ECAR-6564 MARVEL Project Primary Coolant System ASME BPVC Section III Division 5 Design by Analysis

October 2023

Brandon L Moon

Changing the World's Energy Future

Idaho National Laboratory

ECAR-6564 MARVEL Project Primary Coolant System ASME BPVC Section III Division 5 Design by Analysis

Brandon L Moon

October 2023

Idaho National Laboratory
Idaho Falls, Idaho 83415

http://www.inl.gov

1. Effective Date	**10/04/23**	**Professional Engineer's Stamp**
2. Does this ECAR involve a Safety SSC (see def. LWP-10200)?	Yes	
3. Safety SSC Determination Document ID	TBD	
4. SSC ID	----	
5. Project No.	33526	
6. Engineering Job (EJ) or Engineering Change (EC) No.	EC 1755	
7. Building	720	Nathan Seaver Walsh Engineering Services 2023.09.28 12:47:55-06'00'
8. Site Area	MFC	

Professional Engineer's Stamp: PROFESSIONAL ENGINEER LICENSED 16888 STATE OF IDAHO NATHAN ODELL SEAVER

9. Objective / Purpose

This report demonstrates that the MARVEL Reactor Primary Coolant Boundary (herein referred to as the Primary Coolant System, or PCS) is designed to meet ASME BPVC Section III Division 5 [5] elevated temperature service design-by-analysis criteria. The analysis approach that delineates division of responsibilities to meet project objectives is discussed herein. In short, Design and Service Level A, B, and C code calculations are detailed in ECAR-6580 [9] for the majority of the PCS with complex geometry, while the Lower Downcomers, Bottom Head, and Reactor Core Barrel are analyzed in ANL-23/56 [7]. Service Level D code calculations are detailed in this document.

10. If revision, please state the reason and list sections and/or page being affected.

N/A

11. Conclusion / Recommendations

The PCS passes all rules in [5] HBB-3225 for Level D Service Limits and ASME BPVC Section III Appendices [4] Mandatory Appendix XXVII for Unprotected Transient Overpower (UTOP) and two unique directional seismic cases. Compressive stress code checks for buckling from external pressure and local buckling due to flexure pass with sufficient margin. Shear stress checks also pass without concern. See Sections 7.9 and 7.11 as well as Appendix D for detailed calculations and results.

CONTENTS

APPENDICES

1 PROJECT ROLES AND RESPONSIBILITIES

Project Role	Name	Organization	Pages Covered (if applicable)
Performer	K. Francis	Walsh Engineering Services	See DCR 704401, All except Appendix G
Performer	J. Stevenson	Walsh Engineering Services	See DCR 704401, Appendix G
Checker[a]	N. Seaver	Walsh Engineering Services	See DCR 704401
Independent Reviewer[b]	B. Coryell	U710	See DCR 704401
CUI Reviewer[c]	M. Patterson	C120	See DCR 704401
Manager[d]	N. Seaver	Walsh Engineering Services	See DCR 704401
Requestor[ef]	Y. Arafat	C120	See DCR 704401
Nuclear Safety[f]	D. Gerstner	H374	See DCR 704401
Document Owner[f]	B. Moon	U022	See DCR 704401
Reviewer[f]	N/A	N/A	N/A

Responsibilities:

a. Confirmation of completeness, mathematical accuracy, and correctness of data and appropriateness of assumptions.

b. Concurrence of method or approach. See definition, LWP-10106.

c. Concurrence with the document's markings in accordance with LWP-11202.

d. Concurrence of procedure compliance. Concurrence with method/approach and conclusion.

e. Authorizes the commencement of work of the engineering deliverable.

f. Concurrence with the document's assumptions and input information. See definition of Acceptance, LWP-10200.

NOTE: *Delete or mark "N/A" for project roles not engaged. Include ALL personnel and their roles listed above in the DCR system. The list of the roles above is not all inclusive. If needed, the list can be extended or reduced.*

2 SCOPE AND BRIEF DESCRIPTION

This report demonstrates that the MARVEL Reactor Primary Coolant Boundary (herein referred to as the Primary Coolant System, or PCS) is designed to meet ASME BPVC Section III Division 5 [5] elevated temperature service design-by-analysis criteria. The analysis approach that delineates division of responsibilities to meet project objectives is discussed herein. In short, Design and Service Level A, B, and C code calculations are detailed in ECAR-6580 [9] for the majority of the PCS with complex geometry, while the Lower Downcomers, Bottom Head, and Reactor Core Barrel are analyzed in ANL-23/56 [7]. Service Level D code calculations are detailed in this document.

3 DESIGN OR TECHNICAL PARAMETER INPUT AND SOURCES

Engineering inputs are from ECAR-6580 [9], ECAR-6332 [15], and ANL-23/56 [7]. Calculations are administered by ASME BPVC Section III Division 5 [5] and ASCE 4-16 [2]. Technical functional requirements for the MARVEL Reactor Structure are documented in TFR-2576 [18].

4 RESULTS OF LITERATURE SEARCHES AND OTHER BACKGROUND DATA

Drawings used in this analysis, including calculations in the appendices, are referenced in Table 1.

Table 1. Drawing List

Drawing Number	Rev.	Description
1013330	000A	CONTROL DRUM ACTUATOR ASSEMBLY
1013335	000A	CENTRAL INSURANCE ABSORBER ACTUATOR ASSEMBLY
1014540	000A	CONTROL DRUM REFLECTOR ASSEMBLY
1014557	000A	OUTER REFLECTOR
1014579	000A	FUEL CORE SYSTEM
1014605	000B	PRIMARY COOLANT SYSTEM
1014606	000B	DOWNCOMER
1014607	000B	CORE BARREL, LOWER
1014608	000B	BOTTOM HEAD
1014609	000B	DISTRIBUTION PLENUM
1014610	000B	CONTROL DRUM ACTUATOR STANDOFF
1014617	000A	REFLECTOR PRELOAD PLATE ASSEMBLY
1014618	000A	REFLECTOR SUPPORT STRAPS ASSEMBLIES
1014671	000A	OUTER REFLECTOR SUPPORT PLATE
1014672	000A	LOWER REFLECTOR PLATE
1014673	000A	UPPER REFLECTOR SUPPORT PLATE
1014706	000A	AXIAL GAMMA SHIELDING BLOCK
1014707	000A	UPPER AXIAL NEUTRON SHIELDING HOUSING
1014736	000B	INTERMEDIATE HEAT EXCHANGER WELDMENT
1014740	000A	STIRLING ENGINE AND ENGINE BRACKET ASSEMBLY
1014743	000B	STIRLING ENGINE AND SECONDARY SUPPORT STRUCTURE ASSEMBLY
1014744	000B	LOWER STIRLING SUPPORT STRUCTURE WELDMENT

1014746	000A	CENTRAL INSURANCE ABSORBER STRUCTURE FINAL ASSEMBLY
1014747	000A	CENTRAL INSURANCE ABSORBER STRUCTURE WITHOUT BRAZE PLUG ASSEMBLY
1014748	000A	CENTRAL INSURANCE ABSORBER STRUCTURE BRAZE PLUG WITH THERMOCOUPLES ASSEMBLY
1014749	000A	OUTER TUBE WELDMENT
1014750	000A	INNER PIPE WELDMENT
1014751	000A	PCS CLOSURE FLANGE
1014752	000A	BRAZE PLUG
1014753	000A	CENTRAL INSURANCE ABSORBER STRUCTURE CONDUCTIVITY ELEMENT ASSEMBLY
1014754	000A	CENTRAL INSURANCE ABSORBER STRUCTURE ABSORBER SPACER
1014755	000A	CENTRAL INSURANCE ABSORBER STRUCTURE GREY ROD

5 ASSUMPTIONS

1. The bounding design pressure results in the most limiting primary stress intensity contours when applied to each service level.

2. Omitting the lower external Guard Vessel pressure that deducts from the higher PCS design pressure results in the most limiting primary stress intensity contours when applied to each service level.

3. The uniform application of peak hydrostatic pressure results in the most limiting primary stress intensity contours when applied to each service level.

4. The weight of insulation on the PCS is well distributed, small, and is considered negligible.

5. Relatively thin sections of the vessel are modeled at Least Material Condition (LMC) for Service Level D evaluation since the failure criteria focuses on load-controlled stresses only. These sections include the Reactor Core Barrel, IHX, Downcomer piping, Heater Housings, and CIA Housings. All other components have thick sections with tight tolerances and are regions of little concern for Service Level D, so these sections are analyzed at nominal dimensions.

6. NaK corrosion rate is expected to be <0.001 inches per year on 316H SST [7]. The Galinstan secondary coolant is very corrosive; however, the coolant only interfaces with a removable insert that functions as a sacrificial liner and does not contact the PCS. Due to the negligible corrosion rates of NaK, the short lifetime of the MARVEL Reactor, and the sacrificial liner, thickness reductions due to corrosion mechanisms are excluded.

7. The conservative static-equivalent seismic acceleration approach from ECAR-6601 [14] is appropriate since sliding, rocking, and impacts are not anticipated for the PCS.

8. The ASCE 4 static-equivalent seismic acceleration approach from ECAR-6601 [14] is unaffected by the fluid damping response.

6   COMPUTER CODE VALIDATION

A. Computer type: "Sawtooth" HPE SGI 8600 system with 2,052 compute nodes (24 cores per node, Intel 8268 CPUs)

B. Operating System and Version: CentOS 7.9.2009 (kernel release: 3.10.0-1160.66.1.el7.x86_64 #1 SMP Wed May 18 16:02:34 UTC 2022)

C. Computer program name and revision: ABAQUS Standard Version 2021hf6

D. Inputs (may refer to an appendix): Sections 7.1-7.8, all appendices

E. Outputs (may refer to an appendix): Sections 7.9-7.10

F. Evidence of, or reference to, computer program validation: ECAR-5544 Rev. 0 [16], Supplement to ECAR-5544 Rev.0 dated 8/9/2023

G. Bases supporting application of the computer program to the specific physical problem: ABAQUS Standard Version 2021hf6 is a robust implicit solver that performs highly accurate static stress/displacement analysis, among other analysis types. The analyses in this document are linear static problems that fall within the capabilities of the software.

7   DISCUSSION/ANALYSIS

7.1   ASME SERVICE LOADINGS

[5] Subsection HB Subpart B for Class A Metallic Pressure Boundary Components under Elevated Temperature Service requires primary, secondary, and combined stress intensities of the PCS to perform service level calculations for code compliance. Primary stresses result from loading that is necessary to satisfy the laws of equilibrium of external and internal forces and moments and are not self-limiting [5]. Examples of loads that produce primary stress (i.e., primary loads) include pressure and component weights. Secondary stresses are developed by the constraint of adjacent material or the self-constraint of the structure and are self-limiting [5]. Restrained thermal expansion is an example of secondary stresses.

Service levels denote the category of loading that occurs during operational transients at elevated temperature service (>800 °F). Level A Service Loadings include all loadings that would be considered under normal operation [5]. For the MARVEL Reactor, this encompasses start up from cold zero power to hot full power, and shutdown from hot full power to cold zero power over three years of operation. The reactor will undergo normal operations on the weekends, resulting in 156 cycles over the evaluated lifetime. See SPC-70731 [17] for detailed loadings and conditions for the MARVEL Reactor ASME pressure boundary.

Level B Service Loadings are deviations from Level A Service Loadings that are anticipated to occur with moderate frequency, and for which the reactor is designed to withstand without operational impairment [5]. The stirling engines selected for the MARVEL Reactor have components with a life

expectancy of six months in the given operating environment [1]. All four engines will be replaced when one engine fails, resulting in five expected Level B Service Loading cycles over three years (the initial year has one occurrence since the initial state of the reactor assumes four stirling engines with full life). The operational transient is characterized by the failure of one stirling engine followed by a reactor shutdown [17].

Level C Service Loadings are deviations from Level A Service Loadings having low probability of occurrence that require shutdown for correction or repair of damage [5]. There are no Level C Service Loadings classified for the MARVEL Reactor.

Level D Service Loadings are extremely low probability, postulated events that may impair the nuclear system such that only considerations of public health and safety are involved [5]. An Unprotected Transient Over-Power (UTOP), as described above, is classified as such due to its extremely low probability. UTOP occurs when one drum malfunctions and rotates out instantly past critical position to the mechanical hard stop ECAR-6332 [15]. The additional reactivity insertion spikes the system temperature, then intrinsic reactivity feedback returns the reactor to nominal power and temperature. Additionally, seismic events are evaluated to Service Level D. Seismic accelerations are determined using a conservative static equivalency method and are documented in ECAR 6601 [14].

The service levels are summarized in Table 2 below.

Table 2. Service Level Application for the MARVEL Rector [17]

Evaluation Type	Description	Pressure Input (psig)*	Temperature Input (°C)	Number of Cycles
Design	-	55+2.5	570	N/A
Service Level A	Normal Operating Conditions	55+2.5	Provided by [11] and [15]	156
Service Level B	Loss of One Stirling Engine	55+2.5	Provided by [11] and [15]	5
Service Level C	-	-	-	-
Service Level D	Unprotected Transient Over-Power (UTOP), Seismic	55+2.5+1+1	Provided by [15]	1

*Static pressure is evaluated at a constant 55 psig, hydrostatic pressure is applied uniformly as 2.5 psig, and seismic dynamic and hydrostatic pressures are uniformly set to 1 psig each

Loadings are discussed later in this report but note that the static pressure input is the same for each service loading and for the design loading. The design pressure is set to a bounding limit that is greater than all anticipated and postulated service loads at temperature. Calculated pressures for each transient are documented in ECAR-6586 [12].

7.2 ANALYSIS METHODOLOGY

The PCS design is governed by [5] Subsection HB Subpart B as a Class A metallic pressure boundary component seeing service loading temperatures greater than 800 °F (425 °C). Design and Service

Level A, B, and C checks can be grouped into four categories – (1) primary load design or load-controlled stress limits, (2) ratcheting strain limits, (3) creep-fatigue damage accumulation limit, and (4) time-independent and time-dependent buckling limits and special stress limits. Load-controlled stress limits are evaluated using elastic-perfectly plastic (EPP) and simplified inelastic analyses approach that is provided in ASME Code Case N-924. Ratcheting design follows the EPP methodology in ASME Code Case N-861. Creep-fatigue design also relies on EPP methodology as detailed in ASME Code Case N-862. Buckling design is not prescribed by [5]; instead, the method of isochronous curves proposed by Griffin [9] is used. Special stress limits such as bearing stresses and triaxial stresses are considered using elastic structural models.

To meet the MARVEL project objective of an accelerated design schedule while achieving technical excellence and fulfilling rigorous quality standards, the PCS pressure boundary is divided into two sections for Design and Service Level A, B, and C code checks (see Figure 1).

MARVEL Project Primary Coolant System ASME BPVC Section III Division 5 Design by Analysis

Temperature: ECAR-6594
Design, SL-A, SL-B: ECAR-6580

Temperature: ECAR-6332 (Maximums)
SL-D: ECAR-6564 (This Report)

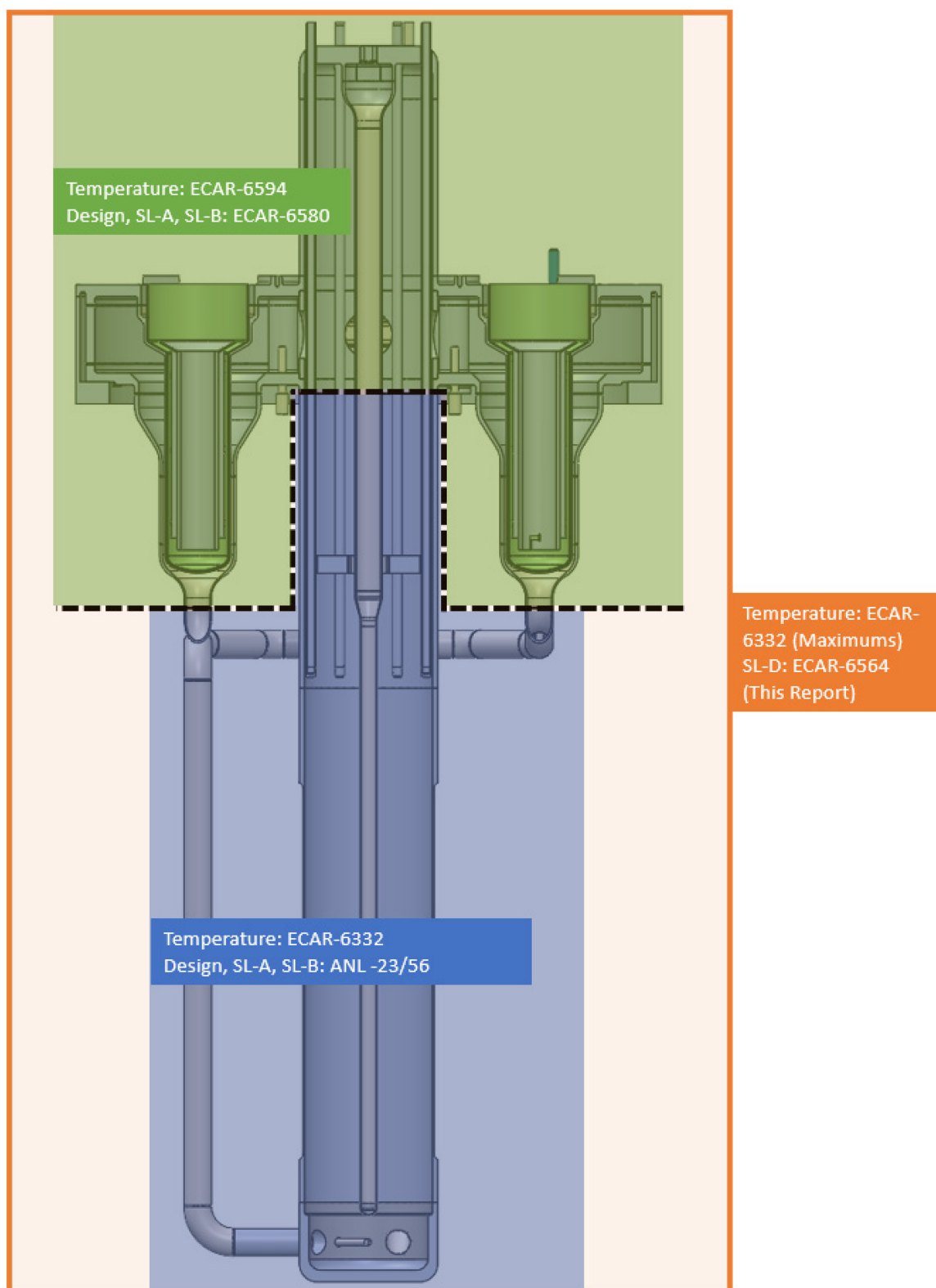Temperature: ECAR-6332
Design, SL-A, SL-B: ANL -23/56

Figure 1. Model Division Based on Temperature Inputs

The dividing boundary is determined from the transient temperature inputs that are required when considering time- and temperature-dependent failure modes. RELAP5-3D is a thermal-hydraulics software that simulates all the design-basis transients for the MARVEL reactor in [15]. It takes hot-channel factors from MCNP neutronics data and generates time-dependent temperature data for the reactor coolants and structural components. [7] uses the mapped temperature distributions from RELAP5-3D on the relatively simple geometry of the Lower Downcomer, Bottom Head, and Reactor Core Barrel to solve the design checks using a Finite Element Analysis (FEA) software called MOOSE. RELAP5-3D is, however, limited to one-dimensional models – this is a concern for the complex geometry and three-dimensional thermal-hydraulic behaviors in the PCS Distribution Plenum and IHX. Star-CCM Computational Fluid Dynamics (CFD) software is employed to provide characteristic temperature distributions in these regions. The CFD tool relies on boundary conditions from RELAP5-3D to generate time-dependent fluid fields with fluid and structural temperature data. Due to model size, resource requirements, and data transmission challenges, CFD is not practical for complete transient runs on a full model of the pressure boundary for the current project objectives; however, this model sectioning approach limits the resource load to an actionable level. In addition, the sectioned model takes advantage of symmetry to further reduce the computational burden. Modelling and results of the CFD analysis are documented in ECAR-6594 [11]. Temperature data on the pressure boundary from [11] is used by [10] to perform the design checks on the remaining, more complex regions of the vessel using ABAQUS FEA software. Boundary conditions between analyses in [10] and [7] at the model divisions are documented in Appendix F.

Service Level D code checks are performed separately on a full model of the PCS using an elastic analysis method in the ABAQUS FEA software. Secondary stresses due to temperature gradients are not considered for the limiting faults, but the maximum temperatures from [15] are used to determine allowable stress limits. The following sections of this report cover the model approach, setup, and results for Service Level D analysis.

7.3 ABAQUS MODELS AND PART GEOMETRY

Figure 2 provides terminology and depicts all ABAQUS part models and their instances within the assembly.

TEM-10200-1, Rev. 12	ENGINEERING CALCULATIONS AND ANALYSIS	ECAR-6564, Rev. 0
04/12/2021		Page 11 of 100

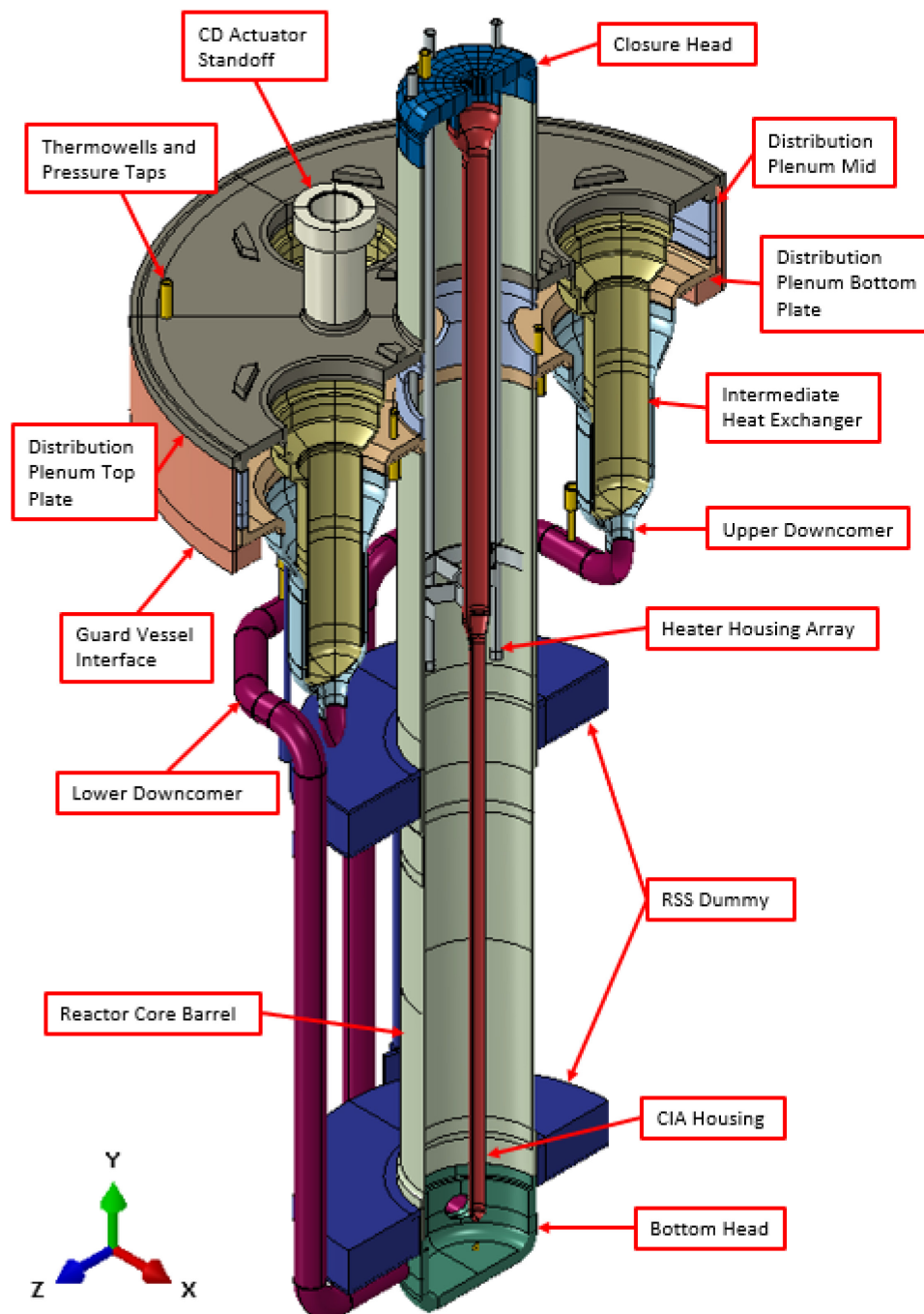MARVEL Project Primary Coolant System ASME BPVC Section III Division 5 Design by Analysis

Figure 2. ABAQUS Parts for the PCS Assembly

The RSS Dummy and Guard Vessel Interface are only modeled for their influences on the PCS and are not considered in the results presentation.

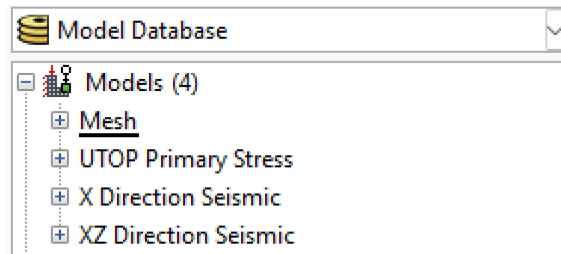The ABAQUS model database has 4 models. See Figure 3 for the nomenclature.

Figure 3. Model Tree in PCS Model Database

The geometry for all models is controlled by model *Mesh* through part and instance linking. Linking the parts and instances of the models to a single model controls geometry and finite element mesh from variance between models. Seismic modeling is comprehensive by considering two directions for the horizontal resultant due to cyclic model symmetry: the X-direction and the XZ-direction at 45° from the former. Table 3 documents the objective of each model.

Table 3. Model Objectives

Model	Objective
Mesh	Geometry and finite element mesh control
UTOP Primary Stress	Service Level D Unprotected Transient Overpower (UTOP) steady state primary stress intensities
X Direction Seismic	Service Level D X-direction resultant seismic primary stress intensities
XZ Direction Seismic	Service Level D X-direction and Z-direction diagonal resultant seismic primary stress intensities

All parts are modeled as 3D deformable solids. Geometry dimensions adhere to the designs detailed in (INL Drawing 1014605) for the PCS and (INL Drawing 1014746) for the Central Insurance Absorber (CIA) Structure and to their respective subordinate drawings with a few exceptions. Model simplifications remove ancillary components having negligible influence that are not part of the pressure boundary and remove weld preps that do not result in the finished vessel geometry. See Figure 4 and Figure 5 for comparisons between the design and the ABAQUS model.
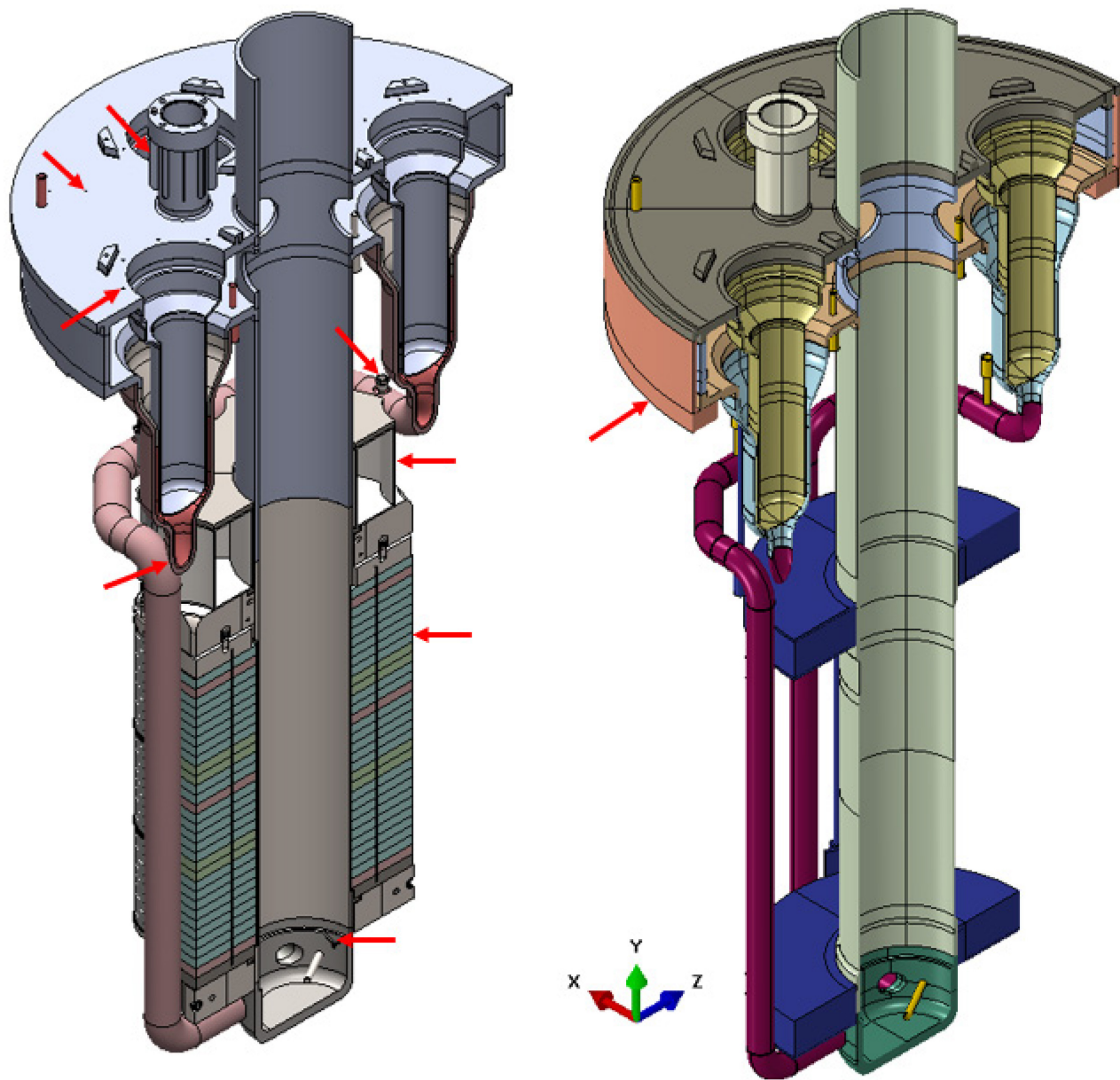
Figure 4. PCS Comparison between Actual Design (Left) and ABAQUS Model (Right)

The liner and internals of the Intermediate Heat Exchanger (IHX) are not included since they are not a part of the pressure boundary and are minimally attached. The Control Drum (CD) Actuator Standoffs are evaluated as an ASME BPVC Section III Division 5 Class B vessel in ECAR-6574 [13], but they are modeled on the PCS for their seismic influence. The thermowell selection changed since the ABAQUS model was developed, but the impacts are negligible. Small, shallow tapped holes and notches in large base metal sections are considered insignificant and are not included. These features are generally located in areas of relatively low stress, creep, and fatigue.
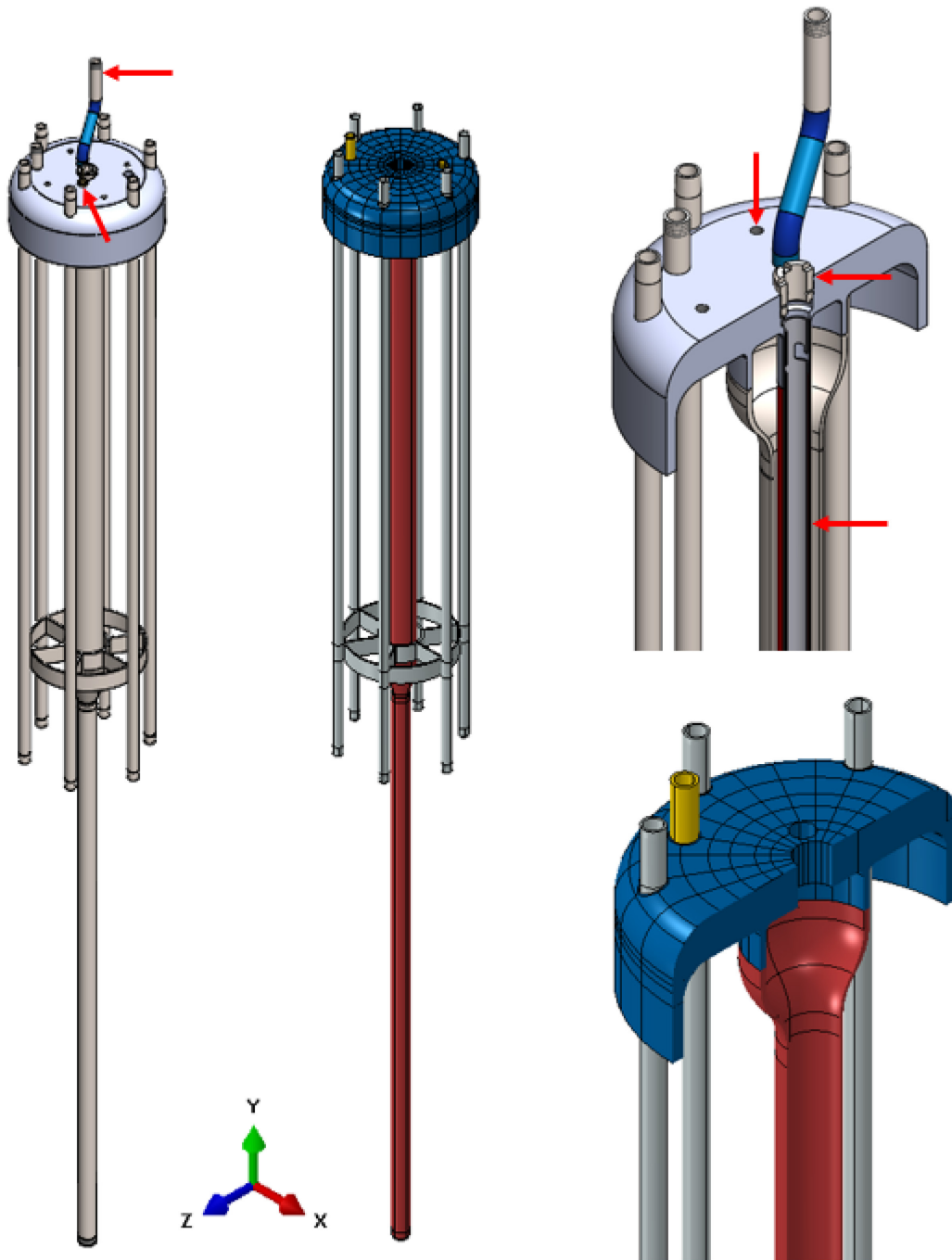
Figure 5. CIA Structure Comparison between Actual Design (Left, Top Right) and ABAQUS Model (Center, Bottom Right)

The CIA Structure has several components that are outside of the pressure boundary and are excluded. This includes penetrations and tubes inside the CIA housing.

Since Service Level D is only concerned with load-controlled stresses, the geometry is modeled at least material condition (LMC) on the critical and thin sections. This includes the Reactor Core Barrel, the

Upper Downcomer, Lower Downcomer, Intermediate Heat Exchangers, Central Insurance Absorber Housing, and Cartridge Heater Housings. The Distribution Plenum, Closure Head, and Bottom Head are sufficiently robust with tight manufacturing tolerances and are considered at nominal dimensions. Corrosion penalties from NaK are an inconsequential <0.001 inches per year for slow-flow systems and are excluded due to the short lifetime of the reactor, see ECAR-6588 [7] for chemical compatibility analyses [17]. See Appendix A for thickness reductions.

[5] HBB-3353 requires consideration for weld geometry in elevated temperature analysis. Welds must be modeled in the condition that would produce the highest strain concentration. All accessible weld surfaces will be ground flush and polished. Complete Joint Penetration (CJP) welds that cannot be accessed on the root side due to limited clearance or assembly sequence (see Figure 7) are modeled with a conservative root geometry in accordance with Figure 6.
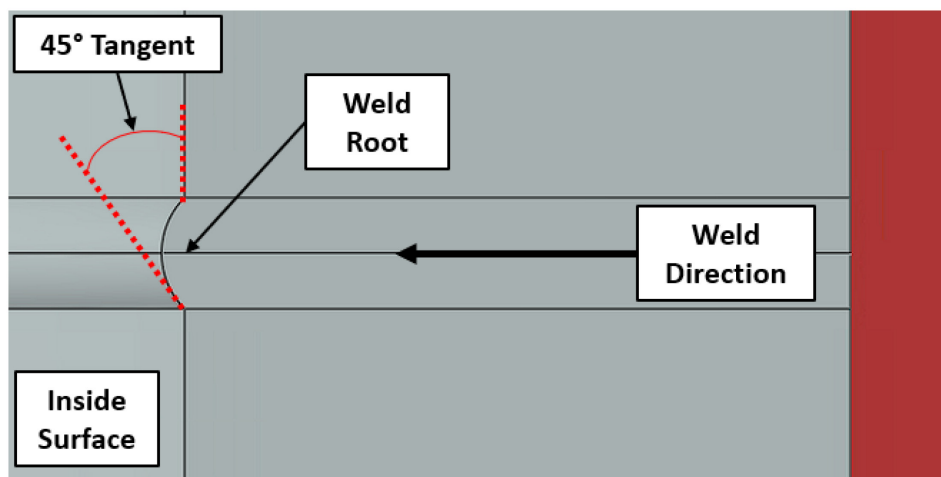

Figure 6. CJP Weld Root Geometry for Inaccessible Weld Surfaces

Consultation with the fabricator has revealed that through prior observation the root reentrant angle can be held to less than 45 degrees. The width of the root is determined based on the thickness of the base metal in accordance with AWS D1.6 [6] Figure 3.5 for a prequalified CJP V-groove weld.

TEM-10200-1, Rev. 12 04/12/2021	ENGINEERING CALCULATIONS AND ANALYSIS	ECAR-6564, Rev. 0 Page 16 of 100

MARVEL Project Primary Coolant System ASME BPVC Section III Division 5 Design by Analysis
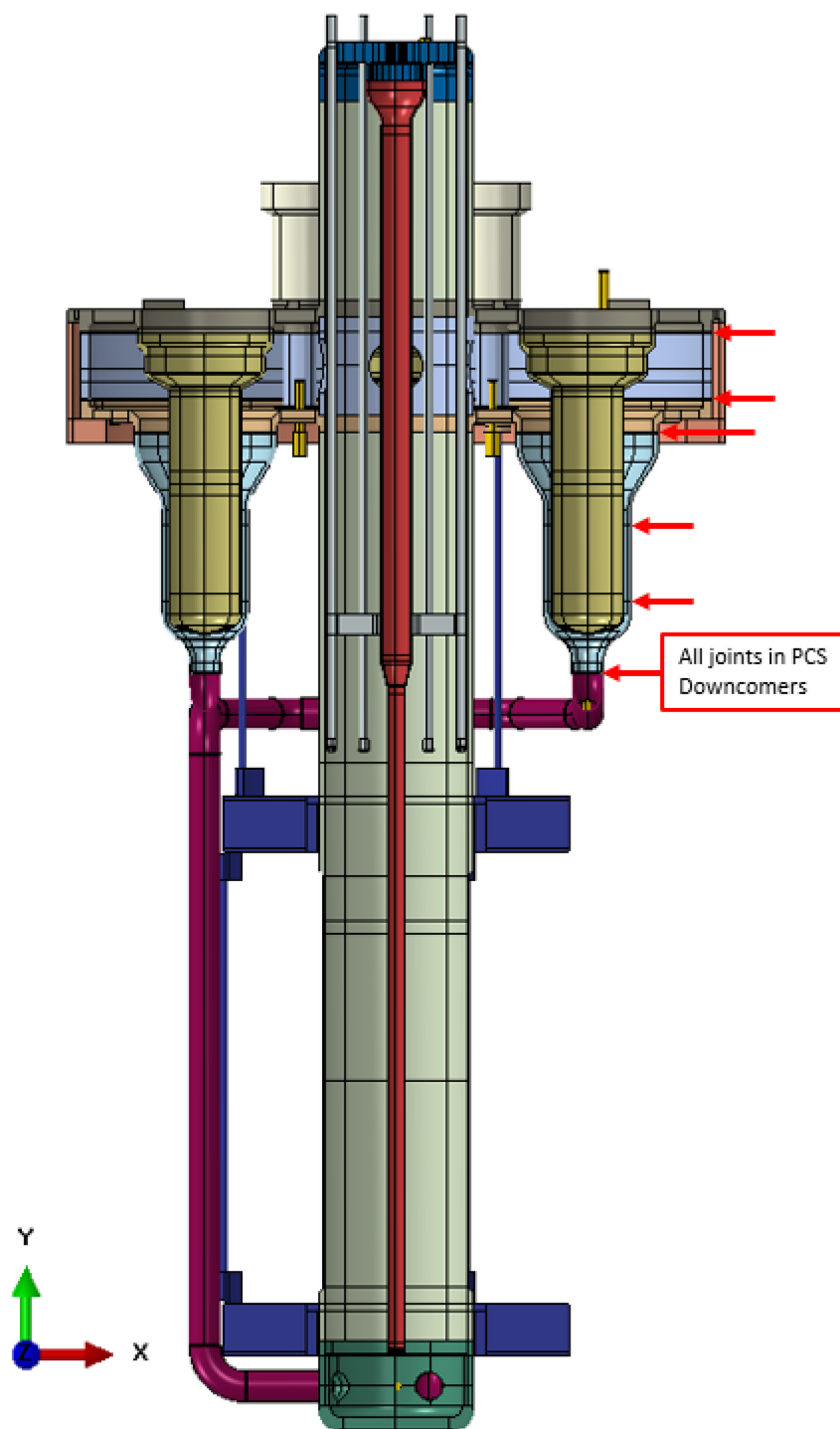
All joints in PCS Downcomers

Figure 7. PCS Weld Joints with Inaccessible Roots Modeled per Figure 6

7.4 MODEL PROPERTY AND MATERIAL

[5] Table HBB-I-14.1(a) prescribes permissible base materials for structures or vessels at elevated temperature service. Type 316H stainless steel is selected for the MARVEL Reactor because of its

TEM-10200-1, Rev. 12 04/12/2021	ENGINEERING CALCULATIONS AND ANALYSIS	ECAR-6564, Rev. 0 Page 17 of 100

MARVEL Project Primary Coolant System ASME BPVC Section III Division 5 Design by Analysis

high temperature strength and availability. Properties of the 316H SST material are shown in Figure 8.

Figure 8. Temperature Dependent Material Properties for 316H SST [3]

All materials in the ABAQUS model are assigned as 316H SST except for the RSS Dummy part. This part, which consists of an upper plate and a lower plate, uses custom densities to simulate the weight of the components which they carry. This approach is conservative since it moves the center of gravities farther away from the braced point above, creating larger than actual moments in a seismic event. The upper plate density brings its weight to 1500 lb, while the lower plate has an even higher density to represent 2500 lb (see Figure 9).
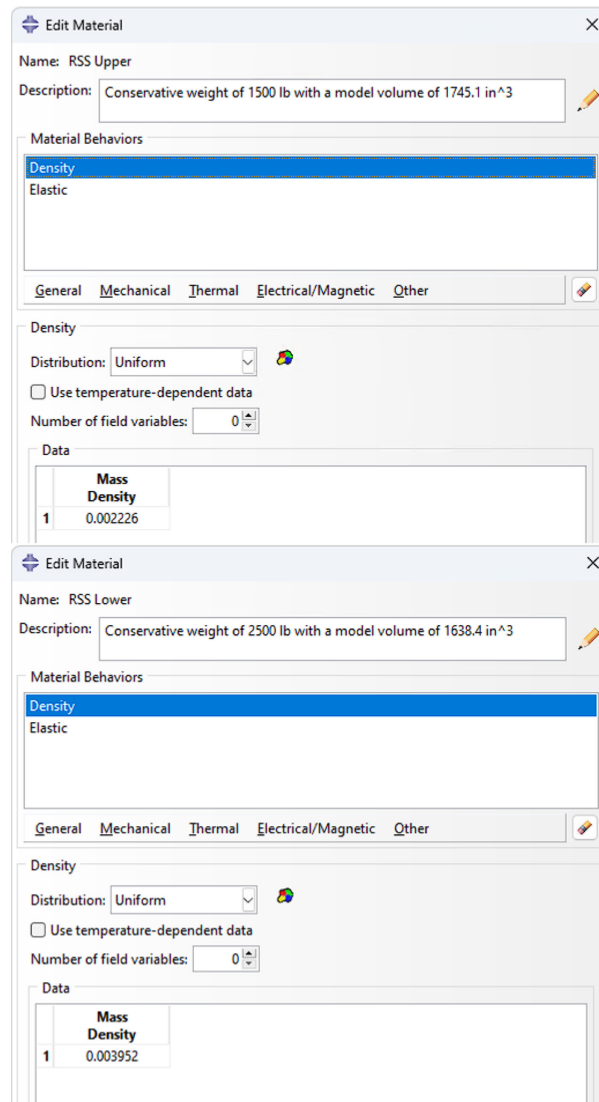
Figure 9. Density Material Properties of the RSS Upper and Lower Plates

7.5 MODEL STEP

All models have similar builds for the model steps, with exception to *Mesh*. Since *Mesh* only supplies part, property, and mesh data to the other models, it does not proceed further in model setup to produce a job. Models have the default initial step followed by a general static step with mostly default settings per Figure 10. The incrementation setup was adjusted to help solution convergence.

ENGINEERING CALCULATIONS AND ANALYSIS

MARVEL Project Primary Coolant System ASME BPVC Section III Division 5 Design by Analysis

Figure 10. General Static Step Setup for Stress Calculation

7.6 MODEL INTERACTIONS

Part instances are tied together to model the PCS as a weldment. The Guard Vessel Interface has one exception where it contacts the bottom of the PCS with a surface-to-surface contact interaction, see Figure 11. The Guard Vessel Interface is included in the model to capture the influence on the PCS.
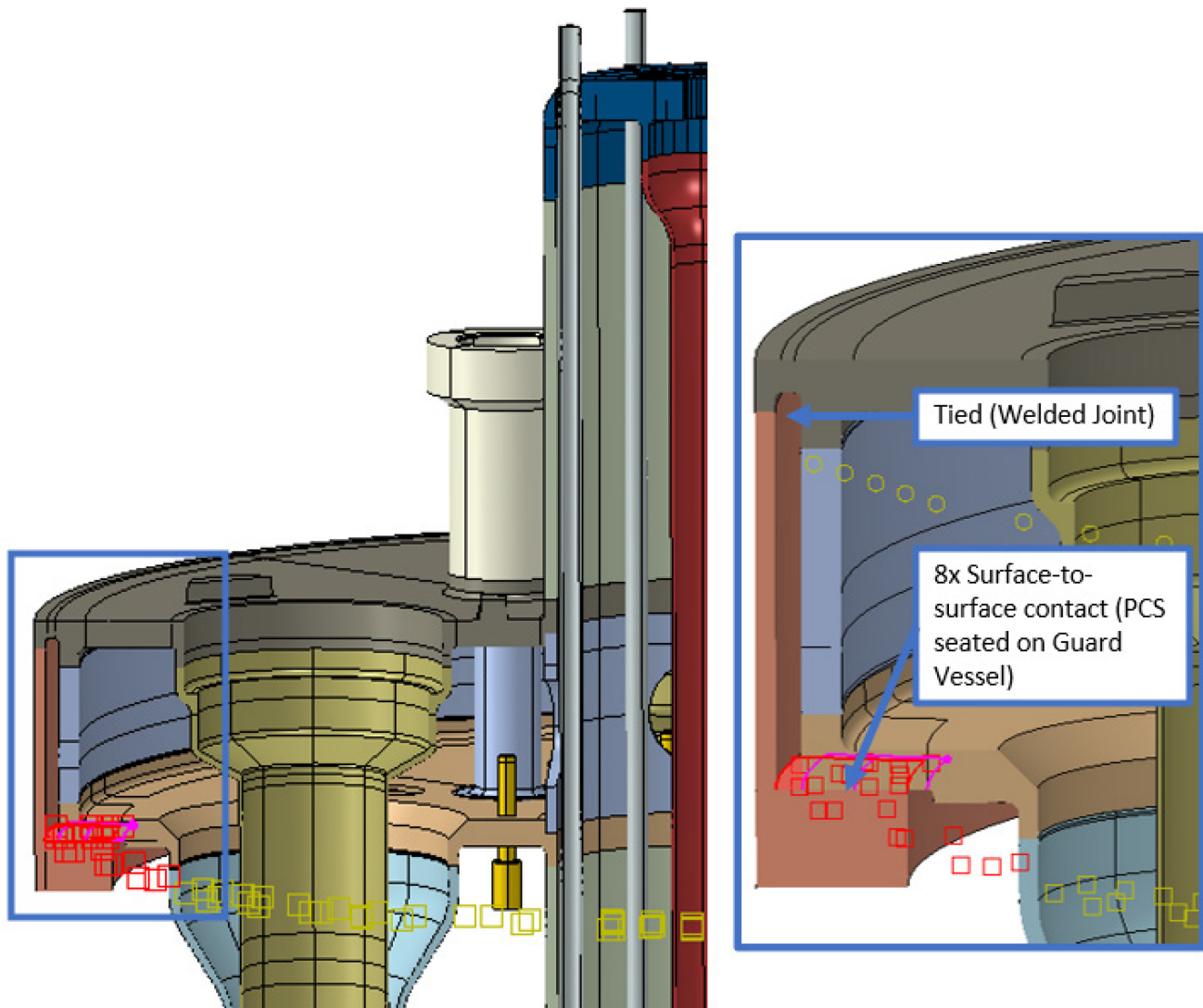
Figure 11. PCS to Guard Vessel Interface Interaction

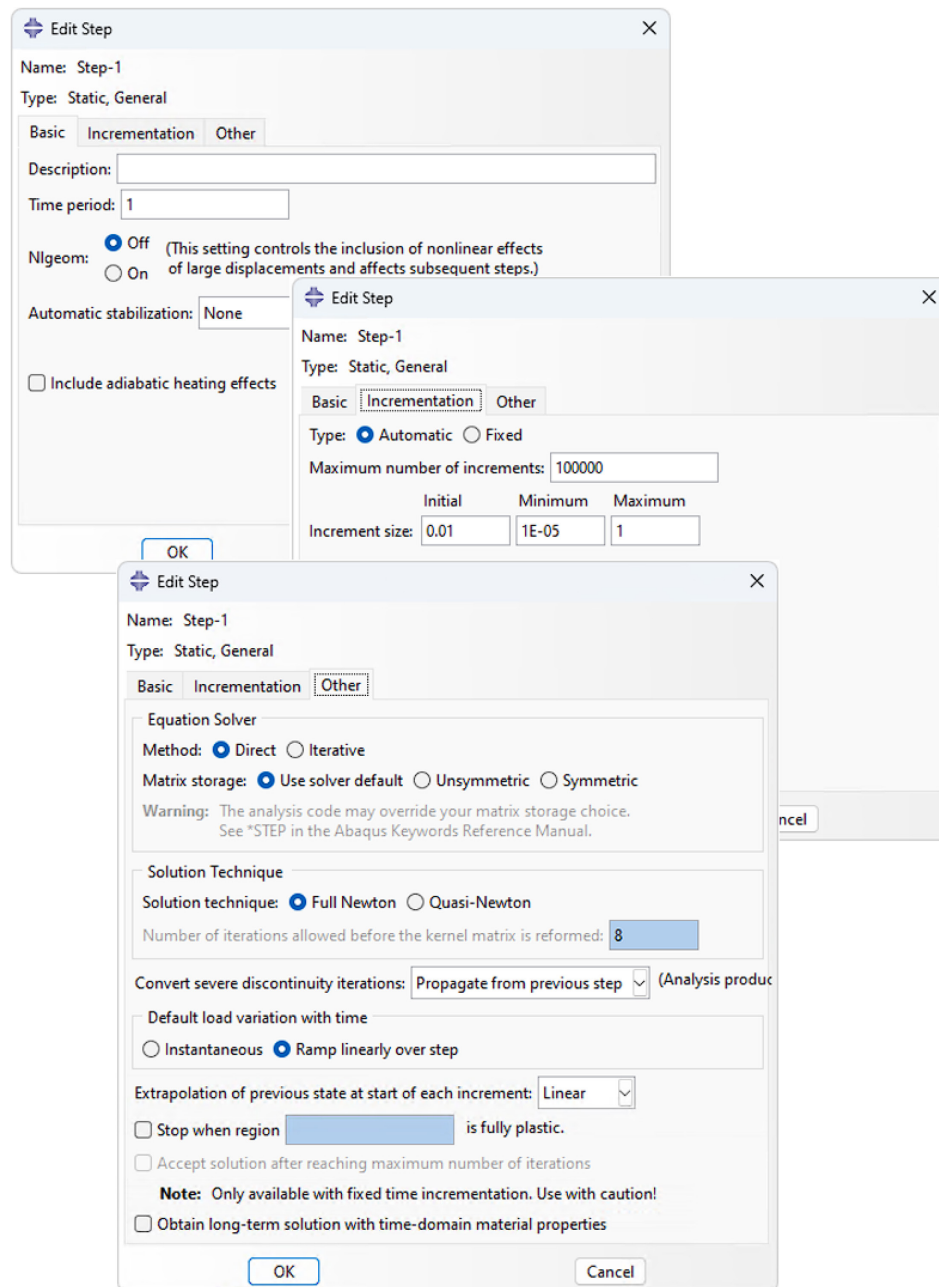Additionally, the RSS Dummy is modeled to capture the interaction with the Core Barrel from horizontal seismic accelerations. There are two centering rings that snug the RSS to the Core Barrel with a small clearance. For stability, these two interfaces are modeled as coincident faces with surface-to-surface contact, see Figure 12. The circular contact area is divided into two halves with separate interactions for proper behavior. The Beryllium Oxide (BeO) plate stacks that are a part of the RSS and surround the Core Barrel have sufficient restraint from the hold-down springs during seismic such that no sliding or movement is expected. See ECAR-6589 [18] for detailed calculations. Therefore, the only contact from the RSS to the PCS is through the two centering rings addressed above. Any stiffness from the excluded RSS components and control drums is omitted from the analysis.
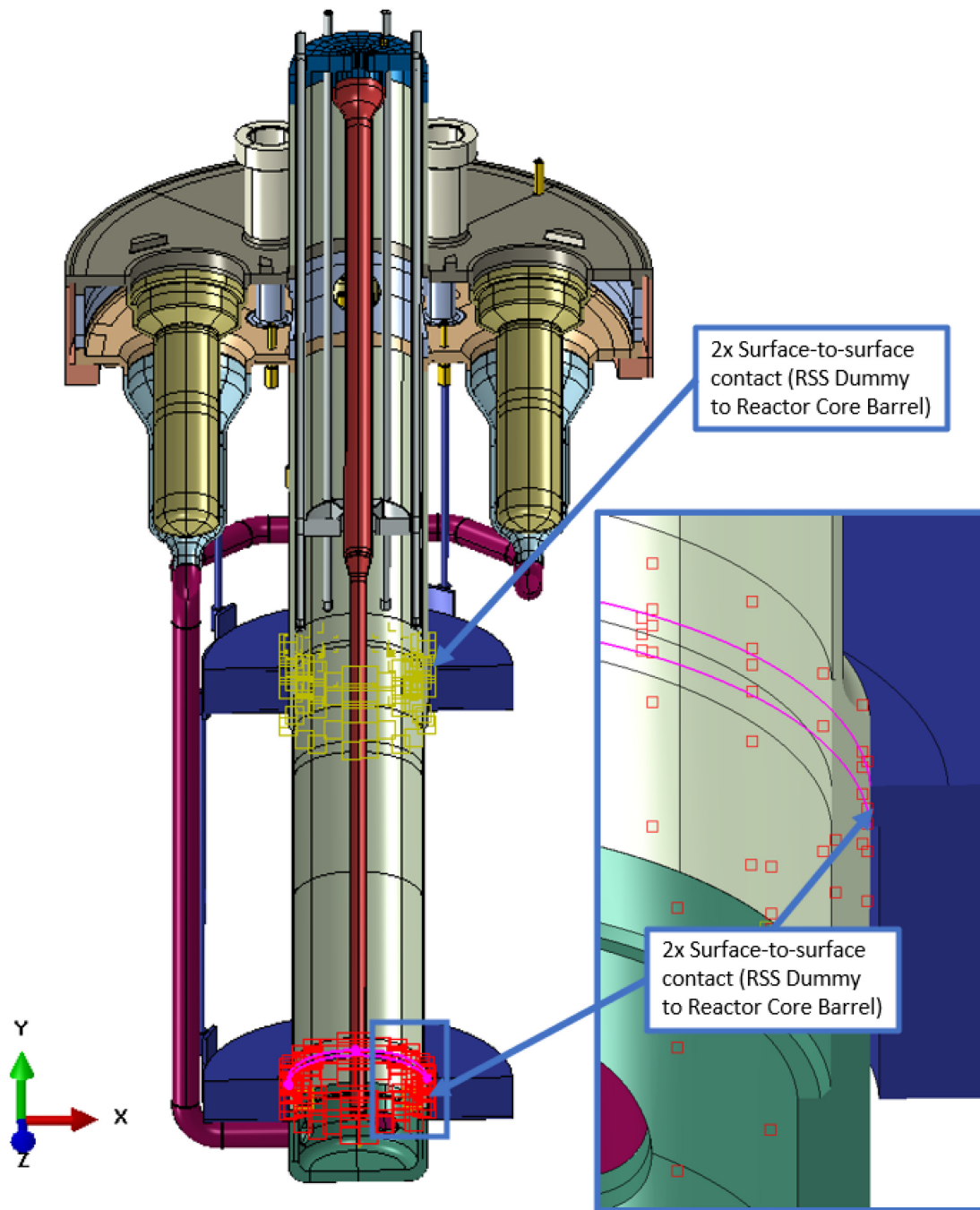
Figure 12. Surface-to-Surface Contact Interactions between the RSS and Axial Shields Dummy and the PCS Core Barrel (Seismic Only)

Attached equipment and internal fluids are modeled using coupling constraints. See Figure 13 for the general arrangements. Reference points set the coordinate location of each coupling control point where the load will be applied. Equipment control points are set to the maximum dimensional extent for conservatism and are coupled to the faces on the PCS that bear the equipment load. The equipment

couplings use a structural distributing coupling type to prevent the attachments from providing any additional model integrity through kinematic couplings. The NaK and molten Galinstan fluids have control points that are calculated from an equivalency method for enforcing hydrodynamic pressures due to seismic forces. These calculations determine impulsive and sloshing hydrodynamic pressure components and their effective weights and heights for overturning moment effects to the vessel. See Appendix C for details. The fluid control points for the overturning moment effects are coupled to wetted surfaces that are positioned in the direction of the horizontal seismic acceleration direction, so the selections are unique in both the X-direction and XZ-direction seismic models. The fluid couplings use a continuum distributing coupling to represent the hydrodynamic loads.
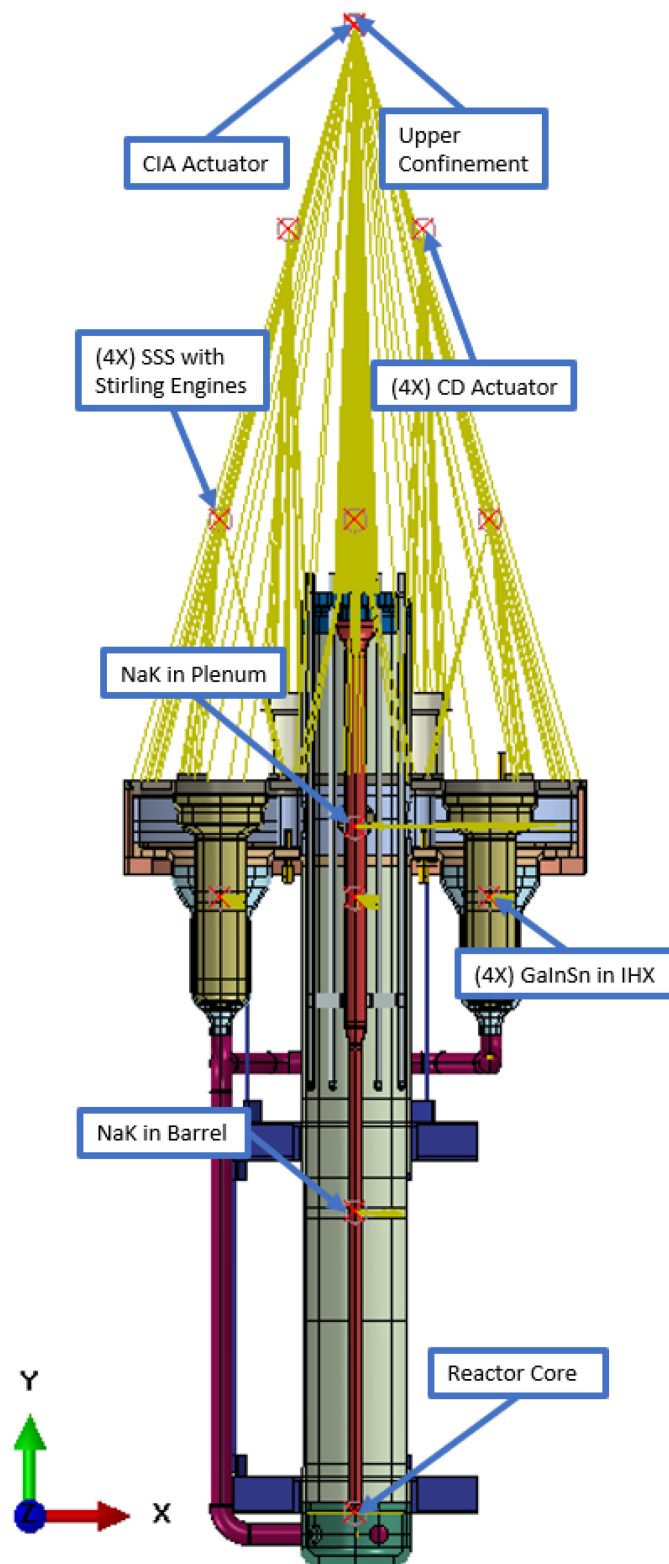
Figure 13. Coupling Constraints for Seismic Models

7.7 MODEL LOADS

Fixturing is accomplished by applying a boundary condition on the bottom surface of the Guard Vessel Interface as shown in Figure 14. The boundary condition uses a polar coordinate system to restrain motion in the axial (vertical) and tangential directions. The PCS rests on the Reactor Support Frame and is allowed to expand radially but not rotate. Seismic uplift is not possible between the PCS and Guard Vessel due to the welded connection, and uplift of the Guard Vessel from the Reactor Support Frame is also determined to not be possible in ECAR-6574 [13]. Therefore, axial modeling restraint is appropriate.

Figure 14. Boundary Condition on the Underside of the Guard Vessel Interface to Represent Seating on Reactor Support Frame

Loads are summarized in Table 4 and are shown Appendix E. See Appendix B for load calculations and comparisons to expected loads. ABAQUS loads have at least a 10% margin over the expected loads. There is also considerable conservatism in the seismic loads and code calculations.

| TEM-10200-1, Rev. 12 | **ENGINEERING CALCULATIONS AND ANALYSIS** | ECAR-6564, Rev. 0 |
| 04/12/2021 | | Page 25 of 100 |

MARVEL Project Primary Coolant System ASME BPVC Section III Division 5 Design by Analysis

Seismic loads are calculated in Appendix C. The MARVEL project uses a static equivalent method to analyze designs for seismic as calculated in ECAR-6601 [14]. The horizontal seismic acce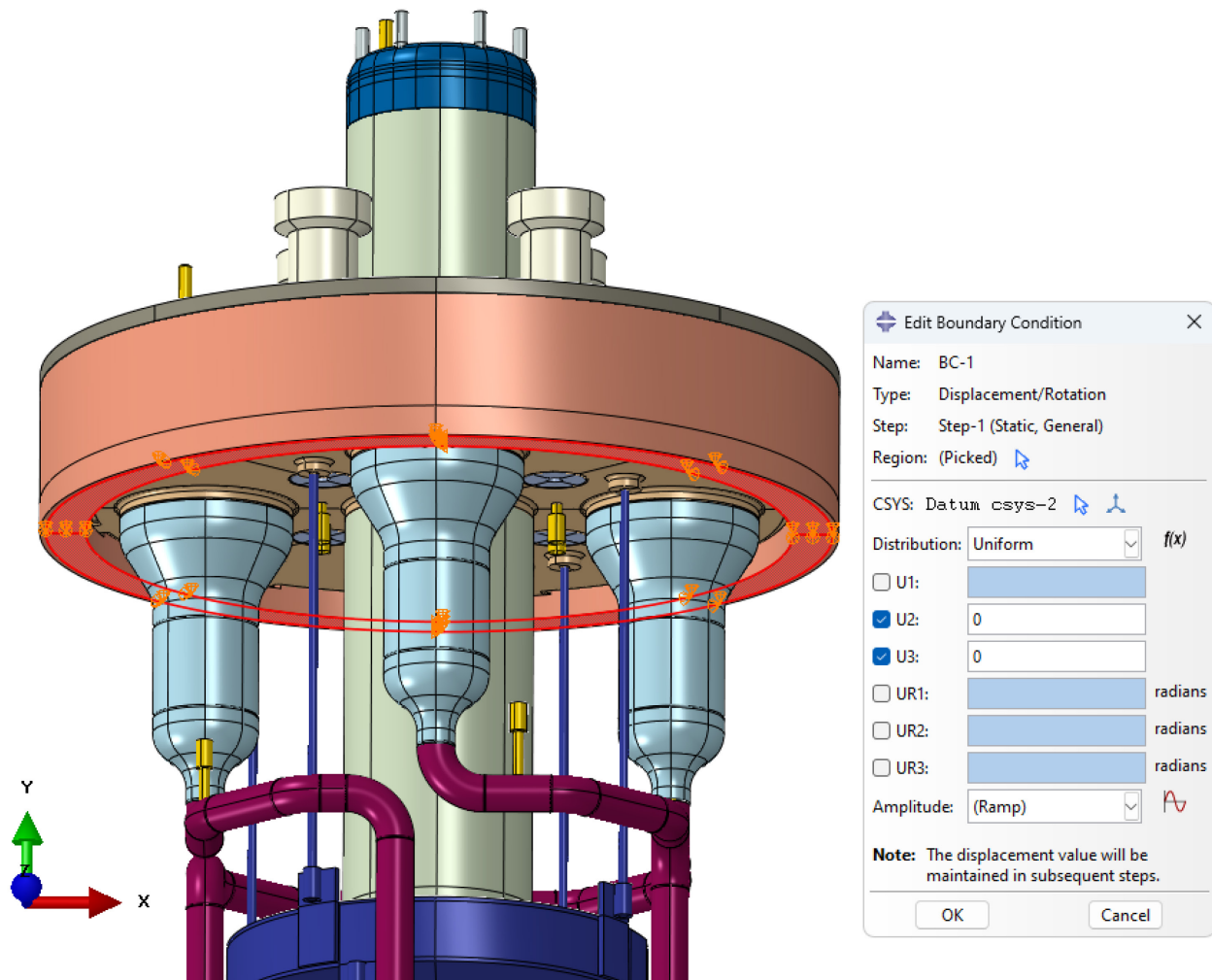leration is 0.377 g applied in a conservative 100-100-100 percent component breakdown. This gives a vertical seismic acceleration of 0.377 g and a resultant horizontal seismic of 0.533 g. Impulsive and sloshing (convective) hydrodynamic seismic forces from the NaK and Galinstan are calculated in Appendix C and applied as loads in the ABAQUS seismic models.

Table 4. Load Summary

Model	Load Description	Load Type	Value
UTOP Primary Stress	CD Actuators Weight 1 (200lb)	Concentrated Force, CF2	-200 lbf
X Direction Seismic,	CD Actuators Weight 2 (200lb)	Concentrated Force, CF2	-200 lbf
XZ Direction Seismic	CD Actuators Weight 3 (200lb)	Concentrated Force, CF2	-200 lbf
	CD Actuators Weight 4 (200lb)	Concentrated Force, CF2	-200 lbf
	CIA Actuator Weight (100lb)	Concentrated Force, CF2	-100 lbf
	Core Weight (800lb)	Concentrated Force, CF2	-800 lbf
	Design Pressure (55 psig)	Pressure, Uniform	55 psi
	Gravity	Gravity, Component 2	-386.089 in/s^2
	NaK Hydrostatic (2_5psi)	Pressure, Uniform	2.5 psi
	SSS Weight and Transmit 1 (500lb)	Concentrated Force, CF2	-500 lbf
	SSS Weight and Transmit 2 (500lb)	Concentrated Force, CF2	-500 lbf
	SSS Weight and Transmit 3 (500lb)	Concentrated Force, CF2	-500 lbf
	SSS Weight and Transmit 4 (500lb)	Concentrated Force, CF2	-500 lbf
	Upper Confinement (1500lb)	Concentrated Force, CF2	-1500 lbf
X Direction Seismic	Seismic (x=0_533g)(y=-0_377g)	Gravity, Component 1, Component 2	205.846 in/s^2 -145.555 in/s^2
	Seismic CD-1 (x=107lb)(y=-76lb)	Concentrated Force, CF1, CF2	107 lbf -76 lbf
	Seismic CD-2 (x=107lb)(y=-76lb)	Concentrated Force, CF1, CF2	107 lbf -76 lbf
	Seismic CD-3 (x=107lb)(y=-76lb)	Concentrated Force, CF1, CF2	107 lbf -76 lbf
	Seismic CD-4 (x=107lb)(y=-76lb)	Concentrated Force, CF1, CF2	107 lbf -76 lbf
	Seismic CIA (x=54lb)(y=-38lb)	Concentrated Force, CF1, CF2	54 lbf -38 lbf
	Seismic Core (x=430lb)(y=-305lb)	Concentrated Force, CF1, CF2	430 lbf -305 lbf
	Seismic Ga Fluid (SCS-1)(80lb)	Concentrated Force, CF1	80 lbf
	Seismic Ga Fluid (SCS-2)(80lb)	Concentrated Force, CF1	80 lbf
	Seismic Ga Fluid (SCS-3)(80lb)	Concentrated Force, CF1	80 lbf
	Seismic Ga Fluid (SCS-4)(80lb)	Concentrated Force, CF1	80 lbf
	Seismic NaK Dynamic P (1psi)	Pressure, Uniform	1 psi
	Seismic NaK Fluid (Barrel)(115lb)	Concentrated Force, CF1	115 lbf
	Seismic NaK Fluid (Plenum)(105lb)	Concentrated Force, CF1	105 lbf
	Seismic NaK Hydrostatic P (1psi)	Pressure, Uniform	1 psi
	Seismic SSS-1 (x=270lb)(y=-190lb)	Concentrated Force, CF1, CF2	270 lbf -190 lbf
	Seismic SSS-2 (x=270lb)(y=-190lb)	Concentrated Force, CF1, CF2	270 lbf -190 lbf
	Seismic SSS-3 (x=270lb)(y=-190lb)	Concentrated Force, CF1, CF2	270 lbf -190 lbf
	Seismic SSS-4 (x=270lb)(y=-190lb)	Concentrated Force, CF1, CF2	270 lbf -190 lbf
	Seismic UC (x=800lb)(y=-570lb)	Concentrated Force, CF1, CF2	800 lbf -570 lbf
XZ Direction Seismic	Seismic (xz=0_377g)(y=-0_377g)	Gravity, Component 1,	145.555 in/s^2

		Component 2, Component 3	-145.555 in/s^2 145.555 in/s^2
	Seismic CD-1 (xz=76lb)(y=-76lb)	Concentrated Force, CF1, CF2, CF3	76 lbf -76 lbf 76 lbf
	Seismic CD-2 (xz=76lb)(y=-76lb)	Concentrated Force, CF1, CF2, CF3	76 lbf -76 lbf 76 lbf
	Seismic CD-3 (xz=76lb)(y=-76lb)	Concentrated Force, CF1, CF2, CF3	76 lbf -76 lbf 76 lbf
	Seismic CD-4 (xz=76lb)(y=-76lb)	Concentrated Force, CF1, CF2, CF3	76 lbf -76 lbf 76 lbf
	Seismic CIA (xz=38lb)(y=-38lb)	Concentrated Force, CF1, CF2, CF3	38 lbf -38 lbf 38 lbf
	Seismic Core (xz=305lb)(y=-305lb)	Concentrated Force, CF1, CF2, CF3	305 lbf -305 lbf 305 lbf
	Seismic Ga Fluid (SCS-1)(xz=57lb)	Concentrated Force, CF1, CF3	57 lbf 57 lbf
	Seismic Ga Fluid (SCS-2)(xz=57lb)	Concentrated Force, CF1, CF3	57 lbf 57 lbf
	Seismic Ga Fluid (SCS-3)(xz=57lb)	Concentrated Force, CF1, CF3	57 lbf 57 lbf
	Seismic Ga Fluid (SCS-4)(xz=57lb)	Concentrated Force, CF1, CF3	57 lbf 57 lbf
	Seismic NaK Dynamic P (1psi)	Pressure, Uniform	1 psi
	Seismic NaK Fluid (Barrel)(xz=82lb)	Concentrated Force, CF1, CF3	82 lbf 82 lbf
	Seismic NaK Fluid (Plenum)(xz=75lb)	Concentrated Force, CF1, CF3	75 lbf 75 lbf
	Seismic NaK Hydrostatic P (1psi)	Pressure, Uniform	1 psi
	Seismic SSS-1 (xz=190lb)(y=-190lb)	Concentrated Force, CF1, CF2, CF3	190 lbf -190 lbf 190 lbf
	Seismic SSS-2 (xz=190lb)(y=-190lb)	Concentrated Force, CF1, CF2, CF3	190 lbf -190 lbf 190 lbf
	Seismic SSS-3 (xz=190lb)(y=-190lb)	Concentrated Force, CF1, CF2, CF3	190 lbf -190 lbf 190 lbf
	Seismic SSS-4 (xz=190lb)(y=-190lb)	Concentrated Force, CF1, CF2, CF3	190 lbf -190 lbf 190 lbf
	Seismic UC (xz=570lb)(y=-570lb)	Concentrated Force, CF1, CF2, CF3	570 lbf -570 lbf 570 lbf

Galinstan alloy fluid sloshing and impulse seismic forces are considered, but the hydrostatic and seismic dynamic pressure is excluded (see Appendix C). NaK hydrostatic pressure is uniformly applied

to all internal NaK-wetted surfaces for conservatism (see Figure 32). The Guard Vessel pressure that acts on all external surfaces of the PCS except for the top of the Distribution Plenum and Upper Core Barrel and Closure Head is omitted since it subtracts from the PCS internal pressure.

7.8   ABAQUS MODEL FINITE ELEMENT MESH

The PCS uses C3D8I linear hexahedral elements, which is an incompatible model element from the 3D Stress family for ABAQUS Standard. Incompatible mode elements mitigate shear locking with additional degrees of freedom as shown in Figure 15.
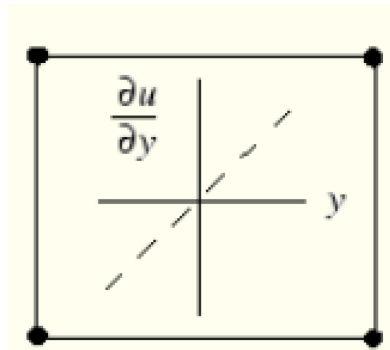
Figure 15. Incompatible Model Element Depiction Showing Additional Diagonal Degree of Freedom

Figure 16 shows the finite element mesh on model *Mesh*, which is used for all models. Critical sections have at least three elements defining the thickness. The Guard Vessel Interface is coarsely defined since it is used only as an interface and is excluded from the evaluation.

MARVEL Project Primary Coolant System ASME BPVC Section III Division 5 Design by Analysis

Figure 16. Finite Element Mesh of Parts in PCS Assembly

All welds with root geometry have adequately refined mesh seeding to capture the root angle while mitigating severe aspect ratio distortion, see Figure 17.
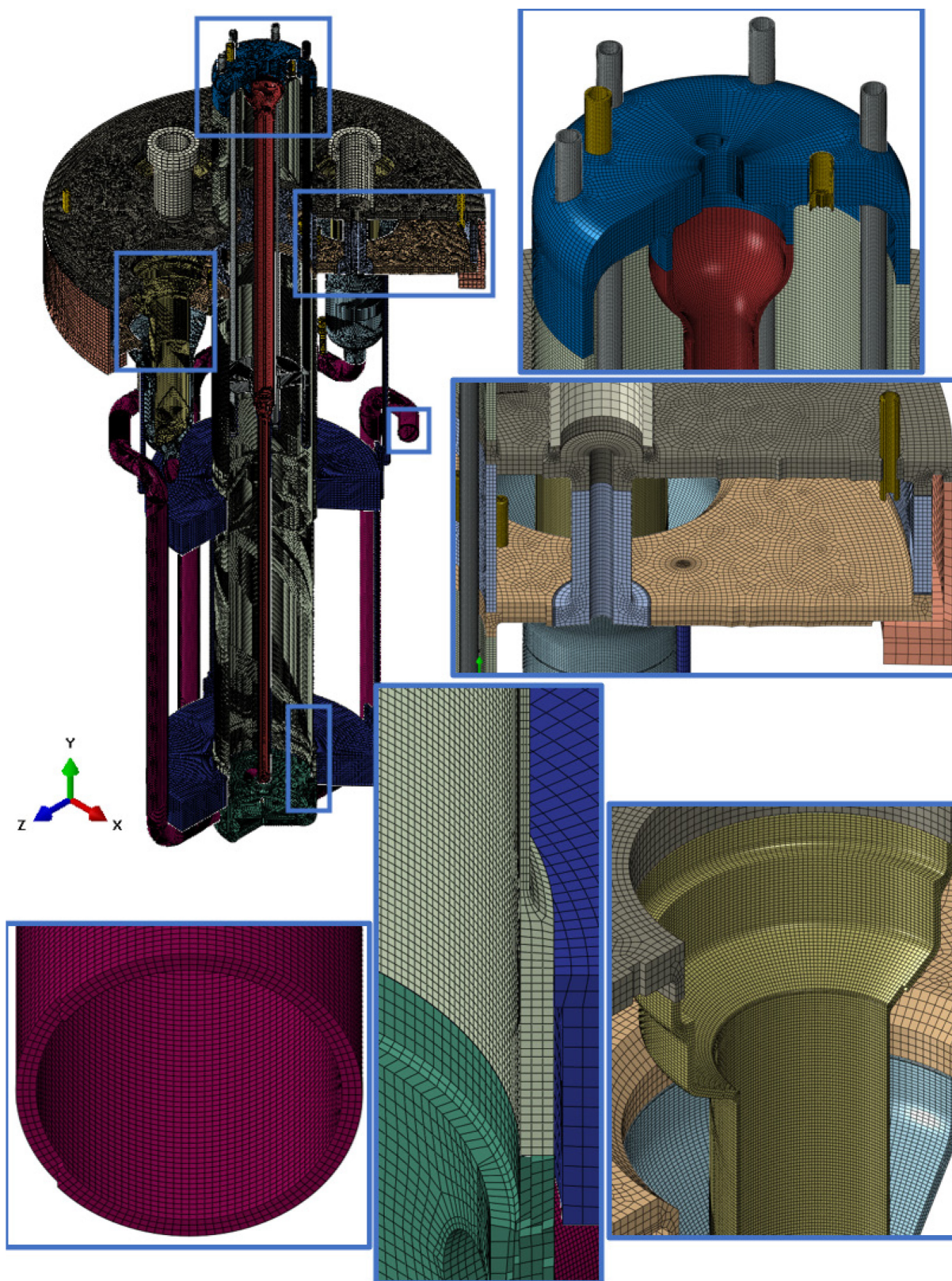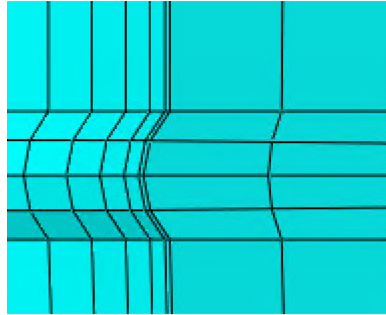

Figure 17. Mesh Refinement on Weld Roots, Typical

Mesh verification ensures that mesh quality is within acceptable limits. Probing element aspect ratio is an overall indicator of the level of distortion in elements. Average aspect ratios should be held under 3, and elements with aspect ratios greater than 10 should be mitigated to less than 1% of the element count as reasonably achievable. Aspect ratio evaluation for model Mesh is summarized in Table 5.

Table 5. Aspect Ratio Mesh Verification for Mesh Model

Part Instance	Element Count	Average Aspect Ratio	Aspect Ratio > 10 (#)	Aspect Ratio > 10 (%)	Worst Aspect Ratio
Distribution Plenum Bottom Plate	157556	2.12	11	0.01	10.59
Distribution Plenum Mid	150006	2.47	444	0.30	10.39
Guard Vessel Interface	11772	1.25	0	0	2.19
CD Actuator Standoff Short No Fins (1 of 4)	1232	2.44	28	2.27	11.72
IHX Pressure Boundary LMC (1 of 4)	171744	2.34	0	0	3.91
Lower Downcomer LMC (1 of 4)	503247	1.38	0	0	2.99
Thermowells and Pressure Taps	184180	1.93	135	0.07	19.63
Upper Downcomer LMC (1 of 4)	112030	1.91	0	0	6.45
Reactor Core Barrel LMC	558800	1.9	0	0	4.03

TEM-10200-1, Rev. 12 04/12/2021	**ENGINEERING CALCULATIONS AND ANALYSIS**	ECAR-6564, Rev. 0 Page 30 of 100

MARVEL Project Primary Coolant System ASME BPVC Section III Division 5 Design by Analysis

CIAS Heater Array 6 Heaters LMC	412532	1.57	0	0	4.51
Distribution Plenum Top Plate	302925	2.43	274	0.09	21.21
CIA Housing LMC	424257	2.63	0	0	5.61
Bottom Head Split Lines	48923	1.63	0	0	8.00
RSS Dummy	146228	1.87	0	0	7.83
CIAS Closure Head Heater LMC	105524	1.73	60	0.06	12.14
Model Totals	**5,655,715**	**1.84**	**1036**	**0.02**	**21.21**

All part instances have aspect ratios that meet the acceptance criteria. The largest aspect ratio is at the SSS mounting features on the Distribution Plenum Top Plate. The part that has the most elements by percentage with an aspect ratio greater than 10 is the Control Drum Actuator Standoff, but it is not a critical component nor is it a primary boundary component.

7.9 SERVICE LEVEL D CODE RESULTS – SUMMARY

Results for Service Level D Code checks are summarized in Table 6 below. Membrane and membrane plus bending limiting demands are investigated in Sections 7.10.1 and 7.11.1 and are all below the allowable limits documented here. Detailed calculations are in Appendix D.

Table 6. Service Level D Results Summary Table

UTOP Membrane and Membrane Plus Bending Checks	
Rule (b): General Primary Membrane Stress Intensity (Allowable Limit)	19.8 ksi
Rule (c): Use-Fraction Sum Associated with General Primary Membrane Stress (D/C Ratio)	0.871
Rule (d): Combined Primary Membrane Plus Bending Stress Intensity (Allowable Limit)	19.8 ksi
Rule (e): Use-Fraction Sum Associated with Primary Membrane Plus Bending Stress (D/C Ratio)	0.871
X and XZ Seismic Membrane and Membrane Plus Bending Checks	
Rule (b): General Primary Membrane Stress Intensity (Allowable Limit)	35.7 ksi
Rule (c): Use-Fraction Sum Associated with General Primary Membrane Stress (D/C Ratio)	0.578
Rule (d): Combined Primary Membrane Plus Bending Stress Intensity (Allowable Limit)	36.1 ksi
Rule (e): Use-Fraction Sum Associated with Primary Membrane Plus Bending Stress (D/C Ratio)	0. 578
UTOP and Seismic Compressive Stress Checks	
CIA Housing External Pressure (D/C Ratio)	0.224
IHX External Pressure (D/C Ratio)	0.185
Cartridge Heater Housing External Pressure (D/C Ratio)	0.023
Local Buckling Due to Flexure (D/C Ratio)	0.779
UTOP and Seismic Shear Stress Checks	
UTOP Shear Stress Check (D/C Ratio)	0.643
X and XZ Seismic Shear Stress Check (D/C Ratio)	0.601

7.10 SERVICE LEVEL D CODE RESULTS – UNPROTECTED TRANSIENT OVERPOWER

7.10.1 HBB-3225 Membrane Stress and Membrane Plus Bending Stress Rules

Rules in [5] HBB-3225 Level D Service Limits and ASME BPVC Section III Appendices [4] Mandatory Appendix XXVII check four criteria: (1) general primary membrane stress intensity, (2) use-fraction sum associated with the general primary membrane stress intensity, (3) combined primary membrane plus bending stress intensity, and (4) use-fraction sum associated with the combined primary membrane

plus bending stress intensity. To calculate (1) – (4), stress classification is required on the stress intensity contours to separate general membrane and combined membrane plus bending stress components, see Figure 18.

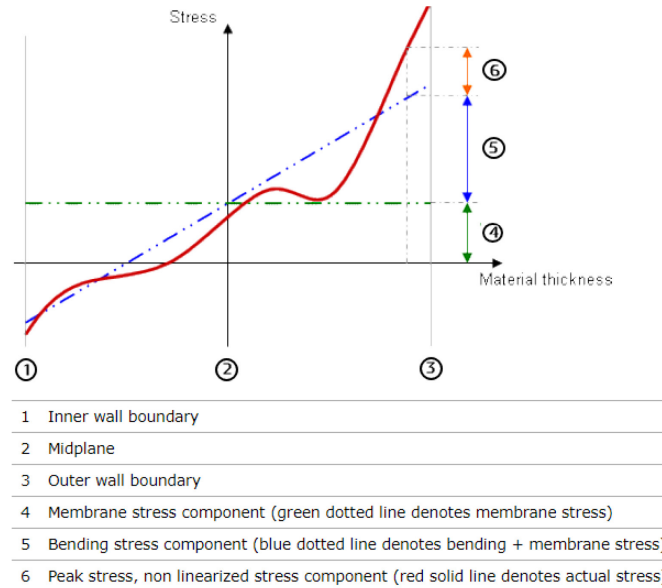|	
1	Inner wall boundary
2	Midplane
3	Outer wall boundary
4	Membrane stress component (green dotted line denotes membrane stress)
5	Bending stress component (blue dotted line denotes bending + membrane stress)
6	Peak stress, non linearized stress component (red solid line denotes actual stress)

Figure 18. Stress Classification through a Wall Thickness

This is generally achieved by generating stress classification lines that characterize a section's thickness. The challenge is that the maximum membrane and maximum combined membrane plus bending stress components in the model are not explicitly defined, so a methodical investigation is required to characterize all potentially limiting sections.

To reduce the analysis burden and submit additional conservatism, a process of elimination is used that takes the maximum model stress intensity that passes all four criteria mentioned above. This means that the stress value used in the calculation includes combined membrane, bending, and peak stress components and conservatively checks those combined values against the limits for general membrane and combined membrane plus bending stress classifications. Engineering judgement is required to eliminate, or disqualify, the maximum stress intensities that fail the code checks due to considerably large peak stress components. See Figure 19 for the UTOP primary stress intensity contour plot.

SS Primary Loads with Max UTOP Temp
ODB: UTOP-Primary.odb   Abaqus/Standard 2021.HF6   Tue Aug 15 16:01:42 Mountain Daylight Time 2023

S, Tresca
(Avg: 75%)
```
  23383.6
  21434.9
  19486.3
  17537.7
  15589.0
  13640.4
  11691.8
   9743.2
   7794.5
   5845.9
   3897.3
   1948.6
      0.0
```
Max: 23383.6
 Elem: Distribution Plenum Top Plate-1.122377
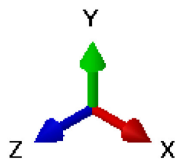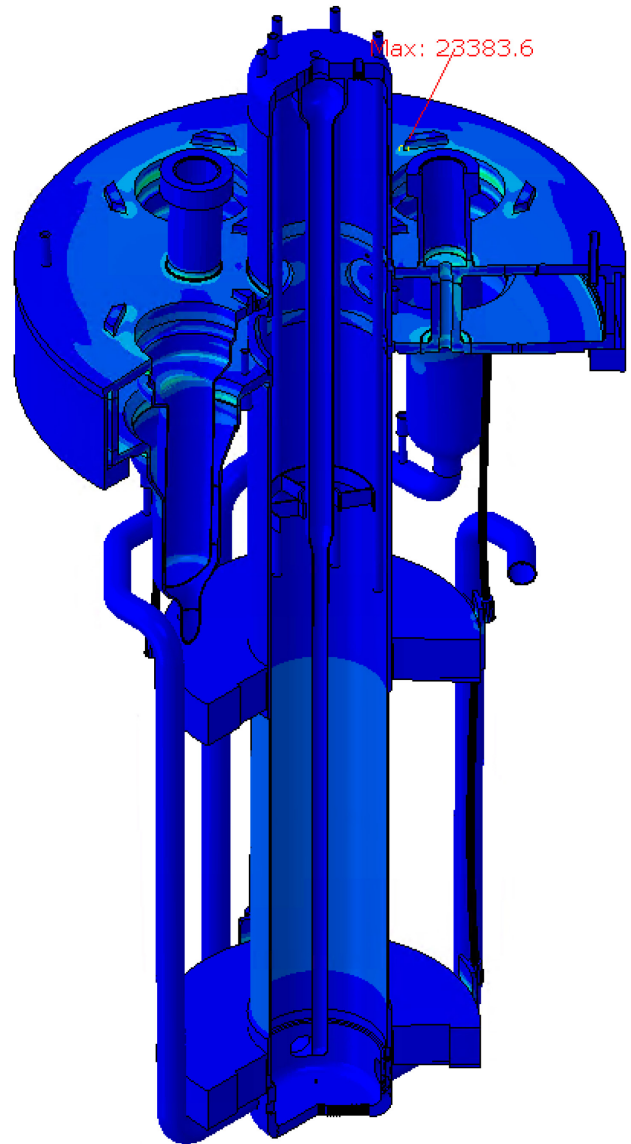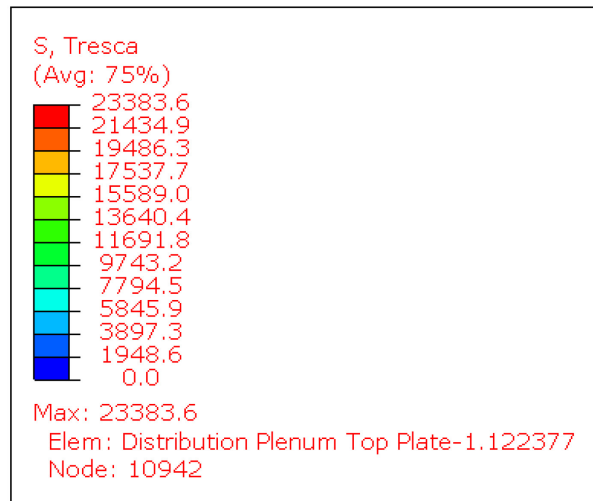 Node: 10942

Max: 23383.6

Figure 19. UTOP Primary Stress Intensity Contour Plot (Max = 23,383.6; 50 Scale Deformation) [psi]

The overall maximum stress intensity is roughly 23.4 ksi. This value does not pass the acceptance criteria from Table 6, so the stress value needs to be classified to verify if it is a membrane or membrane plus bending stress component. Figure 20 shows a zoomed section cut of the stress value, which is on the top plate of the Distribution Plenum.
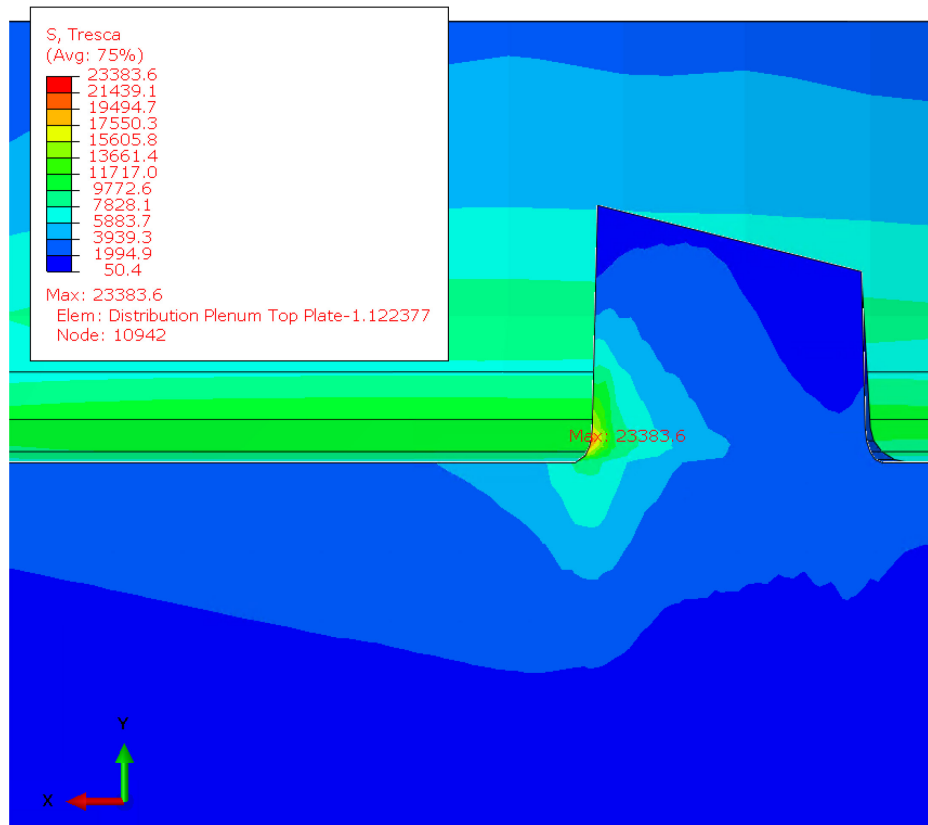
Figure 20. Section View of UTOP Maximum Stress Intensity at Distribution Plenum Top Plate (Max = 23,383.6) [psi]

The section view clearly shows that the maximum stress value is a peak stress component likely caused by a geometric discontinuity on the corner of the SSS mounting feature. The thickness of the section that defines the pressure boundary has considerably lower stress, so this is not the limiting section. The remaining corners have similar peak stresses. Filtering this region out through sectioning, the maximum stress on the Distribution Plenum top plate drops to 17.8 ksi from Figure 21.

TEM-10200-1, Rev. 12 04/12/2021	ENGINEERING CALCULATIONS AND ANALYSIS	ECAR-6564, Rev. 0 Page 35 of 100

MARVEL Project Primary Coolant System ASME BPVC Section III Division 5 Design by Analysis

SS Primary Loads with Max UTOP Temp
ODB: UTOP-Primary.odb   Abaqus/Standard 2021.HF6   Tue Aug 15 16:01:42 Mountain Daylight Time 2023
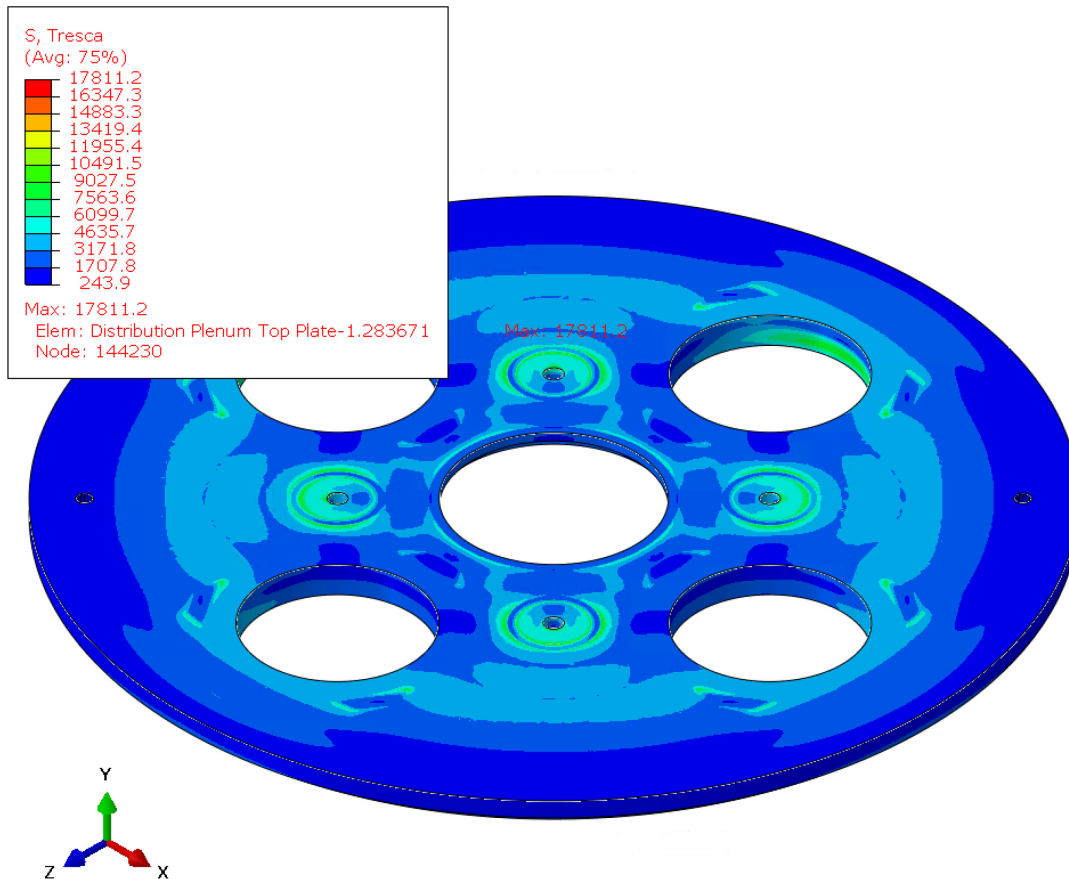

Figure 21. UTOP Distribution Plenum Top Plate Stress Intensity Contour, Sectioned Vertically to Filter Out Peak Stress Identified in Figure 20 (Max = 17,811.2) [psi]

The maximum stress intensity displayed in the model that excludes the top plate (and excludes the Guard Vessel Interface and RSS Dummy since they are not part of the primary boundary) is about 19.6 ksi (see Figure 22).

SS Primary Loads with Max UTOP Temp
ODB: UTOP-Primary.odb   Abaqus/Standard 2021.HF6   Tue Aug 15 16:01:42 Mountain Daylight Time 2023

S, Tresca
(Avg: 75%)
19583.3
17951.4
16319.4
14687.5
13055.5
11423.6
9791.7
8159.7
6527.8
4895.8
3263.9
1632.0
0.0

Max: 19583.3
 Elem: Distribution Plenum Mid-1.122201
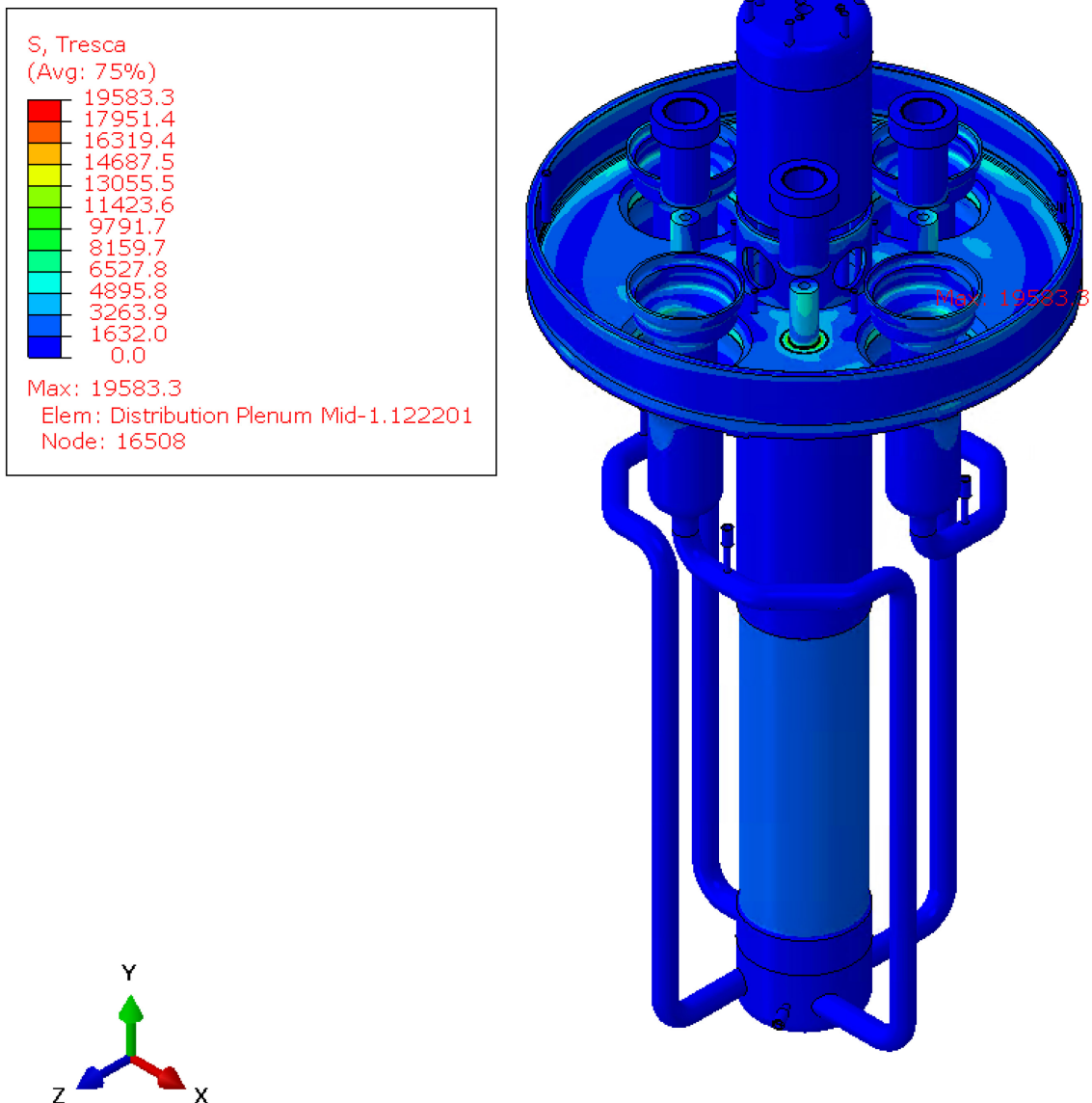 Node: 16508

Figure 22. UTOP Primary Stress Intensity Contour Plot, Distribution Plenum Top Plate Part Instance Excluded (Max = 19,583.3) [psi]

This value passes the criteria for rules (b) and (d), but it fails the use-fraction sum criteria in rules (c) and (e). Closer inspection is required. The stress is located on the bottom inside corner of the Control Drum Shaft Passthrough, see Figure 23.

TEM-10200-1, Rev. 12	**ENGINEERING CALCULATIONS AND ANALYSIS**	ECAR-6564, Rev. 0
04/12/2021		Page 37 of 100

MARVEL Project Primary Coolant System ASME BPVC Section III Division 5 Design by Analysis
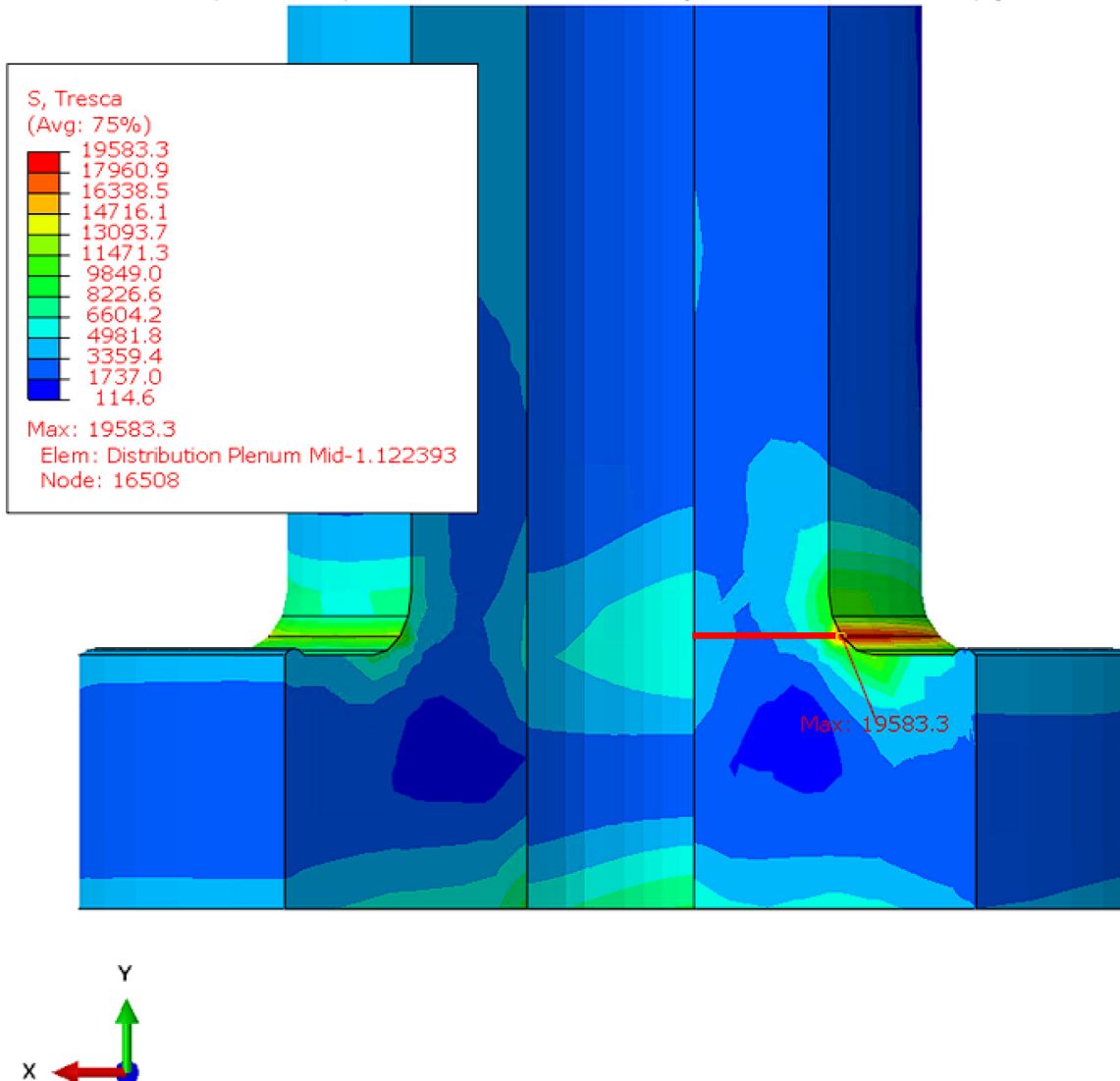
Figure 23. Section View of UTOP Maximum Stress Intensity at Control Drum Shaft Passthrough, Red Line Drawn to Indicate Stress Classification Line for Evaluation (Max = 19,583.3) [psi]

Most of the stress value is again attributed to peak stress, and the plot in Figure 24 indicates that the membrane and bending components are around 5 ksi.

| TEM-10200-1, Rev. 12 | **ENGINEERING CALCULATIONS AND ANALYSIS** | ECAR-6564, Rev. 0 |
| 04/12/2021 | | Page 38 of 100 |

MARVEL Project Primary Coolant System ASME BPVC Section III Division 5 Design by Analysis
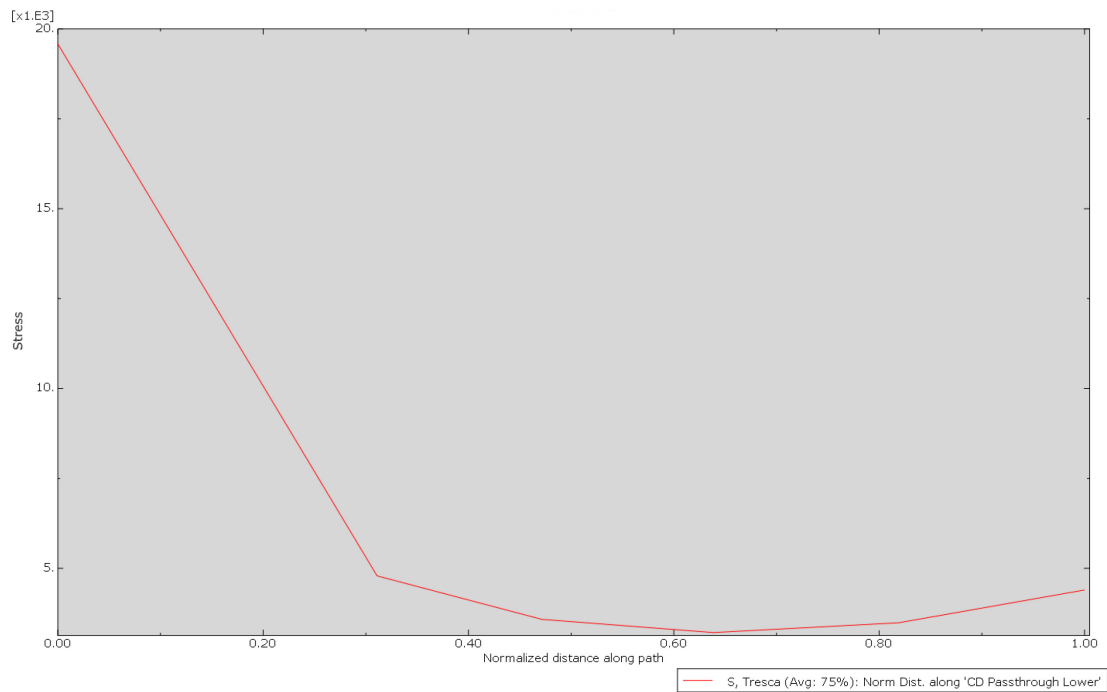
Figure 24. UTOP Stress Classification Line Across the Pressure Boundary Thickness of the Control Drum Shaft Passthrough, Inside Wall to External Wall [inch, psi]

The rest of the Distribution Plenum Mid part instance does not have concerning stress levels, so the part is also filtered out to identify the maximum stress level in the uninvested portion of the model. According to Figure 25, the stress drops to 7.8 ksi.

TEM-10200-1, Rev. 12 04/12/2021	ENGINEERING CALCULATIONS AND ANALYSIS	ECAR-6564, Rev. 0 Page 39 of 100

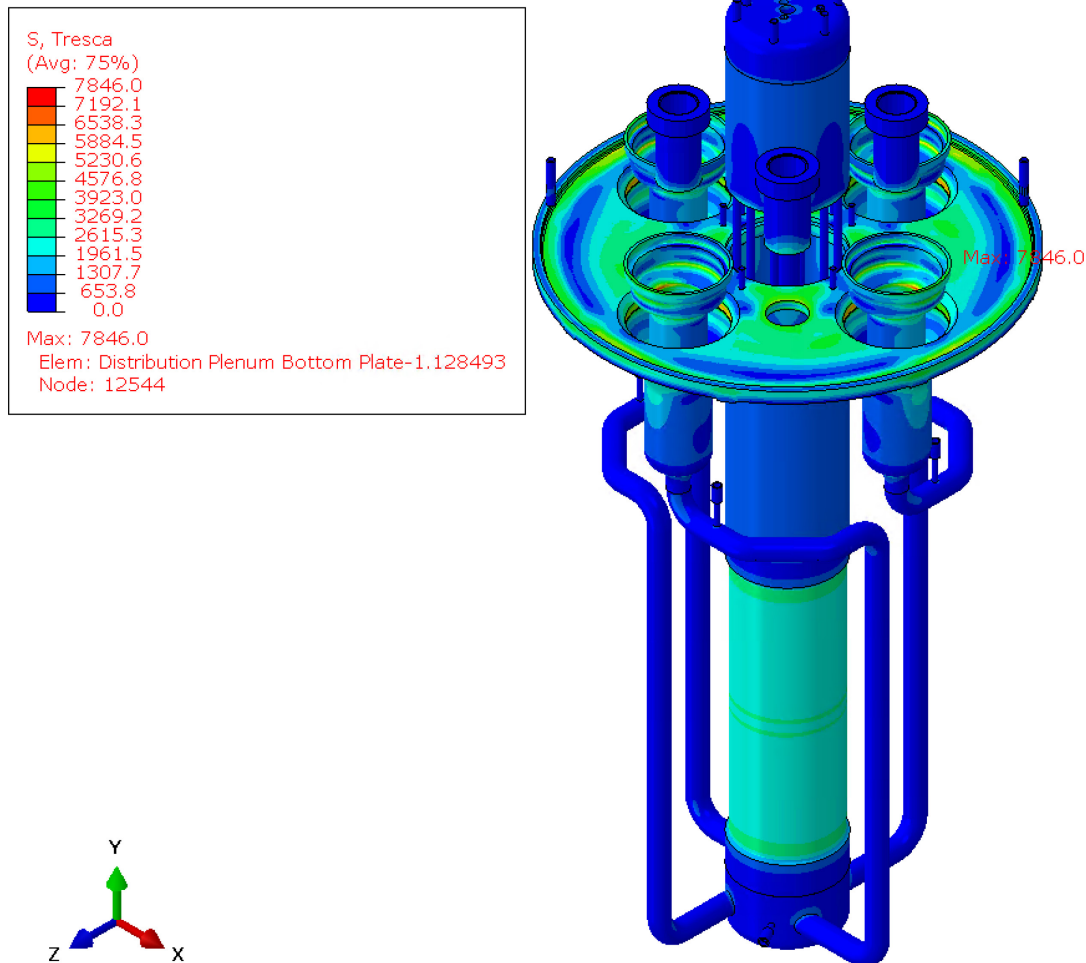MARVEL Project Primary Coolant System ASME BPVC Section III Division 5 Design by Analysis

Figure 25. UTOP Primary Stress Intensity Contour Plot, Distribution Plenum Top Plate and Distribution Plenum Mid Part Instances Excluded (Max = 7,846.0) [psi]

This value is lower than the secondary maximum of 17.8 ksi detected in Figure 21, so 17.8 ksi is evaluated as the next highest stress intensity. When analyzed against the four criteria in [5] HBB-3225, 17.8 ksi passes with margin. See Appendix D for documented calculations.

In summary, 23.4 ksi and 19.6 ksi are identified as the two highest stress values in the model, but neither value met the acceptance criteria and are ruled out based on their peak stress classification. The third highest stress value of 17.8 ksi – without considering its stress classification – passes the criteria. This concludes the process of elimination approach for the UTOP case.

7.10.2 XXVII-3400 Compressive Stress Checks

Compressive stresses are checked for seismic loads at UTOP temperatures (1200°F). Seismic demand is higher than UTOP demand due to the additional primary loads in seismic. Additionally, seismic induces lateral loads on the Reactor Core Barrel that requires local buckling checks due to

flexure. The results of these checks are documented in the seismic results section 7.11.2 and are accredited to the postulated UTOP event.

7.10.3 XXVII-3520 Shear Stress Checks

Maximum shear stress components S_{12}, S_{13}, and S_{23} from output file *UTOP-Primary.odb* pass the calculated maximum allowable shear stress limits. See Appendix D for calculations.

7.11   SERVICE LEVEL D CODE RESULTS – X DIRECTION AND XZ DIRECTION SEISMIC

7.11.1 HBB-3225 Membrane Stress and Membrane Plus Bending Stress Rules

Seismic is evaluated at normal operating temperatures. This provides the design with higher allowable limits for membrane and membrane plus bending stress code checks as indicated in Table 6. As such, the maximum stress intensity values for X and XZ direction seismic models are within limits and pass the four criteria in [5] HBB-3225. See Figure 26 for X direction seismic and Figure 27 for XZ direction seismic stress intensity contour plots.

X-Direction Seismic 0.377g Static Equivalent
ODB: X-Seismic Final.odb   Abaqus/Standard 2021.HF6   Wed Aug 09 23:48:21 Mountain Daylight Time 2023

S, Tresca
(Avg: 75%)
26690.5
24466.3
22242.1
20017.9
17793.7
15569.4
13345.2
11121.0
8896.8
6672.6
4448.4
2224.2
0.0

Max: 26690.5
 Elem: Distribution Plenum Top Plate-1.122377
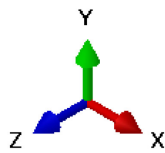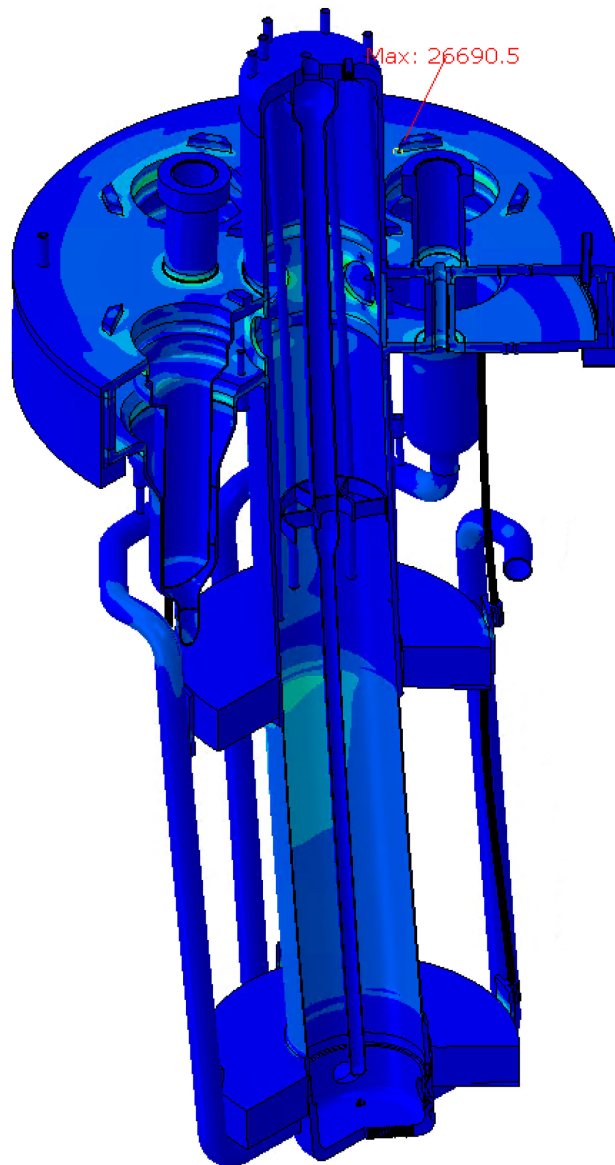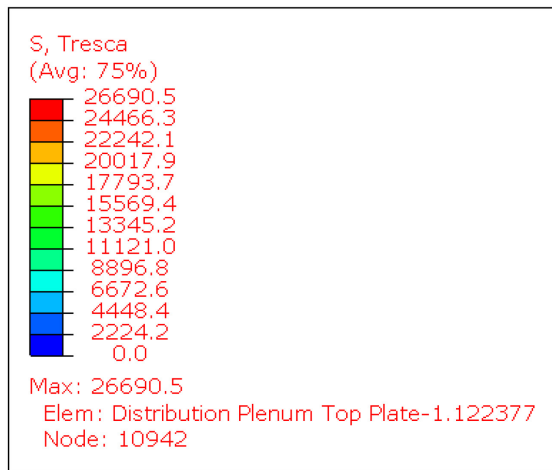 Node: 10942

Max: 26690.5

Figure 26. X Direction Seismic Primary Stress Intensity Contour Plot (Max = 26,690.5; 50 Scale Deformation) [psi]

XZ-Seismic 0.377g
ODB: XZ-Seismic Final.odb   Abaqus/Standard 2021.HF6   Wed Aug 09 17:16:11 Mountain Daylight Time 2023
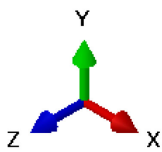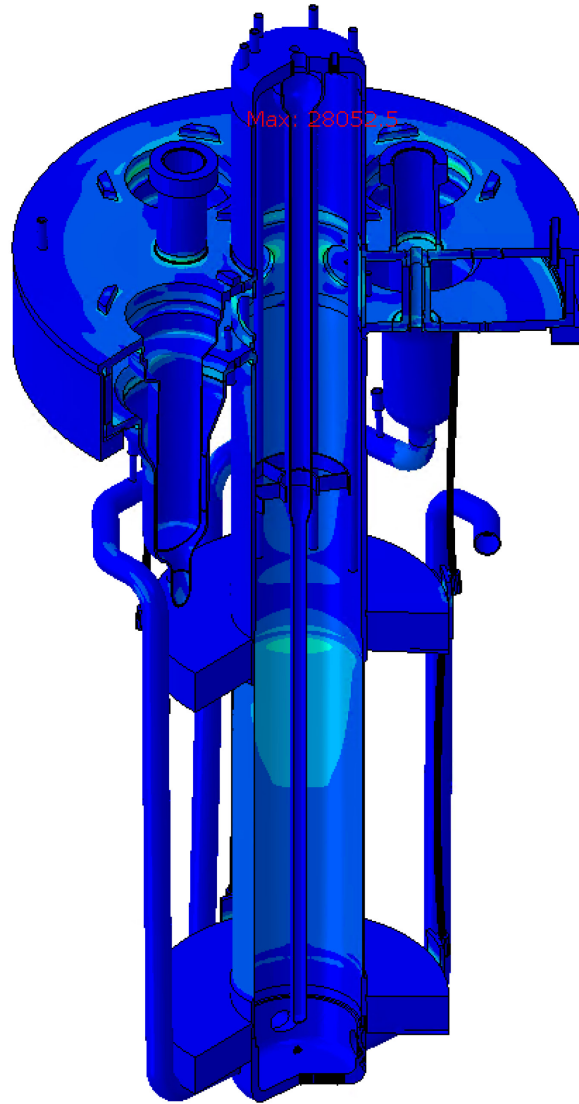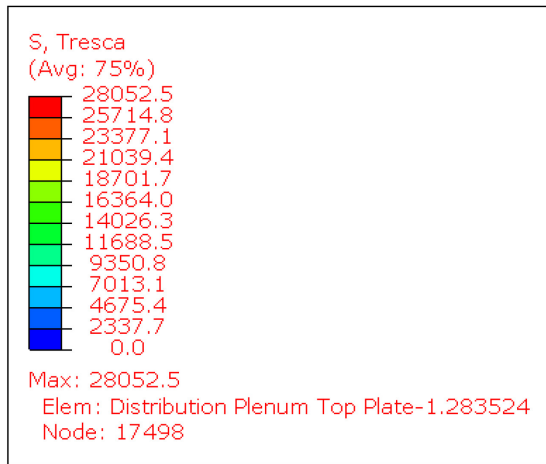

Figure 27. XZ Direction Seismic Primary Stress Intensity Contour Plot (Max = 28,052.5; 50 Scale Deformation) [psi]

Both maximums are peak stresses located in the same feature from the UTOP model that is a result of a geometric discontinuity, so the actual stresses are significantly lower than documented. Still, the 28.1 ksi maximum from both seismic analyses is well within the 35.7 ksi code allowable limit (see Table 6).

7.11.2 XXVII-3400 Compressive Stress Checks

Compressive stress checks are performed in two categories: (1) buckling due to external pressure, and (2) local buckling due to flexure. Compressive forces are minimal due to the design of the vessel where much of the geometry is hanging from the seating surface (or fixturing) and is therefore in tension. The two components that have primary loads supplying compression are the vertical walls of the Distribution

Plenum and the top portion (or top hat) of the Reactor Core Barrel. These sections have relatively small compressive forces that are overcome by the internal pressure pushing outward, so they are not considered.

External pressure is seen on the four Intermediate Heat Exchangers (IHX), the Central Insurance Absorber (CIA) Housing, and the six cartridge heater housings. The most limiting component in the calculation is the CIA, but this is most likely due to the conservative assumption that the thinnest section and the largest diameter exist in the same section across its entire length. Even then, the component passes with a safety factor greater than four. See Appendix D for calculations.

Flexure is considered on the thin section of the Reactor Core Barrel since appreciable lateral loads are applied in the vicinity. The lateral loads are primarily from the Reactor Support Structure (RSS), secondarily from the Reactor Core, and tertiarily from fluid and self-weight seismic forces. Since flexure provisions are not considered in [5], the procedure is followed from ANSI/AISC N690 (which directs the reader to ANSI/AISC 360) for round hollow structural steel (HSS) members. Figure 28 and Figure 29 capture the moments that are applied through the thin section.
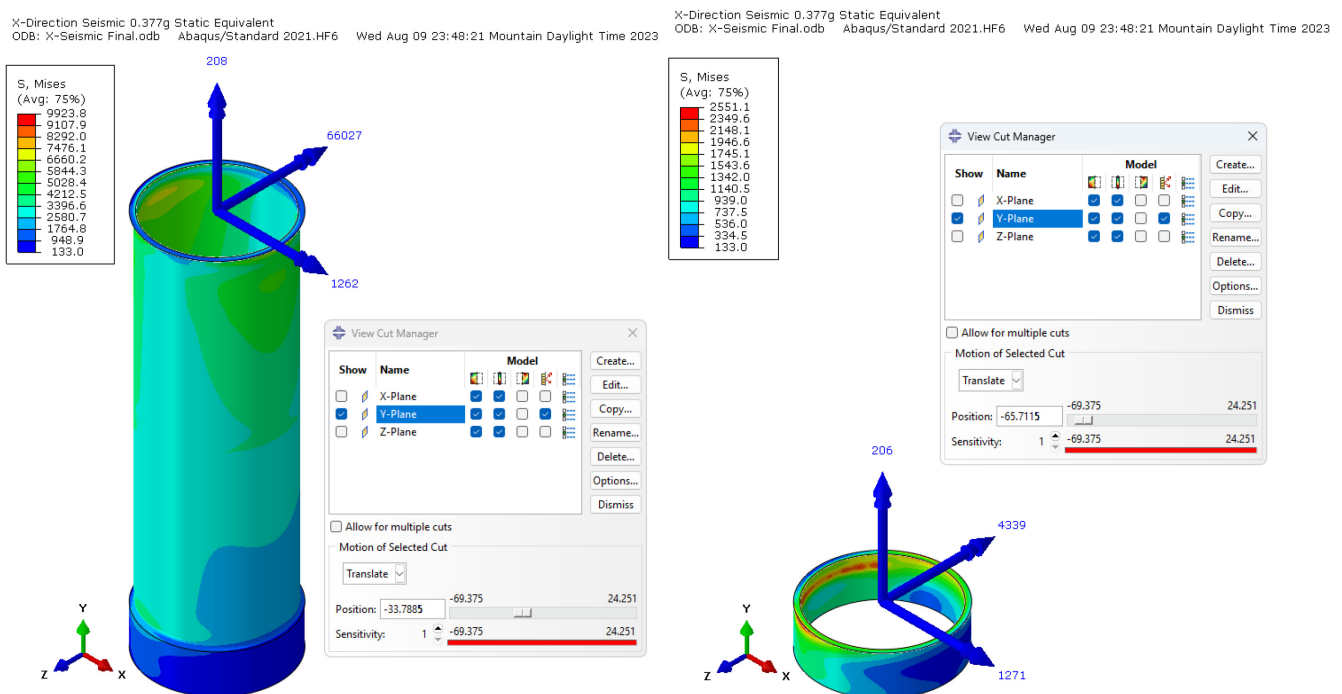

Figure 28. Free Body Cuts at the Top and Bottom of the Thin Section of the Reactor Core Barrel during X Direction Seismic, Moments Only [lbf-in]
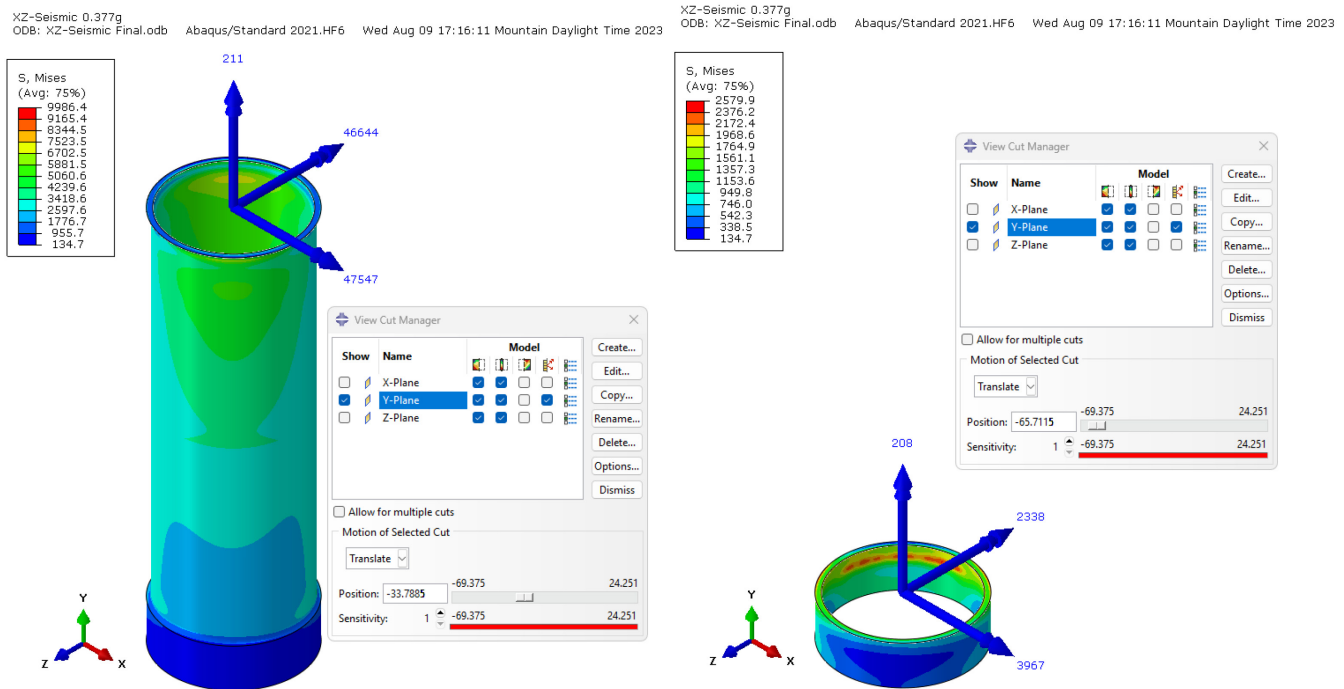
Figure 29. Free Body Cuts at the Top and Bottom of the Thin Section of the Reactor Core Barrel during XZ Direction Seismic, Moments Only [lbf-in]

These moments are compared to calculated allowable limits and pass with 20% margin. See Appendix D for detailed calculations.

7.11.3 XXVII-3520 Shear Stress Checks

Maximum shear stress components S_{12}, S_{13}, and S_{23} from output files *X-Seismic Final.odb* and *XZ-Seismic Final.odb* pass the calculated maximum allowable shear stress limits. See Appendix D for calculations.

7.12 PGS SYSTEM LEAK FAILURE MODES AND EFFECTS ANALYSIS

A PGS system leak that can spill up to approximately 11 gallons of coolant onto the PCS Distribution Plenum top surface is considered via a failure modes and effects analysis (FMEA) in Appendix H. The analysis determines that the PCS pressure boundary is at risk during the worst plausible case and recommends further evaluation to ensure the vessel's integrity is intact.

8 DATA FILES

Table 7 contains names and descriptions of the electronic files associated with this analysis that can be found in the following directories on HPC:

Table 7. ABAQUS File Addresses

/projects/MARVEL/ECAR-6564	
File Name	*Description*

PCS Rev D.cae	ABAQUS cae file
UTOP-Primary.inp X-Seismic Final.inp XZ-Seismic Final.inp	ABAQUS input file
UTOP-Primary.odb X-Seismic Final.odb XZ-Seismic Final.odb	ABAQUS output file

9   REFERENCES

1. Apsher, D., "PGS Stirling Engine Radiation Lifetime Estimate," ECAR-6573, Rev 0, September 2023.
2. ASCE 4-16, "Seismic Analysis of Safety-Related Nuclear Structures," 2016 Ed.
3. ASME Boiler & Pressure Vessel Code Section II Part D, "Materials: Properties (Customary)," 2021 Ed., July 2021.
4. ASME Boiler & Pressure Vessel Code Section III Appendices, "Rules for Construction of Nuclear Facility Components: Appendices," 2021 Ed., July 2021.
5. ASME Boiler & Pressure Vessel Code Section III Division 5, "Rules for Construction of Nuclear Facility Components: High Temperature Reactors," 2021 Ed., July 2021.
6. AWS D1.6, "Structural Welding Code – Stainless Steel," 2007 Ed.
7. Barua, B. and Messner, M, "MARVEL Lower PCS ASME Analysis," ANL-23/56, Rev DRAFT, September 2023.
8. Fish, K., "Chemical Compatibility of MARVEL Components," ECAR-6588, Rev 0, September 2023.
9. Griffin, D.S., 1999. External Pressure: Effect of Initial Imperfections and Temperature Limits-Design Limits for Elevated-Temperature Buckling, in: Welding Research Council, Bulletin 443, New York, pp. 11-26.
10. Hale, C., "ASME Section III, Division 5 Analysis of the MARVEL PCS," ECAR-6580, Rev 0, September 2023.
11. Jesse, C., "Computational Fluid Dynamics Analysis of the Primary Coolant System of MARVEL Microreactor," ECAR-6594, Rev 0, September 2023.
12. Jones, J., "MARVEL Inert Gas System NaK Cover Gas Pressure Calculations and Dissolved Oxygen Control In Lead," ECAR-6586, Rev 0, September 2023.
13. Leal, L., "MARVEL Guard Vessel System FEA and ASME Analysis," ECAR-6574, Rev 0, September 2023.
14. Leal, L., "MARVEL Project Seismic Accelerations," ECAR-6601, Rev 1, September 2023.
15. Parisi, C., "RELAP5-3D Thermal-Hydraulic Analysis of MARVEL Microreactor – Final Design," ECAR-6332, Rev 0, September 2023.
16. Snow, S., "Software Validation Report for Abaqus Standard and Explicit Version 2021.HF6 for Structural Analyses," ECAR-5544, Rev 0, July 2021.
17. SPC-70731, "MARVEL Reactor Project ASME BPVC Section III Division 5 Design Specification," Rev 0, September 2023.
18. Stevenson, J., "Reflector Support Structure Analysis," ECAR-6589, Rev 0, September 2023.

19.   Suyderhoud, P., "MARVEL Reactor Structure (MRS)," TFR-2576, Rev 0, September 2023.

10 APPENDICES

Appendix A -- NPS Pipe Thickness Reductions for ABAQUS Geometry

Appendix B -- ABAQUS Loads Supporting Calculations

Appendix C -- ABAQUS Seismic Supporting Calculations

Appendix D -- ASME BPVC Section III Division 5 Class A Vessel Service Level D Code Calculations for the PCS

Appendix E -- PCS Loading Figures

Appendix F -- Boundary Conditions between Divided PCS Model for Service Level A, B, and C Code Calculations

Appendix G -- Stirling Engine Tube Helium Rupture in Secondary Coolant System Calculation

Appendix H -- PGS Coolant Leak Failure Modes and Effects Analysis

TEM-10200-1, Rev. 12
04/12/2021

ENGINEERING CALCULATIONS AND ANALYSIS

ECAR-6564, Rev. 0
Page 47 of 100

MARVEL Project Primary Coolant System ASME BPVC Section III Division 5 Design by Analysis

Appendix A

NPS Pipe Thickness Reductions for ABAQUS Geometry

08/21/23

PCS NPS Pipe Thickness Reductions
Marvel Project

References
ASTM A312-08a, "Standard Specification for Seamless, Welded, and Heavily Cold Worked Austenitic Stainless Steel Pipes"
ECAR-6588

Reductions due to Manufacturing Tolerances

TABLE 3 Permitted Variations in Wall Thickness

| NPS Designator | Tolerance, % from Nominal | |
	Over	Under
⅛ to 2½ incl., all t/D ratios	20.0	12.5
3 to 18 incl., t/D up to 5 % incl.	22.5	12.5
3 to 18 incl., t/D > 5 %	15.0	12.5
20 and larger, welded, all t/D ratios	17.5	12.5
20 and larger, seamless, t/D up to 5 % incl.	22.5	12.5
20 and larger, seamless, t/D > 5 %	15.0	12.5

where:
t = Nominal Wall Thickness
D = Ordered Outside Diameter

$t_{mintol\_6} := 0.28 \ in \cdot (1 - .125) = 0.245 \ in$ NPS 6 Sch 40 wall thickness at minimum tolerance, reduced from OD for a more limiting section strength

$t_{mintol\_5} := 0.134 \ in \cdot (1 - .125) = 0.117 \ in$ NPS 5 Sch 10 wall thickness at minimum tolerance, reduced from OD for a more limiting section strength

$t_{mintol\_2} := 0.156 \ in \cdot (1 - .125) = 0.137 \ in$ NPS 2 Sch 40 wall thickness at minimum tolerance, reduced from OD for a more limiting section strength

$t_{mintol\_0.5} := 0.109 \ in \cdot (1 - .125) = 0.095 \ in$ NPS 1/2 Sch 40 wall thickness at minimum tolerance, reduced from OD for a more limiting section strength

Reductions due to Corrosion

Corrosion penalties are negligible and are omitted for two reasons: (1) NaK corrosion is <0.001 inches a year for slow-flow systems on 316 SST and provides an indefinite life (see ECAR-6588), and (2) Ga alloy corrosion on the PCS is engineered out of consideration with the design of a sacrificial liner.

TEM-10200-1, Rev. 12
04/12/2021

ENGINEERING CALCULATIONS AND ANALYSIS

ECAR-6564, Rev. 0
Page 49 of 100

MARVEL Project Primary Coolant System ASME BPVC Section III Division 5 Design by Analysis

Appendix B

ABAQUS Loads Supporting Calculations

TEM-10200-1, Rev. 12 04/12/2021	ENGINEERING CALCULATIONS AND ANALYSIS	ECAR-6564, Rev. 0 Page 50 of 100

MARVEL Project Primary Coolant System ASME BPVC Section III Division 5 Design by Analysis

09/13/23

PCS Loads Supporting Calculations
Marvel Project

References

INL Drawings	cont.	INL ECARs	External References
1014743	1014618	ECAR-6576	Materion, BeO Thermalox NRG Material Properties Chart
1014557	1014706	ECAR-6594	American Elements, *americanelements.com*
1014617	1014707	ECAR-6586	Incropera, "Fundamentals of Heat and Mass Transfer," 6th Ed.
1014671	1013335		ASME BPVC Section III Division 5
1014579	1013330		
1014540	1014610		
1014672			
1014673			

Stirling Engine and Secondary Support Structure (SSS) Weight

$W_{SSS} := 391.2 \ lb$ — Total load of stirling engine weight and transmitted load, calculated in ECAR-6576

$A\_W_{SSS} := 500 \ lb$ — Weight of all four SSS with stirling engines in Abaqus, bounding value chosen to uncouple from design iterations

$Margin_{SSS} := \dfrac{A\_W_{SSS}}{W_{SSS}} - 1 = 0.278$ — Margin of Abaqus load above the actual load

Reflector Support Structure (RSS) Weight

$\rho_{BeO} := 2.9 \ \dfrac{gm}{cm^3}$ — BeO Thermalox NRG Material Properties Chart, Materion

$V_{BeO} := 53.751 \ in^3$ — Volume from geometry in INL Drawing 1014557 "Outer Reflector"

$W_{OR} := \rho_{BeO} \cdot V_{BeO} = 5.631 \ lb$ — Outer Reflector weight, applied to each outer reflector plate (unique plates assumed the same)

$W_{OR\_PP} := 27.7 \ lb$ — INL Drawing 1014617, "Reflector Preload Plate Assembly"

$W_{OR\_SP} := 18 \ lb$ — INL Drawing 1014671, "Outer Reflector Support Plate Detail"

$W_{OR\_Stack} := 31 \cdot W_{OR} + W_{OR\_PP} + W_{OR\_SP} = 220.275 \ lb$ — Fixed Outer Reflector stack-up from INL Drawing 1014579

$W_{CD} := 212 \ lb$ — INL Drawing 1014540, "Control Drum Reflector Assembly"

$W_{SP\_L} := 109 \ lb$ — INL Drawing 1014672, "Lower Reflector Plate"

$W_{SP\_U} := 106 \ lb$ — INL Drawing 1014673, "Upper Reflector Support Plate"

$W_{SS} := 16.4 \ lb$ — INL Drawing 1014618, "Reflector Support Strap Assemblies"

09/13/23

$W_{GS} := 31 \; lb$ INL Drawing 1014706, "Axial Gamma Shielding Block"

$W_{NS} := 30 \; lb$ INL Drawing 1014707, "Axial Neutron Shielding Housing Weldment"

$V_{NS} := \pi \cdot \left((12.88 \; in)^2 - (6.10 \; in)^2 \right) \cdot 8.38 \; in = 3387.816 \; in^3$ 4x volume of INL Drawing 1014707, "Axial Neutron Shielding Housing Weldment"

$\rho_{B4C} := 2.7 \; \dfrac{gm}{cm^3}$ Boron carbide (B4C) powder, highest on a range of densities from American Elements, assuming perfect packing factor

$W_{B4C} := V_{NS} \cdot \rho_{B4C} = 330.46 \; lb$ Total weight of B4C powder

$W_{RSS\_upper} := 4 \cdot W_{SP\_U} + 8 \cdot W_{SS} + 4 \cdot W_{GS} + 4 \cdot W_{NS} + W_{B4C} = 1129.66 \; lb$ Total weight supported by the RSS

$A\_W_{RSS\_upper} := 1500 \; lb$ Weight of RSS in Abaqus, bounding value chosen to uncouple from design iterations

$Margin_{RSS\_upper} := \dfrac{A\_W_{RSS\_upper}}{W_{RSS\_upper}} - 1 = 0.328$ Margin of Abaqus load above the actual load

$W_{RSS\_lower} := 4 \cdot W_{OR\_Stack} + 4 \cdot W_{CD} + 4 \cdot W_{SP\_L} = 2165.099 \; lb$ Total weight supported by the RSS

$A\_W_{RSS\_lower} := 2500 \; lb$ Weight of RSS in Abaqus, bounding value chosen to uncouple from design iterations

$Margin_{RSS\_lower} := \dfrac{A\_W_{RSS\_lower}}{W_{RSS\_lower}} - 1 = 0.155$ Margin of Abaqus load above the actual load

Central Insurance Absorber (CIA) Actuator Weight

$W_{CIA} := 80 \; lb$ INL Drawing 1013335, "Actuator Assembly"

$A\_W_{CIA} := 100 \; lb$ Weight of CIA actuator in Abaqus, bounding value chosen to uncouple from design iterations

$Margin_{CIA} := \dfrac{A\_W_{CIA}}{W_{CIA}} - 1 = 0.25$ Margin of Abaqus load above the actual load

Control Drum (CD) Actuator Weight

$W_{CDA} := 75 \; lb$ INL Drawing 1013330, "Actuator Assembly"

$A\_W_{CDA} := 200 \; lb$ 4x weight of CD Actuator in Abaqus, bounding value chosen to uncouple from design iterations

$Margin_{CDA} := \dfrac{A\_W_{CDA}}{W_{CDA}} - 1 = 1.667$ Margin of Abaqus load above the actual load

09/13/23

Reactor Core Weight

$W_{RC} := 700 \; lb$ — INL Drawing 1014579, "Fuel and Core System Assembly"

$A\_W_{RC} := 800 \; lb$ — Weight of reactor core in Abaqus, bounding value chosen to uncouple from design iterations

$Margin_{RC} := \dfrac{A\_W_{RC}}{W_{RC}} - 1 = 0.143$ — Margin of Abaqus load above the actual load

NaK Weight and Hydrostatic Pressure

$Height_{NaK} := 80.625 \; in$ — Height of NaK at operating temperature is 2" from top surface of PCS distribution plenum, see ECAR-6586

$\rho\_NaK := 849 \; \dfrac{kg}{m^3}$ — Density of NaK (22%/78%), Table A.7 in "Fundamentals of Heat and Mass Transfer," 6th Ed. by Incropera

$V_{NaK} := 260 \; L$ — ECAR-6586

$Hydrostat := \rho\_NaK \cdot g \cdot Height_{NaK} = 2.473 \; psi$ — NaK hydrostatic pressure at lowest point in vessel

$A\_Hydrostat := 2.5 \; psi$ — Hydrostatic load in Abaqus, conservatively applied as a constant on all internal surfaces seeing design pressure

Design Pressure

$P_{UTOP} := 46.8 \; psi$ — ECAR-6586, highest pressure the PCS sees in any accident scenario, gauge pressure

$A\_P_D := 55 \; psi$ — Design pressure in Abaqus, bounding value chosen to uncouple from design iterations and to meet overpressure protection requirements in BPVC Section III Division 5 Article HBB-7000, gauge pressure

$Margin_{PD} := \dfrac{A\_P_D}{P_{UTOP}} - 1 = 0.175$ — Margin of Abaqus load above the actual load

MARVEL Project Primary Coolant System ASME BPVC Section III Division 5 Design by Analysis

Appendix C

ABAQUS Seismic Supporting Calculations

TEM-10200-1, Rev. 12 04/12/2021	ENGINEERING CALCULATIONS AND ANALYSIS	ECAR-6564, Rev. 0 Page 54 of 100

MARVEL Project Primary Coolant System ASME BPVC Section III Division 5 Design by Analysis

09/13/23

PCS Seismic Supporting Calculations
Marvel Project

References

INL Drawings	**cont.**	**INL Docs**	**External References**
1014609	1013330	ECAR 6586	ASCE 4-16, "Seismic Analysis of Safety-Related Nuclear Structures"
1014607	1014610	ECAR 6601	Incropera, "Fundamentals of Heat and Mass Transfer," 6th Ed.
1014608	1014614	SPC-70731	
1014736			
1014743			
1014744			
1014740			
1013335			

Inputs for Fluid Seismic Calculations

$H_{NaK\_Plenum} := 4.5\ in$ ECAR 6586

$D_{Plenum} := 46.5\ in$ INL Drawing 1014609 "Distribution Plenum Weldment"

$H_{Plenum} := 6.5\ in$ INL Drawing 1014609 "Distribution Plenum Weldment"

$\rho_{NaK} := 849\ \dfrac{kg}{m^3}$ Density of NaK (22%/78%), Table A.7 in "Fundamentals of Heat and Mass Transfer," 6th Ed. by Incropera

$W_{NaK\_Plenum} := \dfrac{\pi}{4} \cdot D_{Plenum}^2 \cdot H_{NaK\_Plenum} \cdot \rho_{NaK} = 234.397\ lb$ Weight of NaK in PCS Distribution Plenum

$D_{Barrel} := 10.875\ in$ INL Drawing 1014607, "Core Barrel, Lower"

$H_{Barrel} := 5.75\ in + 43.625\ in + 25\ in + 2.5\ in - 0.75\ in = 76.125\ in$ INL Drawings 1014608, "Bottom Head"; 1014607, "Core Barrel, Lower"; 1014609 "Distribution Plenum Weldment"

$W_{NaK\_Barrel} := \dfrac{\pi}{4} \cdot D_{Barrel}^2 \cdot H_{Barrel} \cdot \rho_{NaK} = 216.88\ lb$ Weight of NaK in Core Barrel

$D_{IHX} := 5.295\ in$ INL Drawing 1014736, "Intermediate Heat Exchanger Weldment"

$H_{IHX} := (3 + 15 + 4.75 + 2.75 - 1.125)\ in = 24.375\ in$ INL Drawing 1014736, "Intermediate Heat Exchanger Weldment"

$\rho_{Ga} := 6444\ \dfrac{kg}{m^3}$ Density of EGaInSn (also referred to as Gallium Alloy), room temperature, SPC-70731

$W_{Ga} := 150\ lb$ Conservative weight of EGaInSn for each IHX

$S_{a1} := 0.377\ g \cdot \sqrt{2} = 0.533\ g$ ECAR 6601, horizontal seismic resultant when considering 100-100-100 percent seismic components

$S_{aV} := 0.377\ g$ ECAR 6601, vertical seismic acceleration

Horizontal Impulsive Equations

NaK in Distribution Plenum

$\dfrac{D_{Plenum}}{H_{NaK\_Plenum}} = 10.333$ Since D/H is greater than 4/3, Eq C9-1 and C9-2 apply, pg 143 of ASCE 4-16. Note that since plenum is not full, the height refers to the fill height during operating conditions.

09/13/23

$$W\_imp_{NaK\_Plenum} := \frac{\tanh\left(0.866 \cdot \dfrac{D_{Plenum}}{H_{NaK\_Plenum}}\right)}{0.866 \cdot \dfrac{D_{Plenum}}{H_{NaK\_Plenum}}} \cdot W_{NaK\_Plenum} = 26.193 \ lb \qquad \text{Eq C9-1, pg 143 of ASCE 4-16}$$

$$H\_imp_{NaK\_Plenum} := 0.375 \cdot H_{NaK\_Plenum} = 1.688 \ in \qquad \text{Eq C9-2, pg 143 of ASCE 4-16}$$

$$P\_imp_{Nak\_Plenum} := \frac{W\_imp_{NaK\_Plenum} \cdot H\_imp_{NaK\_Plenum} \cdot S_{a1}}{0.68 \cdot D_{Plenum} \cdot H_{NaK\_Plenum}^2} = 0.037 \ psi \qquad \text{Eq C9-9, pg 144 of ASCE 4-16}$$

NaK in Core Barrel

$$\frac{D_{Barrel}}{H_{Barrel}} = 0.143 \qquad \text{Since D/H is less than 4/3, Eq C9-3 and C9-4 apply, pg 143-144 of ASCE 4-16}$$

$$W\_imp_{NaK\_Barrel} := \left(1 - 0.218 \cdot \frac{D_{Barrel}}{H_{Barrel}}\right) \cdot W_{NaK\_Barrel} = 210.125 \ lb \qquad \text{Eq C9-3, pg 143 of ASCE 4-16}$$

$$H\_imp_{NaK\_Barrel} := \left(0.5 - 0.095 \cdot \frac{D_{Barrel}}{H_{Barrel}}\right) \cdot H_{Barrel} = 37.029 \ in \qquad \text{Eq C9-4, pg 144 of ASCE 4-16}$$

$$P\_imp_{Nak\_Barrel} := \frac{W\_imp_{NaK\_Barrel} \cdot H\_imp_{NaK\_Barrel} \cdot S_{a1}}{0.68 \cdot D_{Barrel} \cdot H_{Barrel}^2} = 0.097 \ psi \qquad \text{Eq C9-9, pg 144 of ASCE 4-16}$$

Gallium alloy in IHX

$$\frac{D_{IHX}}{H_{IHX}} = 0.217 \qquad \text{Since D/H is less than 4/3, Eq C9-3 and C9-4 apply, pg 143-144 of ASCE 4-16}$$

$$W\_imp_{IHX} := \left(1 - 0.218 \cdot \frac{D_{IHX}}{H_{IHX}}\right) \cdot W_{Ga} = 142.897 \ lb \qquad \text{Eq C9-3, pg 143 of ASCE 4-16}$$

$$H\_imp_{IHX} := \left(0.5 - 0.095 \cdot \frac{D_{IHX}}{H_{IHX}}\right) \cdot H_{IHX} = 11.684 \ in \qquad \text{Eq C9-4, pg 144 of ASCE 4-16}$$

$$P\_imp_{IHX} := \frac{W\_imp_{IHX} \cdot H\_imp_{IHX} \cdot S_{a1}}{0.68 \cdot D_{IHX} \cdot H_{IHX}^2} = 0.416 \ psi \qquad \text{Eq C9-9, pg 144 of ASCE 4-16}$$

Horizontal Sloshing Equations

NaK in Distribution Plenum

$$W\_slosh_{NaK\_Plenum} := 0.23 \cdot \frac{D_{Plenum}}{H_{NaK\_Plenum}} \cdot \tanh\left(\frac{3.67}{\dfrac{D_{Plenum}}{H_{NaK\_Plenum}}}\right) \cdot W_{NaK\_Plenum} = 189.934 \ lb \qquad \text{Eq C9-10, pg 144 of ASCE 4-16}$$

09/13/23

$$H\_slosh_{NaK\_Plenum} := \left(1 - \frac{\left(\cosh\left(\frac{3.67}{\frac{D_{Plenum}}{H_{NaK\_Plenum}}}\right) - 1\right)}{\frac{3.67}{\frac{D_{Plenum}}{H_{NaK\_Plenum}}} \cdot \sinh\left(\frac{3.67}{\frac{D_{Plenum}}{H_{NaK\_Plenum}}}\right)}\right) \cdot H_{NaK\_Plenum} = 2.273 \; in$$

Eq C9-11, pg 144 of ASCE 4-16

$$P\_slosh_{NaK\_Plenum} := \frac{0.533 \cdot W_{NaK\_Plenum} \cdot S_{a1}}{D_{Plenum} \cdot H_{NaK\_Plenum}} \cdot \frac{\cosh\left(3.68 \cdot \frac{H_{NaK\_Plenum} - 0}{D_{Plenum}}\right)}{\cosh\left(3.68 \cdot \frac{H_{NaK\_Plenum}}{D_{Plenum}}\right)} = 0.318 \; psi$$

Eq C9-16, pg 145 of ASCE 4-16

NaK in Core Barrel

$$W\_slosh_{NaK\_Barrel} := 0.23 \cdot \frac{D_{Barrel}}{H_{Barrel}} \cdot \tanh\left(\frac{3.67}{\frac{D_{Barrel}}{H_{Barrel}}}\right) \cdot W_{NaK\_Barrel} = 7.126 \; lb$$

Eq C9-10, pg 144 of ASCE 4-16

$$H\_slosh_{NaK\_Barrel} := \left(1 - \frac{\left(\cosh\left(\frac{3.67}{\frac{D_{Barrel}}{H_{Barrel}}}\right) - 1\right)}{\frac{3.67}{\frac{D_{Barrel}}{H_{Barrel}}} \cdot \sinh\left(\frac{3.67}{\frac{D_{Barrel}}{H_{Barrel}}}\right)}\right) \cdot H_{Barrel} = 73.162 \; in$$

Eq C9-11, pg 144 of ASCE 4-16

$$P\_slosh_{NaK\_Barrel} := \frac{0.533 \cdot W_{NaK\_Barrel} \cdot S_{a1}}{D_{Barrel} \cdot H_{Barrel}} \cdot \frac{\cosh\left(3.68 \cdot \frac{H_{Barrel} - 0}{D_{Barrel}}\right)}{\cosh\left(3.68 \cdot \frac{H_{Barrel}}{D_{Barrel}}\right)} = 0.074 \; psi$$

Eq C9-16, pg 145 of ASCE 4-16

Gallium alloy in IHX

$$W\_slosh_{IHX} := 0.23 \cdot \frac{D_{IHX}}{H_{IHX}} \cdot \tanh\left(\frac{3.67}{\frac{D_{IHX}}{H_{IHX}}}\right) \cdot W_{Ga} = 7.494 \; lb$$

Eq C9-10, pg 144 of ASCE 4-16

$$H\_slosh_{IHX} := \left(1 - \frac{\left(\cosh\left(\frac{3.67}{\frac{D_{IHX}}{H_{IHX}}}\right) - 1\right)}{\frac{3.67}{\frac{D_{IHX}}{H_{IHX}}} \cdot \sinh\left(\frac{3.67}{\frac{D_{IHX}}{H_{IHX}}}\right)}\right) \cdot H_{IHX} = 22.932 \; in$$

Eq C9-11, pg 144 of ASCE 4-16

$$P\_slosh_{IHX} := \frac{0.533 \cdot W_{Ga} \cdot S_{a1}}{D_{IHX} \cdot H_{IHX}} \cdot \frac{\cosh\left(3.68 \cdot \frac{H_{IHX} - 0}{D_{IHX}}\right)}{\cosh\left(3.68 \cdot \frac{H_{IHX}}{D_{IHX}}\right)} = 0.33 \; psi$$

Eq C9-16, pg 145 of ASCE 4-16

09/13/23

Vertical Fluid Response Equations

Nak in Distribution Plenum

$$P_{v\_Plenum} := S_{aV} \cdot \rho_{NaK} \cdot H_{NaK\_Plenum} = 0.052 \; psi$$
Eq 9-1, pg 42 of ASCE 4-16

NaK in Core Barrel

$$P_{v\_Barrel} := S_{aV} \cdot \rho_{NaK} \cdot H_{Barrel} = 0.88 \; psi$$
Eq 9-1, pg 42 of ASCE 4-16

Gallium alloy in IHX

$$P_{v\_IHX} := S_{aV} \cdot \rho_{Ga} \cdot H_{IHX} = 2.139 \; psi$$
Eq 9-1, pg 42 of ASCE 4-16

Hydrodynamic Pressure Combinations

$$P_{d\_Plenum} := \sqrt{P\_imp_{Nak\_Plenum}^2 + P\_slosh_{NaK\_Plenum}^2 + P_{v\_Plenum}^2} = 0.325 \; psi$$
Total dynamic pressure in Distribution Plenum, Eq C9-20, pg 145 of ASCE 4-16

$$P_{d\_Barrel} := \sqrt{P\_imp_{Nak\_Barrel}^2 + P\_slosh_{NaK\_Barrel}^2 + P_{v\_Barrel}^2} = 0.889 \; psi$$
Total dynamic pressure in Core Barrel, Eq C9-20, pg 145 of ASCE 4-16

$$P_{d\_IHX} := \sqrt{P\_imp_{IHX}^2 + P\_slosh_{IHX}^2 + P_{v\_IHX}^2} = 2.204 \; psi$$
Total dynamic pressure in IHX, Eq C9-20, pg 145 of ASCE 4-16

Applied Fluid Seismic Loads

Considering the hydrodynamic pressure combinations, a bounding pressure of 1 psi will be used in Abaqus for all internal surfaces of the PCS wetted with NaK. The hydrodynamic pressure in the IHX will be omitted since it subtracts from the larger NaK side pressures, which acts as external pressure on the IHX. This is conservative.

$$A\_P_{d\_NaK} := 1 \; psi$$

$$A\_P_{d\_IHX} := 0 \; psi$$

The overturning moments will consider both impulsive and sloshing horizontal effects. This will be applied to the model using a SRSS combination to the effective weights, following paragraph 9.5.1.(a) of ASCE 4-16. The height component that results in the larger moment will be used for the effective weight SRSS combination.

$$W\_comb_{NaK\_Plenum} := \sqrt{W\_imp_{NaK\_Plenum}^2 + W\_slosh_{NaK\_Plenum}^2} = 191.732 \; lb$$
Effective weight combination for fluid NaK in the Distribution Plenum

$$W_{NaK\_Plenum\_hs} := W\_comb_{NaK\_Plenum} \cdot S_{a1} = 102.224 \; lbf$$ Horizontal seismic force for NaK fluid in Distribution Plenum

$$A\_W_{NaK\_Plenum\_hs} := 105 \; lbf$$
Horizontal seismic force for NaK fluid in Distribution Plenum in Abaqus, rounded up

$$H_{NaK\_Plenum\_hs} := \max\left(H\_imp_{NaK\_Plenum}, H\_slosh_{NaK\_Plenum}\right) = 2.273 \; in$$
Since the Distribution Plenum height is above the fixturing in the model, the larger height will result in a larger moment

TEM-10200-1, Rev. 12
04/12/2021

ENGINEERING CALCULATIONS AND ANALYSIS

ECAR-6564, Rev. 0
Page 58 of 100

MARVEL Project Primary Coolant System ASME BPVC Section III Division 5 Design by Analysis

09/13/23

$A\_H_{NaK\_Plenum\_hs} := 2.5\ in$ Height to apply effective weight in Abaqus, rounded up

$W\_comb_{NaK\_Barrel} := \sqrt{W\_imp_{NaK\_Barrel}{}^2 + W\_slosh_{NaK\_Barrel}{}^2} = 210.246\ lb$ Effective weight combination for fluid NaK in the Core Barrel

$W_{NaK\_Barrel\_hs} := W\_comb_{NaK\_Barrel} \cdot S_{a1} = 112.095\ lbf$ Horizontal seismic force for NaK fluid in Core Barrel

$A\_W_{NaK\_Barrel\_hs} := 115\ lbf$ Horizontal seismic force for NaK fluid in Core Barrel in Abaqus, rounded up

$H_{NaK\_Barrel\_hs} := min\left(H\_imp_{NaK\_Barrel}, H\_slosh_{NaK\_Barrel}\right) = 37.029\ in$ Since the Core Barrel height is below the fixturing in the model, the smaller height will result in a larger moment

$A\_H_{NaK\_Barrel\_hs} := 37\ in$ Height to apply effective weight in Abaqus, rounded down

$W\_comb_{IHX} := \sqrt{W\_imp_{IHX}{}^2 + W\_slosh_{IHX}{}^2} = 143.093\ lb$ Effective weight combination for Gallium alloy in the IHX

$W_{IHX\_hs} := W\_comb_{IHX} \cdot S_{a1} = 76.291\ lbf$ Horizontal seismic force for Gallium alloy in IHX

$A\_W_{IHX\_hs} := 80\ lbf$ Horizontal seismic force for Gallium alloy in IHX in Abaqus, rounded up

$H_{IHX\_hs} := min\left(H\_imp_{IHX}, H\_slosh_{IHX}\right) = 11.684\ in$ Since the IHX height is below the joint that ties it to the PCS in the model, the smaller height will result in a larger moment at the IHX joint

$A\_H_{IHX\_hs} := 11.75\ in$ Height to apply effective weight in Abaqus, rounded down

Applied Equipment Seismic Loads

SSS with Stirling Engine

$A\_W_{SSS} := 500\ lb$ Weight of SSS with stirling engines in Abaqus

$W_{SSS\_hs} := A\_W_{SSS} \cdot S_{a1} = 266.579\ lbf$ Horizontal seismic force of each SSS with stirling engine

$A\_W_{SSS\_hs} := 270\ lbf$ Horizontal seismic force of each SSS with stirling engine in Abaqus, rounded up

$H_{SSS} := (33.10 - 8.45 + 1.5 + 2.4 - 0.75)\ in = 27.8\ in$ INL Drawings 1014743, 1014744, and 1014740 to get overall height of SSS with stirling engine from mounting point

$A\_H_{SSS} := 28\ in$ Height of SSS with stirling engine in Abaqus for horizontal seismic, rounded up

$W_{SSS\_vs} := A\_W_{SSS} \cdot S_{aV} = 188.5\ lbf$ Vertical seismic force of each SSS with stirling engine

$A\_W_{SSS\_vs} := 190\ lbf$ Vertical seismic force of each SSS with stirling engine in Abaqus, rounded up

09/13/23

RSS

The RSS hangs from the Distribution Plenum, which is the only contact concerned with vertical acceleration. However, it also is wrapped around the Core Barrel which will bear the majority of the horizontal seismic acceleration on the RSS. So instead of arithmetically breaking up the RSS loadings between the points of contact, the RSS is modeled as the upper plate and bottom plate with specific densities to capture the entire RSS weight. The two contact points with the Core Barrel are modeled as coincident contacts, and they are not tied to induce the hanging weight and vertical seismic on the Distribution Plenum.

$A\_W_{RSS} := 4000 \; lb$

$A\_W_{RSS\_hs} := A\_W_{RSS} \cdot S_{a1} = 2132.634 \; lbf$ For reference only, horizontal seismic force of RSS with axial shields

$A\_W_{RSS\_vs} := A\_W_{RSS} \cdot S_{aV} = 1508 \; lbf$ For reference only, vertical seismic force of RSS with axial shields

CIA Actuator

$A\_W_{CIA} := 100 \; lb$ Weight of CIA actuator in Abaqus

$W_{CIA\_hs} := A\_W_{CIA} \cdot S_{a1} = 53.316 \; lbf$ Horizontal seismic force of CIA Actuator

$A\_W_{CIA\_hs} := 54 \; lbf$ Horizontal seismic force of CIA Actuator in Abaqus, rounded up

$H_{CIA} := 60.8 \; in$ INL Drawing 1013335, "Actuator Assembly"; overall height

$A\_H_{CIA} := 61 \; in$ CIA Actuator overall height in Abaqus, rounded up

$W_{CIA\_vs} := A\_W_{CIA} \cdot S_{aV} = 37.7 \; lbf$ Vertical seismic force of CIA Actuator

$A\_W_{CIA\_vs} := 38 \; lbf$ Vertical seismic force of CIA Actuator in Abaqus, rounded up

Control Drum (CD) Actuator

$A\_W_{CDA\_tot} := 200 \; lb$ Weight of CD Actuator in Abaqus

$W_{CDA\_hs} := A\_W_{CDA\_tot} \cdot S_{a1} = 106.632 \; lbf$ Horizontal seismic force of CD Actuator

$A\_W_{CDA\_hs} := 107 \; lbf$ Horizontal seismic force of CD Actuator in Abaqus, rounded up

$H_{CDA} := 57.77 \; in$ INL Drawing 1013330, 1014610 overall height of CD Actuator with Standoff

$A\_H_{CDA} := 58 \; in$ CD Actuator overall height in Abaqus, rounded up

$W_{CDA\_vs} := \dfrac{A\_W_{CDA\_tot}}{4} \cdot S_{aV} = 18.85 \; lbf$ Vertical seismic force of CD Actuator

$A\_W_{CDA\_vs} := 76 \; lbf$ Vertical seismic force of CD Actuator in Abaqus, rounded up

MARVEL Project Primary Coolant System ASME BPVC Section III Division 5 Design by Analysis

09/13/23

Reactor Core

$A\_W_{RC} := 800 \ lb$ Weight of reactor core in Abaqus

$W_{RC\_hs} := A\_W_{RC} \cdot S_{a1} = 426.527 \ lbf$ Horizontal seismic force of Reactor Core

$A\_W_{RC\_hs} := 430 \ lbf$ Horizontal seismic force of Reactor Core in Abaqus, rounded up

The horizontal seismic force will be enacted on the bearing surface near the bottom of the Reactor Barrel where the Core is seated to provide the largest moment.

$W_{RC\_vs} := A\_W_{RC} \cdot S_{aV} = 301.6 \ lbf$ Vertical seismic force of Reactor Core

$A\_W_{RC\_vs} := 305 \ lbf$ Vertical seismic force of Reactor Core in Abaqus, rounded up

Upper Confinement

$A\_W_{UC} := 1500 \ lb$ Weight of Upper Confinement in Abaqus

$W_{UC\_hs} := A\_W_{UC} \cdot S_{a1} = 799.738 \ lbf$ Horizontal seismic force of Upper Confinement

$A\_W_{UC\_hs} := 800 \ lbf$ Horizontal seismic force of Upper Confinement in Abaqus, rounded up

$H_{UC} := 81.5 \ in$ INL Drawing 1014614; overall height

$A\_H_{UC} := 81.5 \ in$ Upper Confinement overall height in Abaqus, rounded up

$W_{UC\_vs} := A\_W_{UC} \cdot S_{aV} = 565.5 \ lbf$ Vertical seismic force of Upper Confinement

$A\_W_{UC\_vs} := 570 \ lbf$ Vertical seismic force of Upper Confinement in Abaqus, rounded up

NaK Hydrostatic Pressure

$A\_Hydrostat := 2.5 \ psi$ NaK Hydrostatic load in Abaqus

$Hydrostat_{vs} := P_{v\_Plenum} + P_{v\_Barrel} = 0.932 \ psi$ Vertical seismic NaK hydrostatic pressure at lowest point in vessel

$A\_Hydrostat_{vs} := 1 \ psi$ Vertical seismic NaK hydrostatic pressure in Abaqus, rounded up and uniformly applied for conservatism

Appendix D

ASME BPVC Section III Division 5 Class A Vessel Service Level D Code

Calculations for the PCS

TEM-10200-1, Rev. 12	ENGINEERING CALCULATIONS AND ANALYSIS	ECAR-6564, Rev. 0
04/12/2021		Page 62 of 100

MARVEL Project Primary Coolant System ASME BPVC Section III Division 5 Design by Analysis

09/13/23

PCS Service Level D ASME BPVC Section III Division 5 Code Calculations
Marvel Project

References

INL Drawings	INL ECARs	External References
1014749	ECAR-6580	ASME BPVC Section II Part D, 2021
1014736	ECAR-6332	ASME BPVC Section III Division 1, 2021
		ASME BPVC Section III Division 5, 2021
		ASME BPVC Section III Appendices, 2021

UTOP HBB-3225 Membrane Stress and Membrane Plus Bending Stress Rules

Rule (b): General Primary Membrane Stress Intensity

$S_{UTOP\_peak} := 17820 \; psi$
Limiting stress intensity from model *UTOP Primary Stress*, output file *UTOP-Primary.odb*, rounded up. See body of report for process of elimination approach.

$T_{max\_UTOP} := 645 \; °C = 1193 \; °F$
Maximum temperature during UTOP, taken from ECAR-6332, rounded up.

$S_{u\_UTOP} := \text{linterp}\left(\begin{bmatrix} 1150 \; °F \\ 1200 \; °F \end{bmatrix}, \begin{bmatrix} 54.7 \; ksi \\ 50.6 \; ksi \end{bmatrix}, T_{max\_UTOP}\right) = 51.174 \; ksi$
Tensile strength values, Su, from ASME BPVC Sect III Div 5 Table HBB-3225-1

$S_{r\_UTOP} := \text{linterp}\left(\begin{bmatrix} 1150 \; °F \\ 1200 \; °F \end{bmatrix}, \begin{bmatrix} 34 \; ksi \\ 29 \; ksi \end{bmatrix}, T_{max\_UTOP}\right) = 29.7 \; ksi$
Minimum Stress-to-Rupture Value, Sr, from ASME BPVC Sect III Div 5 Table HBB-I-14.6B for Type 316 SS at t=30 hr

$R_{UTOP} := \text{linterp}\left(\begin{bmatrix} 1150 \; °F \\ 1200 \; °F \end{bmatrix}, \begin{bmatrix} 0.91 \\ 0.89 \end{bmatrix}, T_{max\_UTOP}\right) = 0.893$
Stress Rupture Factor, R, from ASME BPVC Sect III Div 5 Table HBB-I-14.10B-2 for Type 316 SS welded with SFA-5.9 ER 16-8-2 at t=30 hr

$R_{TS\_UTOP} := 0.8$
Tensile strength reduction factor, Table HBB-3225-2, enforced by Rule (f) from ASME BPVC Sect III Div 5 HBB-3225.(f) on tensile strength values used in Section III Appendices, Mandatory Appendix XXVII calculations

$Sb_{limit\_UTOP} := min\left(0.7 \cdot R_{TS\_UTOP} \cdot S_{u\_UTOP}, 0.67 \cdot S_{r\_UTOP}, 0.8 \cdot R_{UTOP} \cdot S_{r\_UTOP}\right) = 19.899 \; ksi$
Minimum allowable limit

$\textbf{rule}_{b\_UTOP}\left(P_m\right) := \text{if}\left(P_m \le Sb_{limit\_UTOP}, \text{"PASS"}, \text{"FAIL"}\right)$
Rule (b) is ASME BPVC Sect III Div 5 HBB-3225.(b) for general primary membrane stress intensity

$\textbf{rule}_{b\_UTOP}\left(S_{UTOP\_peak}\right) = \text{"PASS"}$
General primary membrane stress intensity is a stress classification. Stress classifications are components of stress, so it is conservative to compare the general primary membrane stress intensity allowable to a limiting stress value that includes membrane, bending, and peak stress components.

Rule (c): Use-Fraction Sum Associated with General Primary Membrane Stress

$P_{mi\_UTOP} := S_{UTOP\_peak}$
Setting Pmi equal to S_peak will yield the least maximum allowable time under load, which is conservative

$S\_t_{ir\_UTOP} := max\left(1.5 \cdot P_{mi\_UTOP}, \dfrac{1.25}{R_{UTOP}} \cdot P_{mi\_UTOP}\right) = 26.73 \; ksi$
Stress intensity that correlates to the maximum allowed time under load -- since primary loading does not change from Service Level A and B to UTOP, this value is used for each.

$S_{r\_100hr\_UTOP} := \text{linterp}\left(\begin{bmatrix} 1150 \; °F \\ 1200 \; °F \end{bmatrix}, \begin{bmatrix} 30.5 \; ksi \\ 25.6 \; ksi \end{bmatrix}, T_{max\_UTOP}\right) = 26.286 \; ksi$
Upper bounds for allowed time under load using expected minimum stress-to-rupture values, Table HBB-I-14.6B

09/13/23

$$S_{r\_30hr\_UTOP} := \text{linterp}\left(\begin{bmatrix} 1150\ °F \\ 1200\ °F \end{bmatrix}, \begin{bmatrix} 34\ ksi \\ 29\ ksi \end{bmatrix}, T_{max\_UTOP}\right) = 29.7\ ksi$$

Lower bounds for allowed time under load using expected minimum stress-to-rupture values, Table HBB-I-14.6B

$$t_{ir\_UTOP} := \text{linterp}\left(\begin{bmatrix} S_{r\_100hr\_UTOP} \\ S_{r\_30hr\_UTOP} \end{bmatrix}, \begin{bmatrix} 100\ hr \\ 30\ hr \end{bmatrix}, S\_t_{ir\_UTOP}\right) = 90.896\ hr$$

Interpolated allowed time under load using upper and lower bounds

$$T_{max\_NormOps} := 815\ K = 1007.33\ °F$$ Maximum temperature during Service Level A, taken from ECAR-6332, rounded up.

$$S_{r\_100000hr\_NormOps} := \text{linterp}\left(\begin{bmatrix} 1000\ °F \\ 1050\ °F \end{bmatrix}, \begin{bmatrix} 24.6\ ksi \\ 18.8\ ksi \end{bmatrix}, T_{max\_NormOps}\right) = 23.75\ ksi$$

Upper bounds for allowed time under load using expected minimum stress-to-rupture values, Table HBB-I-14.6B

$$S_{r\_30000hr\_NormOps} := \text{linterp}\left(\begin{bmatrix} 1000\ °F \\ 1050\ °F \end{bmatrix}, \begin{bmatrix} 28.8\ ksi \\ 22.3\ ksi \end{bmatrix}, T_{max\_NormOps}\right) = 27.847\ ksi$$

Lower bounds for allowed time under load using expected minimum stress-to-rupture values, Table HBB-I-14.6B

$$t_{ir\_NormOps} := \text{linterp}\left(\begin{bmatrix} S_{r\_100000hr\_NormOps} \\ S_{r\_30000hr\_NormOps} \end{bmatrix}, \begin{bmatrix} 100000\ hr \\ 30000\ hr \end{bmatrix}, S\_t_{ir\_UTOP}\right) = 49084.635\ hr$$ Interpolated allowed time under load using upper and lower bounds

$$T_{max\_LOHS} := 554\ °C = 1029.2\ °F$$ Maximum temperature during Loss of One Stirling Engine, taken from ECAR-6332, rounded up.

$$S_{r\_30000hr\_LOHS} := \text{linterp}\left(\begin{bmatrix} 1000\ °F \\ 1050\ °F \end{bmatrix}, \begin{bmatrix} 28.8\ ksi \\ 22.3\ ksi \end{bmatrix}, T_{max\_LOHS}\right) = 25.004\ ksi$$

Upper bounds for allowed time under load using expected minimum stress-to-rupture values, Table HBB-I-14.6B

$$S_{r\_10000hr\_LOHS} := \text{linterp}\left(\begin{bmatrix} 1000\ °F \\ 1050\ °F \end{bmatrix}, \begin{bmatrix} 33.6\ ksi \\ 26.4\ ksi \end{bmatrix}, T_{max\_LOHS}\right) = 29.395\ ksi$$

Lower bounds for allowed time under load using expected minimum stress-to-rupture values, Table HBB-I-14.6B

$$t_{ir\_LOHS} := \text{linterp}\left(\begin{bmatrix} S_{r\_30000hr\_LOHS} \\ S_{r\_10000hr\_LOHS} \end{bmatrix}, \begin{bmatrix} 30000\ hr \\ 10000\ hr \end{bmatrix}, S\_t_{ir\_UTOP}\right) = 22138.823\ hr$$ Interpolated allowed time under load using upper and lower bounds

$$t_{UTOP} := 30\ hr$$ Conservative expected time under load for UTOP

$$t_{NormOps} := 3\ yr = 26297.438\ hr$$ Expected time under load for Service Level A per SPC-70731, ASME Design Specification

$$t_{LOHS} := 5 \cdot 24\ hr = 120\ hr$$ Expected time under load for Service Level B per SPC-70731, ASME Design Specification, assuming each event occurs for 24 hr

$$UF_{SUM\_UTOP} := \frac{t_{UTOP}}{t_{ir\_UTOP}} + \frac{t_{NormOps}}{t_{ir\_NormOps}} + \frac{t_{LOHS}}{t_{ir\_LOHS}} = 0.871$$ Use-fraction sum of Service Level A, B, and D (UTOP)

$$\text{rule}_{c\_UTOP} := \text{if}\left(UF_{SUM\_UTOP} \le 1, \text{"PASS"}, \text{"FAIL"}\right)$$ Rule (c) is ASME BPVC Sect III Div 5 HBB-3225.(c) for use-fraction sum associated with general primary membrane stresses that arise from all service loadings

$$\text{rule}_{c\_UTOP} = \text{"PASS"}$$ The rule passes with conservative loading, conservative peak stress values, conservative application of temperature, and conservative time under load

Rule (d): Combined Primary Membrane Plus Bending Stress Intensity

$$Sd_{limit\_UTOP} := \min\left(0.67 \cdot S_{r\_UTOP}, 0.8 \cdot R_{UTOP} \cdot S_{r\_UTOP}\right) = 19.899\ ksi$$ Minimum allowable limit

09/13/23

$$\text{rule}_{d\_UTOP}\left(P_{lm\_b}\right) := \text{if}\left(P_{lm\_b} \le Sd_{limit\_UTOP}, \text{"PASS"}, \text{"FAIL"}\right)$$

Rule (d) is ASME BPVC Sect III Div 5 HBB-3225.(d) for combined primary membrane plus bending stress intensity. Calculation of Kt is omitted since it only reduces the bending component based on section factors.

$$\text{rule}_{d\_UTOP}\left(S_{UTOP\_peak}\right) = \text{"PASS"}$$

Rule (d) is approached the same as Rule (b). By comparing the combined primary plus bending stress intensity allowable to the limiting peak stress value noted above, the calculation is nearly identical to Rule (b) and is conservative.

Rule (e): Use-Fraction Sum Associated with Primary Membrane Plus Bending Stress

$$P_{lm\_b\_UTOP} := S_{UTOP\_peak}$$

Setting primary membrane plus bending (Plm + Pb) equal to S_peak will yield the least maximum allowable time under load, which is conservative

$$\text{rule}_{e\_UTOP} := \text{rule}_{c\_UTOP} = \text{"PASS"}$$

Rule (e) is equivalent to Rule (c) since there is no distinction in the stress component being compared.

X and XZ Seismic HBB-3225 Membrane Stress and Membrane Plus Bending Stress Rules

Rule (b): General Primary Membrane Stress Intensity

$$S_{X\_peak} := 26700 \; psi$$

Limiting stress intensity from model *X Direction Seismic*, output file *X-Seismic Final.odb*, rounded up. See body of report for process of elimination approach.

$$S_{XZ\_peak} := 28100 \; psi$$

Limiting stress intensity from model *XZ Direction Seismic*, output file *XZ-Seismic Final.odb*, rounded up. See body of report for process of elimination approach.

$$S_{max} := \max\left(S_{X\_peak}, S_{XZ\_peak}\right) = 28100 \; psi$$

Maximum value between X direction seismic and XZ direction seismic models used for calculation

$$T_{max\_Seismic} := T_{max\_NormOps} = 1007.33 \; °F$$

Maximum temperature during Service Level A, taken from ECAR-6332 since seismic is postulated during normal operations.

$$S_u := \text{linterp}\left(\begin{bmatrix} 1000 \; °F \\ 1050 \; °F \end{bmatrix}, \begin{bmatrix} 64.3 \; ksi \\ 61.5 \; ksi \end{bmatrix}, T_{max\_Seismic}\right) = 63.89 \; ksi$$

Tensile strength values, Su, from ASME BPVC Sect II Part D Table U and ASME BPVC Sect III Div 5 Table HBB-3225-1

$$S_r := \text{linterp}\left(\begin{bmatrix} 1000 \; °F \\ 1050 \; °F \end{bmatrix}, \begin{bmatrix} 55 \; ksi \\ 47.5 \; ksi \end{bmatrix}, T_{max\_Seismic}\right) = 53.901 \; ksi$$

Minimum Stress-to-Rupture Value, Sr, from ASME BPVC Sect III Div 5 Table HBB-I-14.6B for Type 316 SS at t=30 hr

$$R := \text{linterp}\left(\begin{bmatrix} 1000 \; °F \\ 1050 \; °F \end{bmatrix}, \begin{bmatrix} 0.93 \\ 0.92 \end{bmatrix}, T_{max\_Seismic}\right) = 0.929$$

Stress Rupture Factor, R, from ASME BPVC Sect III Div 5 Table HBB-I-14.10B-2 for Type 316 SS welded with SFA-5.9 ER 16-8-2 at t=30 hr

$$R_{TS} := 0.8$$

Tensile strength reduction factor, enforced by Rule (f) from ASME BPVC Sect III Div 5 HBB-3225.(f) on tensile strength values used in Section III Appendices, Mandatory Appendix XXVII calculations

$$Sb_{limit} := \min\left(0.7 \cdot R_{TS} \cdot S_u, 0.67 \cdot S_r, 0.8 \cdot R \cdot S_r\right) = 35.778 \; ksi$$

Minimum allowable limit

$$\text{rule}_b\left(P_m\right) := \text{if}\left(P_m \le Sb_{limit}, \text{"PASS"}, \text{"FAIL"}\right)$$

Rule (b) is ASME BPVC Sect III Div 5 HBB-3225.(b) for general primary membrane stress intensity

$$\text{rule}_b\left(S_{max}\right) = \text{"PASS"}$$

General primary membrane stress intensity is a stress classification. Stress classifications are components of stress, so it is conservative to compare the general primary membrane stress intensity allowable to a limiting stress value that includes membrane, bending, and peak stress components.

TEM-10200-1, Rev. 12 04/12/2021	**ENGINEERING CALCULATIONS AND ANALYSIS**	ECAR-6564, Rev. 0 Page 65 of 100

MARVEL Project Primary Coolant System ASME BPVC Section III Division 5 Design by Analysis

09/13/23

Rule (c): Use-Fraction Sum Associated with General Primary Membrane Stress

$P_{mi} := S_{max}$

Setting Pmi equal to Smax will yield the least maximum allowable time under load, which is conservative

$S\_t_{ir\_seismic} := \max\left(1.5 \cdot P_{mi}, \frac{1.25}{R} \cdot P_{mi}\right) = 42.15 \ ksi$

Stress intensity that correlates to the maximum allowed time under load

$S_{r\_1000hr\_seismic} := \mathrm{linterp}\left(\begin{bmatrix} 1000 \ °F \\ 1050 \ °F \end{bmatrix}, \begin{bmatrix} 42.1 \ ksi \\ 34.4 \ ksi \end{bmatrix}, T_{max\_Seismic}\right) = 40.971 \ ksi$

Upper bounds for allowed time under load using expected minimum stress-to-rupture values, Table HBB-I-14.6B

$S_{r\_300hr\_seismic} := \mathrm{linterp}\left(\begin{bmatrix} 1000 \ °F \\ 1050 \ °F \end{bmatrix}, \begin{bmatrix} 47 \ ksi \\ 38.2 \ ksi \end{bmatrix}, T_{max\_Seismic}\right) = 45.71 \ ksi$

Lower bounds for allowed time under load using expected minimum stress-to-rupture values, Table HBB-I-14.6B

$t_{ir\_seismic} := \mathrm{linterp}\left(\begin{bmatrix} S_{r\_1000hr\_seismic} \\ S_{r\_300hr\_seismic} \end{bmatrix}, \begin{bmatrix} 1000 \ hr \\ 300 \ hr \end{bmatrix}, S\_t_{ir\_seismic}\right) = 825.866 \ hr$

Interpolated allowed time under load using upper and lower bounds

$t_{seismic} := 30 \ hr$ Conservative expected time under load for Seismic

$UF_{SUM\_seismic} := \frac{t_{seismic}}{t_{ir\_seismic}} + \frac{t_{NormOps}}{t_{ir\_NormOps}} + \frac{t_{LOHS}}{t_{ir\_LOHS}} = 0.578$ Use-fraction sum of Service Level A, B, and D (Seismic)

$\mathrm{rule}_c := \mathrm{if}\left(UF_{SUM\_seismic} \le 1, \text{"PASS"}, \text{"FAIL"}\right)$

Rule (c) is ASME BPVC Sect III Div 5 HBB-3225.(c) for use-fraction sum associated with general primary membrane stresses that arise from all service loadings

$\mathrm{rule}_c = \text{"PASS"}$

The rule passes with conservative loading, conservative peak stress values, conservative application of temperature, and conservative time under load

Rule (d): Combined Primary Membrane Plus Bending Stress Intensity

$Sd_{limit} := \min\left(0.67 \cdot S_r, 0.8 \cdot R \cdot S_r\right) = 36.113 \ ksi$ Minimum allowable limit

$\mathrm{rule}_d\left(P_{lm\_b}\right) := \mathrm{if}\left(P_{lm\_b} \le Sd_{limit}, \text{"PASS"}, \text{"FAIL"}\right)$

Rule (d) is ASME BPVC Sect III Div 5 HBB-3225.(d) for combined primary membrane plus bending stress intensity. Calculation of Kt is omitted since it only reduces the bending component based on section factors.

$\mathrm{rule}_d\left(S_{max}\right) = \text{"PASS"}$

Rule (d) is approached the same as Rule (b). By comparing the combined primary plus bending stress intensity allowable to the limiting peak stress value noted above, the calculation is nearly identical to Rule (b) and is conservative.

Rule (e): Use-Fraction Sum Associated with Primary Membrane Plus Bending Stress

$P_{lm\_b} := S_{max}$

Setting primary membrane plus bending (Plm + Pb) equal to S_peak will yield the least maximum allowable time under load, which is conservative

$\mathrm{rule}_e := \mathrm{rule}_c = \text{"PASS"}$

Rule (e) is equivalent to Rule (c) since there is no distinction in the stress component being compared.

09/13/23

XXVII-3400 Compressive Stresses

Compressive stresses are analyzed against seismic primary loads. Since seismic loading is more limiting than UTOP loading, passing results for seismic also conclude that UTOP passes.

ASME BPVC Section III Appendices, Mandatory Appendix XXVII-3400.(b) states that the maximum compressive load shall be limited to a value equal to 150% of the limit established by the referencing design rules for compression, except that the value is permitted to be 250% of the given value when the ovality is limited to 1% or less. For this analysis, the referencing design rules for compression are NB-3133 for time-independent buckling and the external pressure calculations in ECAR-6580 that consider time-dependent buckling with creep effects.

ASME BPVC Sect III Div 1 NB-3133 will be used to analyze three components under external pressure: (1) the CIA housing, (2) the IHX, and (3) the cartridge heater housings.

CIA Housing External Pressure

$D_{CIA} := 2.375 \; in$ Limiting outer diameter of CIA housing, INL Drawing 1014749

$th_{CIA} := 0.060 \; in$ Limiting thickness of CIA housing, INL Drawing 1014749 (not the same region as the limiting diameter for conservatism)

$L_{CIA} := 92.19 \; in$ Length of CIA housing, INL Drawing 1014749

$$\frac{L_{CIA}}{D_{CIA}} = 38.817 \qquad \frac{D_{CIA}}{th_{CIA}} = 39.583$$

$$A_{CIA} := \mathrm{linterp}\left(\begin{bmatrix} 30 \\ 40 \end{bmatrix}, \begin{bmatrix} 0.122 \cdot 10^{-2} \\ 0.688 \cdot 10^{-3} \end{bmatrix}, \frac{D_{CIA}}{th_{CIA}}\right) = 0.0007$$ ASME BPVC Sect II Part D Subpart 3 Table G, L/D = 40

$B_{CIA} := 5250 \; psi$ Approximated from ASME BPVC Sect II Part D Subpart 3 Figure HA-2 for Type 316 SST at 1200 F

$$P_{a\_CIA} := \frac{4 \cdot B_{CIA}}{3 \cdot \left(\frac{D_{CIA}}{th_{CIA}}\right)} = 176.842 \; psi$$ Maximum allowable external pressure in calculated from ASME BPVC Sect III Div 1 NB-3133.3.(a) Step 6

$P\_creep_{a\_CIA} := 479 \; psi$ Maximum allowable external pressure calculated in ECAR-6580 for time-dependent buckling analysis that includes the effects of creep

$P_{PCS} := (55 + 2.5 + 1 + 1) \; psi = 59.5 \; psi$ Pressure in PCS that acts externally to the CIA housing. Combines design pressure, NaK hydrostatic pressure, seismic NaK fluid dynamic pressure, and seismic NaK hydrostatic pressure. Ignores pressure in CIA housing.

$$Pmin_{a\_CIA} := \min\left(1.5 \cdot P_{a\_CIA}, 1.5 \cdot P\_creep_{a\_CIA}\right) = 265.263 \; psi$$

$$CIA_{DC} := \frac{P_{PCS}}{Pmin_{a\_CIA}} = 0.224$$ External buckling Demand-to-Capacity ratio

$Comp\_check_{CIA} := \mathrm{if}\left(P_{PCS} \le Pmin_{a\_CIA}, \text{"PASS"}, \text{"FAIL"}\right) = \text{"PASS"}$ CIA will not buckle under external pressure during Service Level D loadings

IHX External Pressure

$D_{IHX} := 5.563 \; in$ Outer diameter of IHX pipe, INL Drawing 1014736

$$th_{IHX} := \frac{5.563 - 5.295}{2} \; in$$ Limiting thickness of IHX pipe, INL Drawing 1014736

$L_{IHX} := (15 + 3.5 + 0.5) \; in$ Length of IHX pipe, INL Drawing 1014736

TEM-10200-1, Rev. 12 04/12/2021	ENGINEERING CALCULATIONS AND ANALYSIS	ECAR-6564, Rev. 0 Page 67 of 100

MARVEL Project Primary Coolant System ASME BPVC Section III Division 5 Design by Analysis

09/13/23

$$\frac{L_{IHX}}{D_{IHX}} = 3.415 \qquad \frac{D_{IHX}}{th_{IHX}} = 41.515$$

$$A_{IHX} := \text{linterp}\left(\begin{bmatrix} 2 \\ 4 \end{bmatrix}, \begin{bmatrix} 0.252 \cdot 10^{-2} \\ 0.117 \cdot 10^{-2} \end{bmatrix}, \frac{L_{IHX}}{D_{IHX}}\right) = 0.0016 \qquad$$ ASME BPVC Sect II Part D Subpart 3 Table G, D/t = 40

$$B_{IHX} := 6750 \; psi \qquad$$ Approximated from ASME BPVC Sect II Part D Subpart 3 Figure HA-2 for Type 316 SST at 1200 F

$$P_{a\_IHX} := \frac{4 \cdot B_{IHX}}{3 \cdot \left(\frac{D_{IHX}}{th_{IHX}}\right)} = 216.79 \; psi \qquad$$ Maximum allowable external pressure in calculated from ASME BPVC Sect III Div 1 NB-3133.3.(a) Step 6

$$P\_creep_{a\_IHX} := 214.5 \; psi \qquad$$ Maximum allowable external pressure calculated in ECAR-6580 for time-dependent buckling analysis that includes the effects of creep

$$P_{PCS} = 59.5 \; psi \qquad$$ Pressure in PCS that acts externally to the IHX. Combines design pressure, NaK hydrostatic pressure, seismic NaK fluid dynamic pressure, and seismic NaK hydrostatic pressure. Ignores pressure in IHX.

$$Pmin_{a\_IHX} := \min\left(1.5 \cdot P_{a\_IHX}, 1.5 \cdot P\_creep_{a\_IHX}\right) = 321.75 \; psi$$

$$IHX_{DC} := \frac{P_{PCS}}{Pmin_{a\_IHX}} = 0.185 \qquad$$ External buckling Demand-to-Capacity ratio

$$Comp\_check_{IHX} := \text{if}\left(P_{PCS} \leq Pmin_{a\_IHX}, \text{"PASS"}, \text{"FAIL"}\right) = \text{"PASS"} \qquad$$ IHX will not buckle under external pressure during Service Level D loadings

Heater Housing External Pressure

$$D_{HH} := 0.84 \; in \qquad$$ Outer diameter of Heater Housing pipe, INL Drawing 1014750

$$th_{HH} := \frac{0.84 - 0.622}{2} \; in \qquad$$ Thickness of Heater Housing pipe, INL Drawing 1014750

$$L_{HH} := 52.07 \; in \qquad$$ Length of Heater Housing pipe, INL Drawing 1014750

$$\frac{L_{HH}}{D_{HH}} = 61.988 \qquad \frac{D_{HH}}{th_{HH}} = 7.706$$

$$A_{HH} := 0.0174 \qquad$$ ASME BPVC Sect II Part D Subpart 3 Table G, D/t = 8, L/D = 50 (highest listed)

$$B_{HH} := 10000 \; psi \qquad$$ Approximated from ASME BPVC Sect II Part D Subpart 3 Figure HA-2 for Type 316 SST at 1200 F

$$P_{a\_HH} := \frac{4 \cdot B_{HH}}{3 \cdot \left(\frac{D_{HH}}{th_{HH}}\right)} = 1730.159 \; psi \qquad$$ Maximum allowable external pressure in calculated from ASME BPVC Sect III Div 1 NB-3133.3.(a) Step 6

$$P\_creep_{a\_HH} := 2120.25 \; psi \qquad$$ Maximum allowable external pressure calculated in ECAR-6580 for time-dependent buckling analysis that includes the effects of creep

TEM-10200-1, Rev. 12 04/12/2021	ENGINEERING CALCULATIONS AND ANALYSIS	ECAR-6564, Rev. 0 Page 68 of 100

MARVEL Project Primary Coolant System ASME BPVC Section III Division 5 Design by Analysis

09/13/23

$P_{PCS} = 59.5 \ psi$ Pressure in PCS that acts externally to the Heater Housing . Combines design pressure, NaK hydrostatic pressure, seismic NaK fluid dynamic pressure, and seismic NaK hydrostatic pressure. Ignores pressure in Heater Housing .

$Pmin_{a\_HH} := min \left(1.5 \cdot P_{a\_HH} , 1.5 \cdot P\_creep_{a\_HH} \right) = 2595.238 \ psi$

$HH_{DC} := \dfrac{P_{PCS}}{Pmin_{a\_HH}} = 0.023$ External buckling Demand-to-Capacity ratio
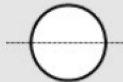
$Comp\_check_{HH} := if \left(P_{PCS} \le Pmin_{a\_HH} , \text{"PASS"} , \text{"FAIL"} \right) = \text{"PASS"}$ The Heater Housing will not buckle under external pressure during Service Level D loadings

Flexure Check for Thin Section of Reactor Core Barrel

The thin section of the Reactor Core Barrel has lateral loading in the seismic event. To consider limit states due to flexure, AISC N690 -- which directs to AISC 360 -- will be used. Section F8 applies to Round HSS, which is an equivalent shape to the Reactor Core Barrel and will be used for the flexure check.

TABLE USER NOTE F1.1
Selection Table for the Application
of Chapter F Sections

Section in Chapter F	Cross Section	Flange Slenderness	Web Slenderness	Limit States
F8	⊖	N/A	N/A	Y, LB

AISC 360 Table F1.1 states that, for a circular cross section, the limit states are yielding and local buckling. Local buckling will be considered.

TEM-10200-1, Rev. 12	ENGINEERING CALCULATIONS AND ANALYSIS	ECAR-6564, Rev. 0
04/12/2021		Page 69 of 100

MARVEL Project Primary Coolant System ASME BPVC Section III Division 5 Design by Analysis

09/13/23

F8. ROUND HSS

This section applies to round HSS having D/t ratios of less than $\frac{0.45E}{F_y}$.

The nominal flexural strength, M_n, shall be the lower value obtained according to the limit states of yielding (plastic moment) and local buckling.

1. Yielding

$$M_n = M_p = F_y Z \tag{F8-1}$$

2. Local Buckling

(a) For compact sections, the limit state of flange local buckling does not apply.

(b) For noncompact sections

$$M_n = \left[\frac{0.021E}{\left(\frac{D}{t}\right)} + F_y \right] S \tag{F8-2}$$

(c) For sections with slender walls

$$M_n = F_{cr} S \tag{F8-3}$$

where
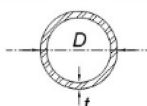
D = outside diameter of round HSS, in. (mm)

$$F_{cr} = \frac{0.33E}{\left(\frac{D}{t}\right)} \tag{F8-4}$$

t = design wall thickness of HSS member, in. (mm)

First, Width-to-Thickness ratios are determined for the Reactor Core Barrel using the round HSS element in Table B4.1b

TABLE B4.1b (continued)
Width-to-Thickness Ratios: Compression Elements
Members Subject to Flexure

Case	Description of Element	Width-to-Thickness Ratio	Limiting Width-to-Thickness Ratio		Examples
			λ_p (compact/ noncompact)	λ_r (noncompact/ slender)	
20	Round HSS	D/t	$0.07\dfrac{E}{F_y}$	$0.31\dfrac{E}{F_y}$	

$OD_{RCB\_thin\_MMC} := 11.125\ in + 0.020\ in$ OD of Reactor Core Barrel at thin section at MMC tolerance

$OD_{RCB\_thin\_LMC} := 11.125\ in - 0\ in$ OD of Reactor Core Barrel at thin section at LMC tolerance

$ID_{RCB\_thin\_MMC} := 10.875\ in - 0\ in$ ID of Reactor Core Barrel at thin section at MMC tolerance

$ID_{RCB\_thin\_LMC} := 10.875\ in + 0.010\ in$ ID of Reactor Core Barrel at thin section at LMC tolerance

$t_{RCB\_thin\_MMC} := \dfrac{OD_{RCB\_thin\_MMC} - ID_{RCB\_thin\_MMC}}{2} = 0.135\ in$ Thickness of Reactor Core Barrel at thin section at MMC tolerance

09/13/23

$$t_{RCB\_thin\_LMC} := \frac{OD_{RCB\_thin\_LMC} - ID_{RCB\_thin\_LMC}}{2} = 0.12 \ in$$

Thickness of Reactor Core Barrel at thin section at LMC tolerance

$$r_{wt} := \frac{OD_{RCB\_thin\_MMC}}{t_{RCB\_thin\_LMC}} = 92.875$$

Limiting Width-to-Thickness Ratio

$$E_{316H\_70F} := 28300000 \ psi$$

Elastic Modulus of 316H SST at 70 F, Table TM-1, Group G, ASME BPVC Section II Part D

$$E_{316H\_1100F} := 22000000 \ psi$$

Elastic Modulus of 316H SST at 1100 F, Table TM-1, Group G, ASME BPVC Section II Part D

$$Fy_{316H\_70F} := 30000 \ psi$$

Yield Strength of SA-240 316H SST at 70 F, Table Y-1, ASME BPVC Section II Part D

$$Fy_{316H\_1100F} := 16600 \ psi$$

Yield Strength of SA-240 316H SST at 1100 F, Table HBB-I-14.5, ASME BPVC Section III Division 5

$$\lambda_{p\_70F} := 0.07 \cdot \frac{E_{316H\_70F}}{Fy_{316H\_70F}} = 66.033$$

Limiting Width-to-Thickness Ratio for compact/noncompact at 70 F

$$\lambda_{r\_70F} := 0.31 \cdot \frac{E_{316H\_70F}}{Fy_{316H\_70F}} = 292.433$$

Limiting Width-to-Thickness Ratio for noncompact/slender at 70 F

$$F8_{70F} := 0.45 \cdot \frac{E_{316H\_70F}}{Fy_{316H\_70F}} = 424.5$$

Threshold for applying Section F8 to a round HSS section at 70 F

$$\lambda_{p\_1100F} := 0.07 \cdot \frac{E_{316H\_1100F}}{Fy_{316H\_1100F}} = 92.771$$

Limiting Width-to-Thickness Ratio for compact/noncompact at 1100 F

$$\lambda_{r\_1100F} := 0.31 \cdot \frac{E_{316H\_1100F}}{Fy_{316H\_1100F}} = 410.843$$

Limiting Width-to-Thickness Ratio for noncompact/slender at 1100 F

$$F8_{1100F} := 0.45 \cdot \frac{E_{316H\_1100F}}{Fy_{316H\_1100F}} = 596.386$$

Threshold for applying Section F8 to a round HSS section at 70 F

$$\text{if} \left(r_{wt} < \lambda_{p\_70F} , \text{"Compact"} , \text{"Noncompact"} \right) = \text{"Noncompact"}$$

$$\text{if} \left(r_{wt} > \lambda_{r\_70F} , \text{"Slender"} , \text{"Noncompact"} \right) = \text{"Noncompact"}$$

$$\text{if} \left(r_{wt} < F8_{70F} , \text{"Section F8 Applies"} , \text{"Section F8 Does Not Apply"} \right) = \text{"Section F8 Applies"}$$

$$\text{if} \left(r_{wt} < \lambda_{p\_1100F} , \text{"Compact"} , \text{"Noncompact"} \right) = \text{"Noncompact"}$$

$$\text{if} \left(r_{wt} > \lambda_{r\_1100F} , \text{"Slender"} , \text{"Noncompact"} \right) = \text{"Noncompact"}$$

$$\text{if} \left(r_{wt} < F8_{1100F} , \text{"Section F8 Applies"} , \text{"Section F8 Does Not Apply"} \right) = \text{"Section F8 Applies"}$$

Based on the above check, Section F8 applies to the thin section of the Reactor Core Barrel and is a noncompact element. Local Buckling shall be evaluated in accordance with equation F8-2.

TEM-10200-1, Rev. 12 04/12/2021	**ENGINEERING CALCULATIONS AND ANALYSIS**	ECAR-6564, Rev. 0 Page 71 of 100

MARVEL Project Primary Coolant System ASME BPVC Section III Division 5 Design by Analysis

09/13/23

$$S_{RCB\_thin} := \frac{\pi}{32} \cdot \frac{\left(OD_{RCB\_thin\_LMC}^4 - ID_{RCB\_thin\_LMC}^4\right)}{OD_{RCB\_thin\_LMC}} = 11.293 \ in^3$$

Most limiting (smallest) elastic section modulus for a hollow circle, derived from I/c

$$M_{n\_70F} := \left(\frac{0.021 \cdot E_{316H\_70F}}{\left(\frac{OD_{RCB\_thin\_MMC}}{t_{RCB\_thin\_LMC}} \right)} + Fy_{316H\_70F} \right) \cdot S_{RCB\_thin} = 34.253 \ kip \cdot ft$$

70 F, equation F8-2.

$$M_{n\_1100F} := \left(\frac{0.021 \cdot E_{316H\_1100F}}{\left(\frac{OD_{RCB\_thin\_MMC}}{t_{RCB\_thin\_LMC}} \right)} + Fy_{316H\_1100F} \right) \cdot S_{RCB\_thin} = 20.303 \ kip \cdot ft$$

1100 F, equation F8-2.

$$M_n := min\left(M_{n\_70F}, M_{n\_1100F}\right) = 20.303 \ kip \cdot ft$$

Minimum allowable flexure strength

$$\Omega_b := 1.67$$

$$M_c := \frac{M_n}{\Omega_b} = 12.157 \ kip \cdot ft$$

Allowable flexural strength, including the safety factor for Allowable Strength Design
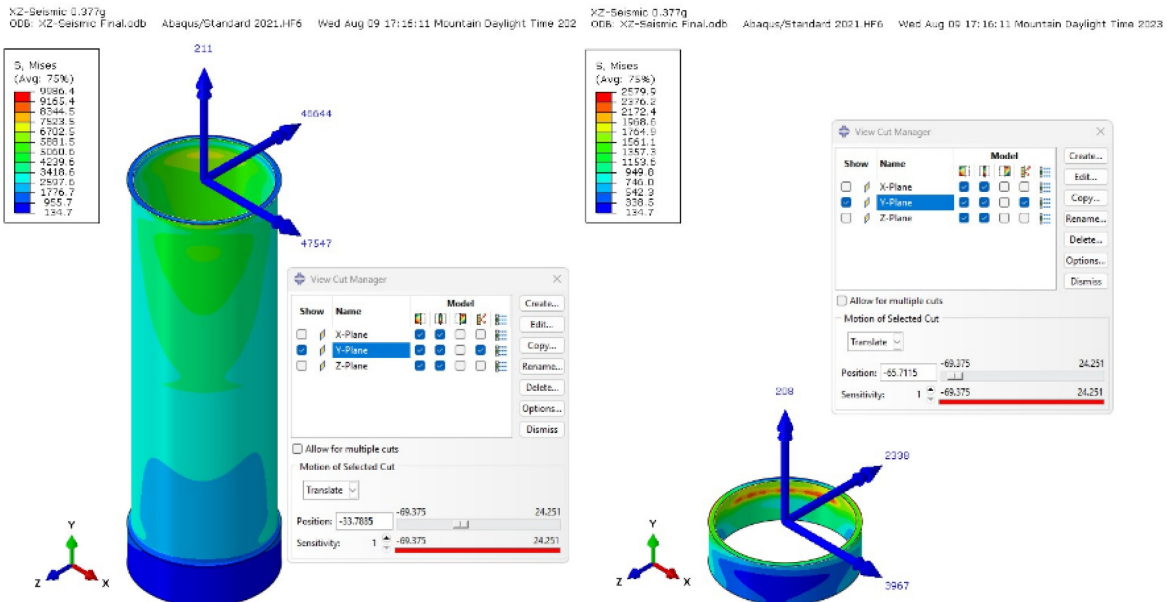
$$Mt_{XZ\_x} := 47600 \ lbf \cdot in = 3.967 \ kip \cdot ft$$

Top end x-component moment magnitude in ABAQUS at y=-33.7885 inches, *XZ Direction Seismic, XZ-Seismic Final.odb*, rounded up

$$Mt_{XZ\_z} := 46700 \ lbf \cdot in = 3.892 \ kip \cdot ft$$

Top end z-component moment magnitude in ABAQUS at y=-33.7885 inches, *XZ Direction Seismic, XZ-Seismic Final.odb*, rounded up

$$Mb_{XZ\_x} := 4000 \ lbf \cdot in = 0.333 \ kip \cdot ft$$

Bottom end x-component moment magnitude in ABAQUS at y=-65.7115 inches, *XZ Direction Seismic, XZ-Seismic Final.odb*, rounded up
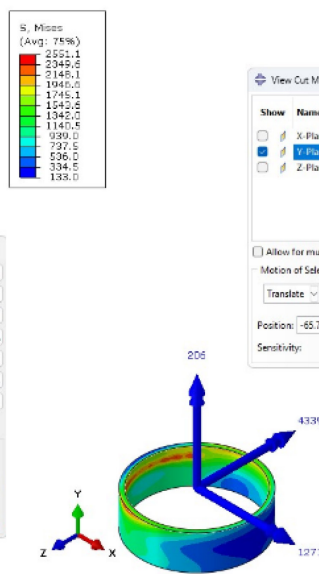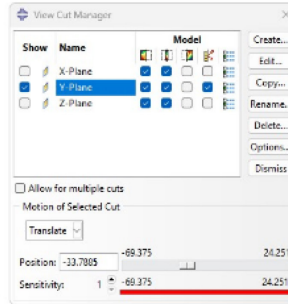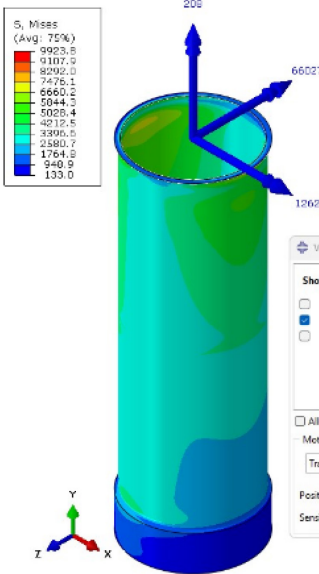
$$Mb_{XZ\_z} := 2400 \ lbf \cdot in = 0.2 \ kip \cdot ft$$

Bottom end z-component moment magnitude in ABAQUS at y=-65.7115 inches, *XZ Direction Seismic, XZ-Seismic Final.odb*, rounded up

TEM-10200-1, Rev. 12 04/12/2021	**ENGINEERING CALCULATIONS AND ANALYSIS**	ECAR-6564, Rev. 0 Page 72 of 100

MARVEL Project Primary Coolant System ASME BPVC Section III Division 5 Design by Analysis

09/13/23

$$M_{XZ\_x} := \max\left(Mt_{XZ\_x}, Mb_{XZ\_x}\right) = 3.967 \; kip \cdot ft \qquad \text{Largest x-component moment magnitude, XZ seismic}$$

$$M_{XZ\_z} := \max\left(Mt_{XZ\_z}, Mb_{XZ\_z}\right) = 3.892 \; kip \cdot ft \qquad \text{Largest z-component moment magnitude, XZ seismic}$$
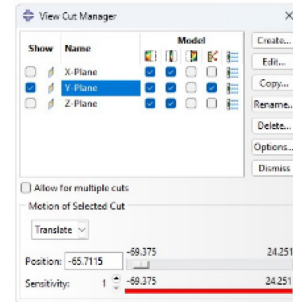
$$Mt_{X\_x} := 1300 \; lbf \cdot in = 0.108 \; kip \cdot ft \qquad \text{Top end x-component moment magnitude in ABAQUS at y=-33.7885 inches, } X \text{ Direction Seismic, X-Seismic Final.odb, rounded up}$$

$$Mt_{X\_z} := 66050 \; lbf \cdot in = 5.504 \; kip \cdot ft \qquad \text{Top end z-component moment magnitude in ABAQUS at y=-33.7885 inches, } X \text{ Direction Seismic, X-Seismic Final.odb, rounded up}$$

$$Mb_{X\_x} := 1300 \; lbf \cdot in = 0.108 \; kip \cdot ft \qquad \text{Bottom end x-component moment magnitude in ABAQUS at y=-65.7115 inches, } X \text{ Direction Seismic, X-Seismic Final.odb, rounded up}$$

$$Mb_{X\_z} := 4350 \; lbf \cdot in = 0.363 \; kip \cdot ft \qquad \text{Bottom end z-component moment magnitude in ABAQUS at y=-65.7115 inches, } X \text{ Direction Seismic, X-Seismic Final.odb, rounded up}$$

$$M_{X\_x} := \max\left(Mt_{X\_x}, Mb_{X\_x}\right) = 0.108 \; kip \cdot ft \qquad \text{Largest x-component moment magnitude, X seismic}$$

$$M_{X\_z} := \max\left(Mt_{X\_z}, Mb_{X\_z}\right) = 5.504 \; kip \cdot ft \qquad \text{Largest z-component moment magnitude, X seismic}$$

$$M_x := \max\left(M_{XZ\_x}, M_{X\_x}\right) = 3.967 \; kip \cdot ft \qquad \text{Largest x-component moment magnitude between X and XZ seismic models}$$

$$M_z := \max\left(M_{XZ\_z}, M_{X\_z}\right) = 5.504 \; kip \cdot ft \qquad \text{Largest z-component moment magnitude between X and XZ seismic models}$$

$$Flex_{DC} := \frac{M_x}{M_c} + \frac{M_z}{M_c} = 0.779 \qquad \text{Combined forces equation H1-1b, neglecting axial force since section is in tension}$$

$$Flex\_check_{RCB} := \text{if}\left(Flex_{DC} \le 1, \text{"PASS", "FAIL"}\right) = \text{"PASS"} \qquad \text{The thin section of the Reactor Core Barrel passes local buckling flexure checks in accordance with Allowable Strength Design in AISC 360 during conservative static equivalent x-direction and xz-direction seismic forces.}$$

11 of 12

09/13/23

XXVII-3520 Shear Stress

UTOP

$\tau_{UTOP\_12} := 11050 \; psi$ Maximum component shear stress from model *UTOP Primary Stress*, output file *UTOP-Primary.odb*, rounded up

$\tau_{UTOP\_13} := 4000 \; psi$ Maximum component shear stress from model *UTOP Primary Stress*, output file *UTOP-Primary.odb*, rounded up

$\tau_{UTOP\_23} := |-11050| \; psi$ Maximum component shear stress from model *UTOP Primary Stress*, output file *UTOP-Primary.odb*, rounded up

$\tau_{max\_UTOP} := \max\left(\tau_{UTOP\_12}, \tau_{UTOP\_13}, \tau_{UTOP\_23}\right) = 11050 \; psi$ Maximum shear stress component

$\tau_{a\_UTOP} := 0.42 \cdot R_{TS} \cdot S_{u\_UTOP} = 17194.464 \; psi$ ASME BPVC Section III Appendices, Mandatory Appendix XXVII-3520.(a) and (b) maximum allowable shear stress

$\tau_{DC\_UTOP} := \dfrac{\tau_{max\_UTOP}}{\tau_{a\_UTOP}} = 0.643$ Demand to capacity ratio

$Shear\_check\_UTOP := \text{if}\left(\tau_{max\_UTOP} < \tau_{a\_UTOP}, \text{"PASS"}, \text{"FAIL"}\right) = \text{"PASS"}$ Shear stress limits are not exceeded for Service Level D when conservatively considering maximum shear stress of all shear components
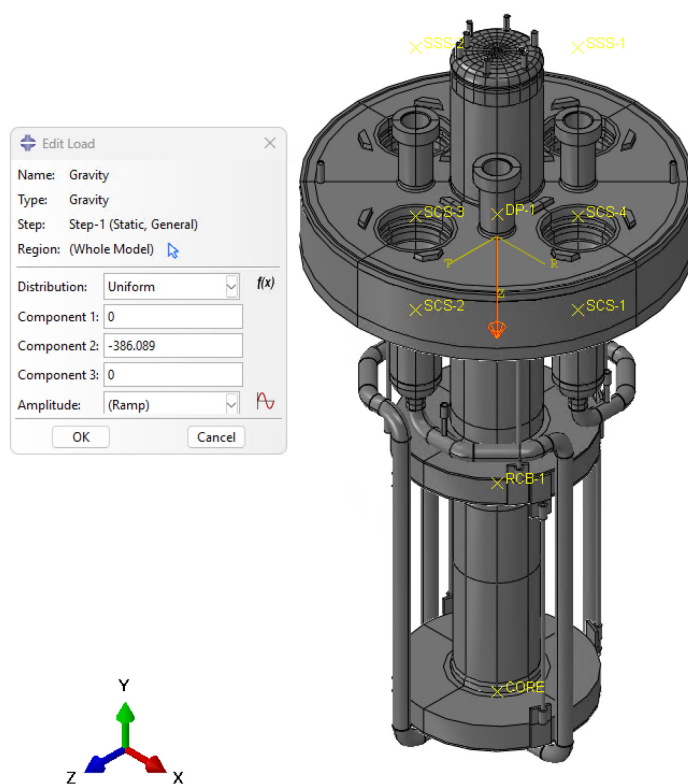
Seismic

$\tau_{X\_12} := |-12000| \; psi$ Maximum component shear stress from model *X Direction Seismic*, output file *X-Seismic Final.odb*, rounded up

$\tau_{X\_13} := 4850 \; psi$ Maximum component shear stress from model *X Direction Seismic*, output file *X-Seismic Final.odb*, rounded up

$\tau_{X\_23} := |-12550 \; psi|$ Maximum component shear stress from model *X Direction Seismic*, output file *X-Seismic Final.odb*, rounded up

$\tau_{XZ\_12} := |-12800| \; psi$ Maximum component shear stress from model *XZ Direction Seismic*, output file *XZ-Seismic Final.odb*, rounded up

$\tau_{XZ\_13} := 5200 \; psi$ Maximum component shear stress from model *XZ Direction Seismic*, output file *XZ-Seismic Final.odb*, rounded up

$\tau_{XZ\_23} := |-12900 \; psi|$ Maximum component shear stress from model *XZ Direction Seismic*, output file *XZ-Seismic Final.odb*, rounded up

$\tau_{max\_seismic} := \max\left(\tau_{X\_12}, \tau_{X\_13}, \tau_{X\_23}, \tau_{XZ\_12}, \tau_{XZ\_13}, \tau_{XZ\_23}\right) = 12900 \; psi$ Maximum shear stress component from both X direction seismic and XZ direction seismic models

$\tau_{a\_seismic} := 0.42 \cdot R_{TS} \cdot S_u = 21466.879 \; psi$ ASME BPVC Section III Appendices, Mandatory Appendix XXVII-3520.(a) and (b) maximum allowable shear stress

$\tau_{DC\_seismic} := \dfrac{\tau_{max\_seismic}}{\tau_{a\_seismic}} = 0.601$ Demand to capacity ratio

$Shear\_check\_seismic := \text{if}\left(\tau_{max\_seismic} < \tau_{a\_seismic}, \text{"PASS"}, \text{"FAIL"}\right) = \text{"PASS"}$ Shear stress limits are not exceeded for Service Level D when conservatively considering maximum shear stress of all shear components

TEM-10200-1, Rev. 12
04/12/2021

ENGINEERING CALCULATIONS AND ANALYSIS

ECAR-6564, Rev. 0
Page 74 of 100

MARVEL Project Primary Coolant System ASME BPVC Section III Division 5 Design by Analysis

Appendix E

PCS Loading Figures

TEM-10200-1, Rev. 12	ENGINEERING CALCULATIONS AND ANALYSIS	ECAR-6564, Rev. 0
04/12/2021		Page 75 of 100

MARVEL Project Primary Coolant System ASME BPVC Section III Division 5 Design by Analysis

Figure 30. Gravity Load
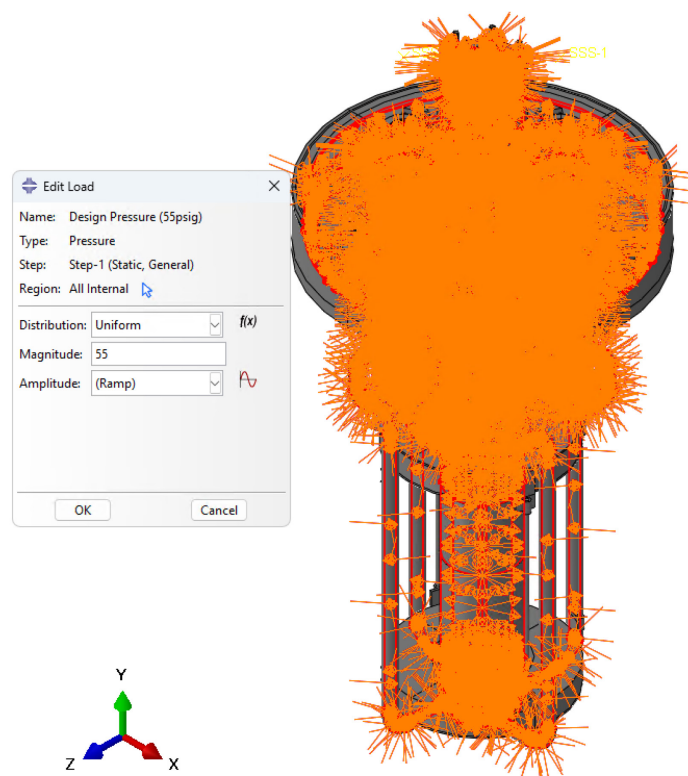
Figure 31. Design Pressure

| TEM-10200-1, Rev. 12 | **ENGINEERING CALCULATIONS AND ANALYSIS** | ECAR-6564, Rev. 0 |
| 04/12/2021 | | Page 76 of 100 |

MARVEL Project Primary Coolant System ASME BPVC Section III Division 5 Design by Analysis
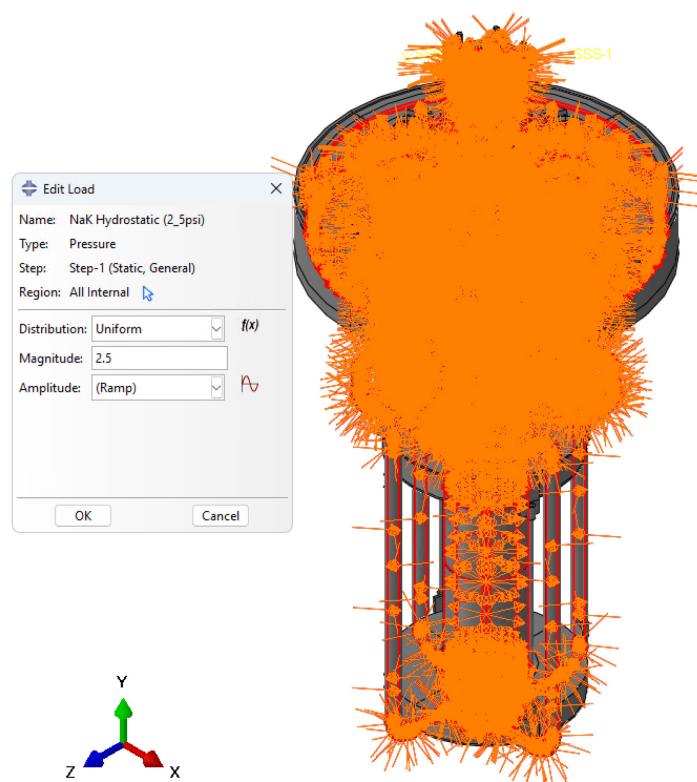
Figure 32. NaK Hydrostatic Pressure
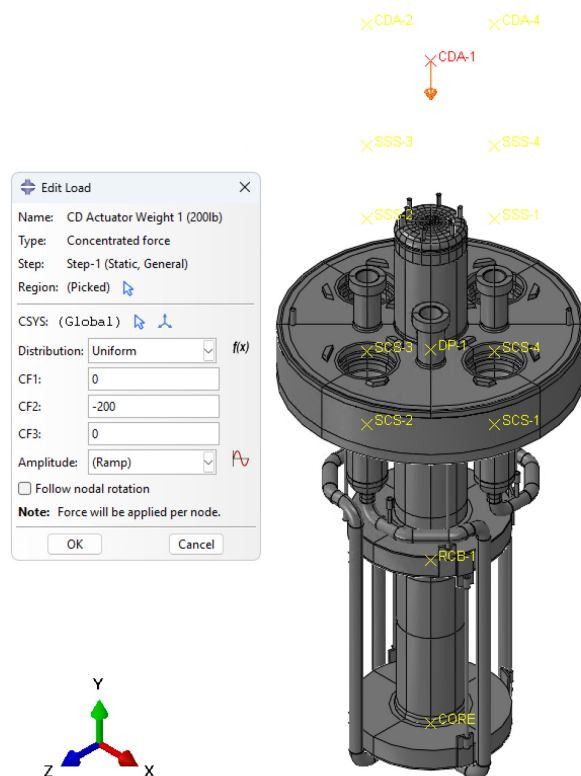
Figure 33. CD Actuators Weight (4x)

TEM-10200-1, Rev. 12	ENGINEERING CALCULATIONS AND ANALYSIS	ECAR-6564, Rev. 0
04/12/2021		Page 77 of 100

MARVEL Project Primary Coolant System ASME BPVC Section III Division 5 Design by Analysis
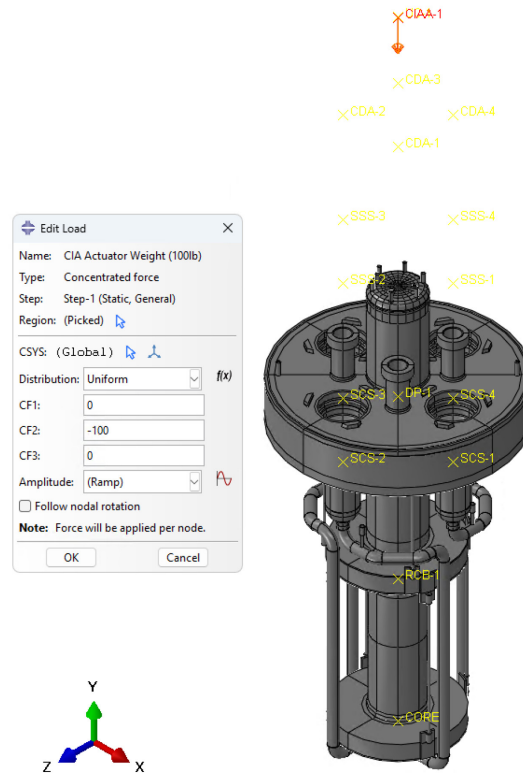
Figure 34. CIA Actuators Weight
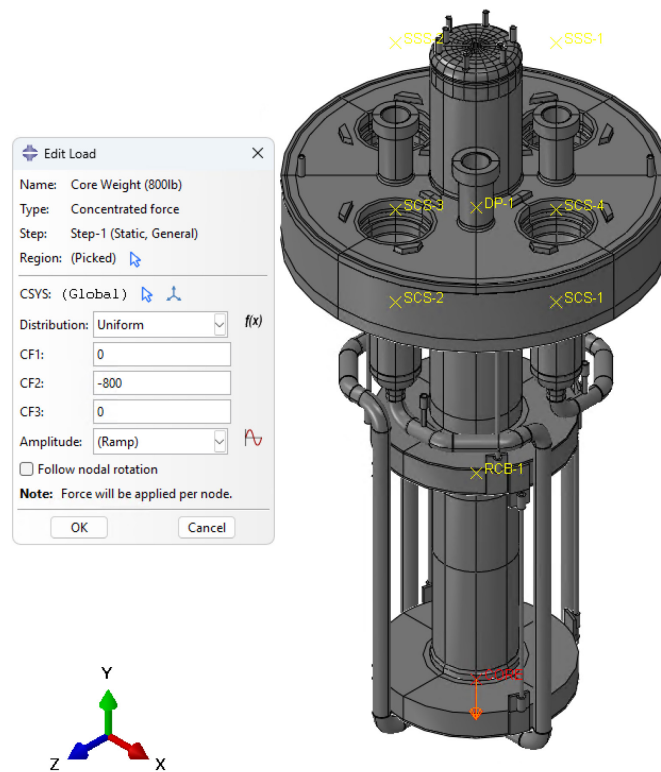
Figure 35. Reactor Core Weight
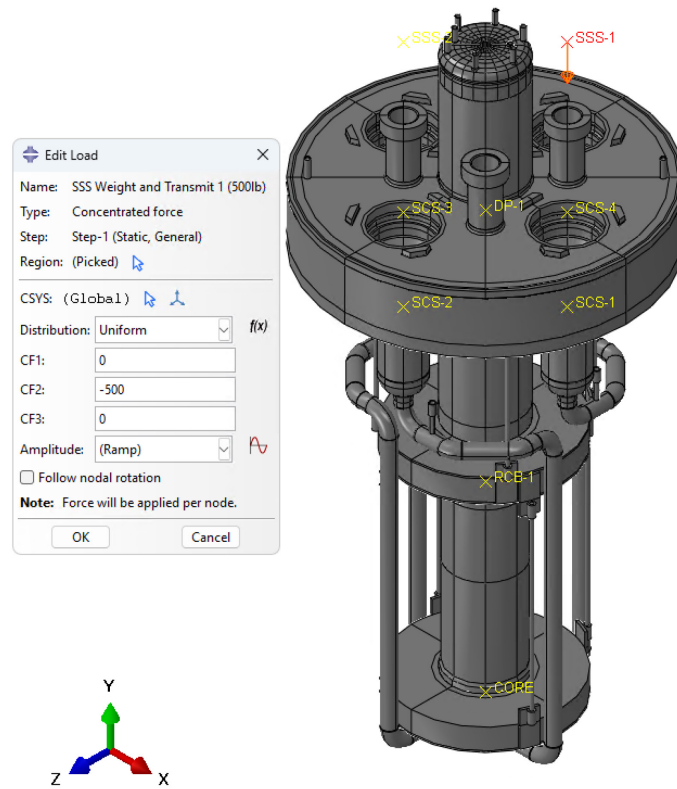
Figure 36. SSS with Stirling Engines Weight and Transmitted Load (4x)
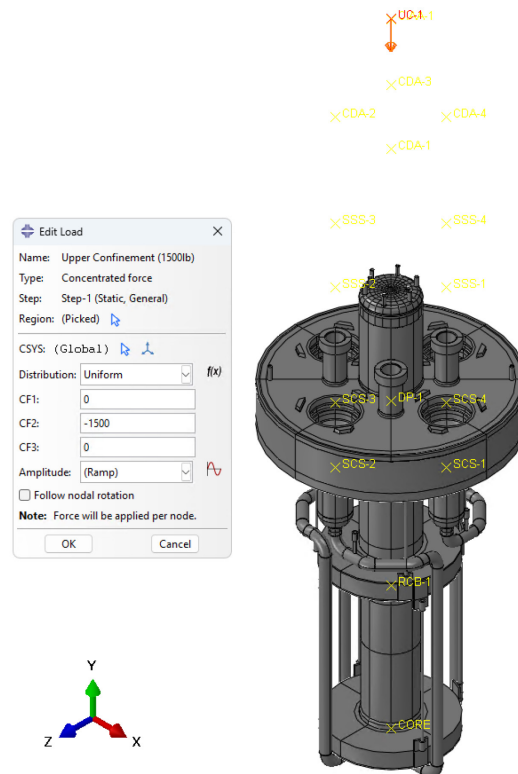
Figure 37. Upper Confinement Weight
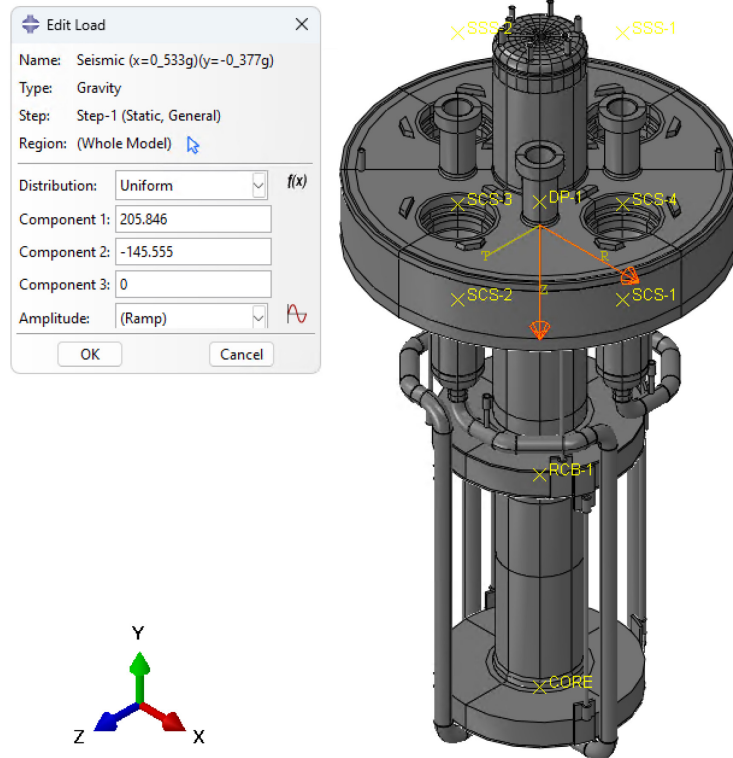
Figure 38. X Direction Seismic Gravity
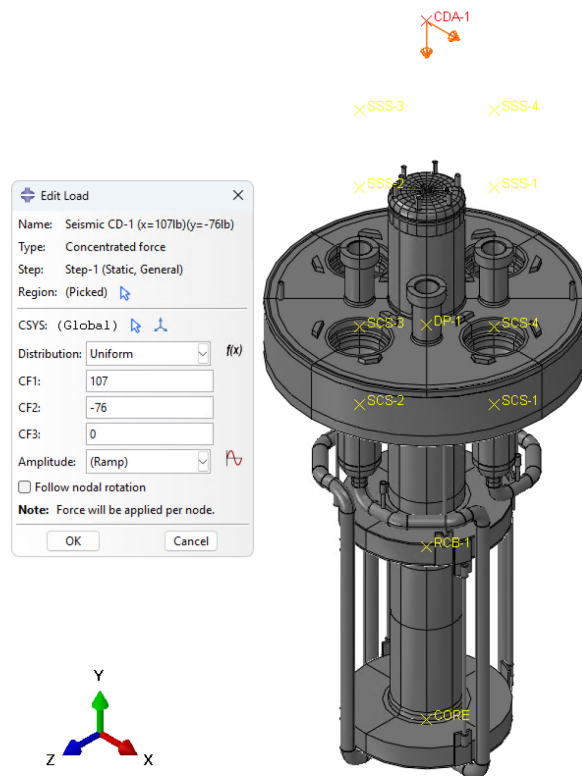
Figure 39. CD Actuators X Direction Seismic (4x)
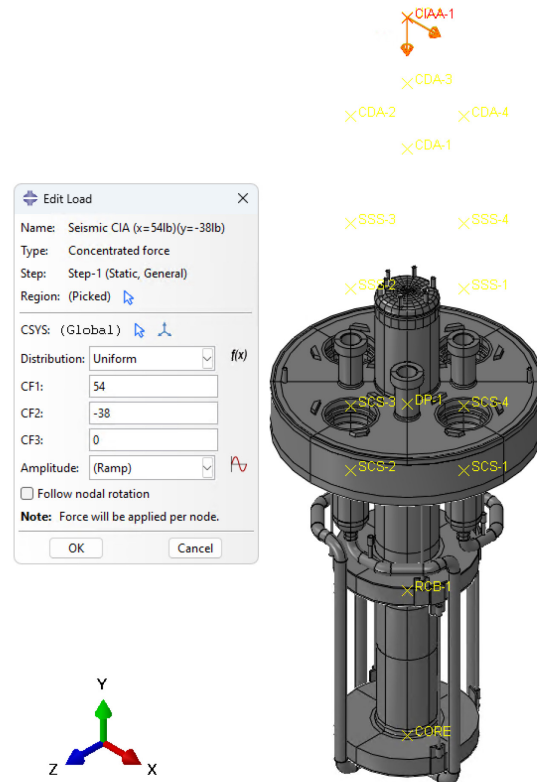
Figure 40. CIA Actuator X Direction Seismic
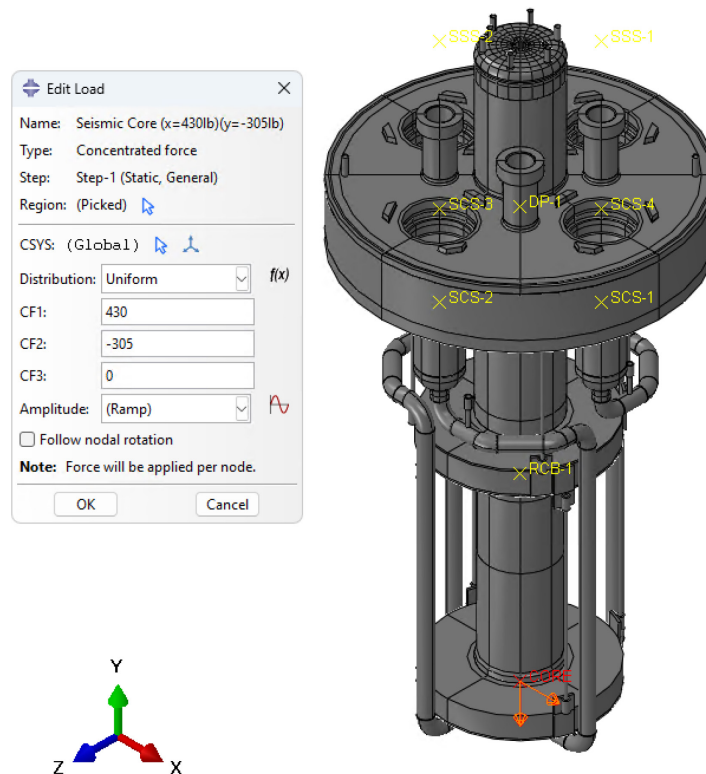
Figure 41. Core X Direction Seismic

TEM-10200-1, Rev. 12 04/12/2021	**ENGINEERING CALCULATIONS AND ANALYSIS**	ECAR-6564, Rev. 0 Page 81 of 100

MARVEL Project Primary Coolant System ASME BPVC Section III Division 5 Design by Analysis
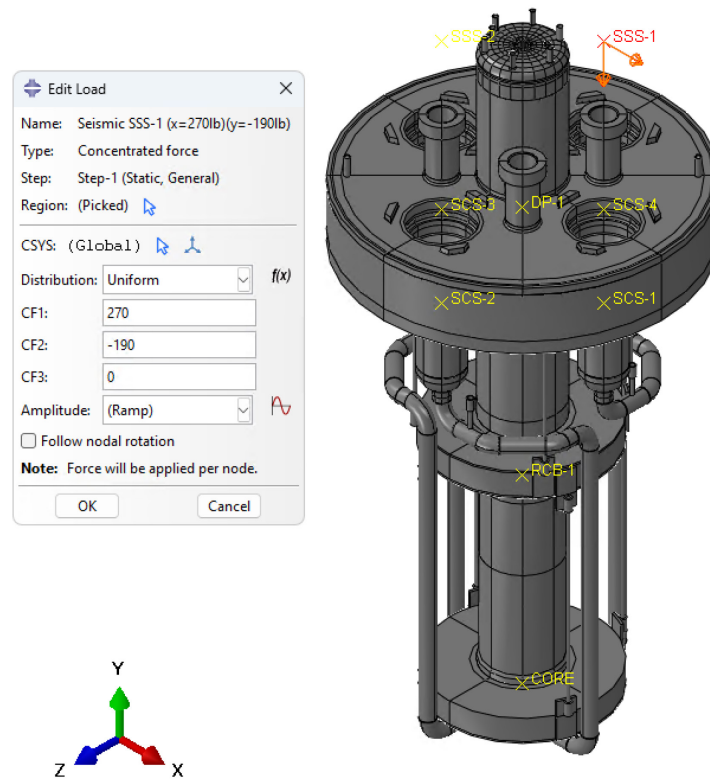
Figure 42. SSS with Stirling Engines X Direction Seismic (4x)
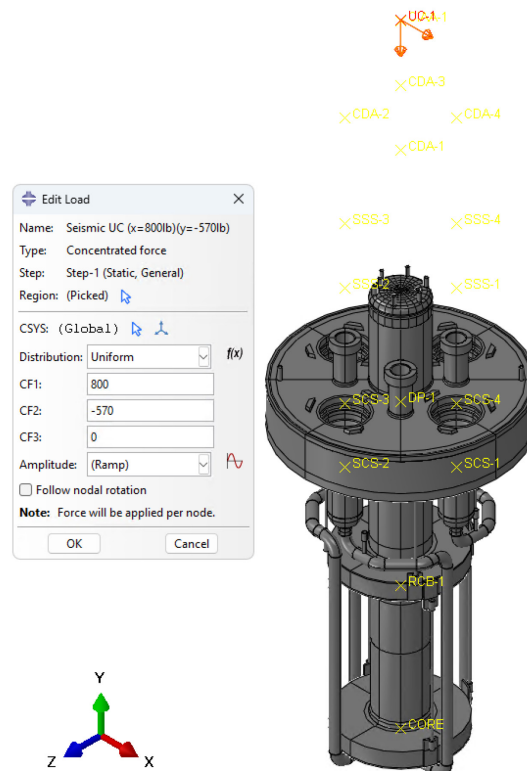
Figure 43. Upper Confinement X Direction Seismic
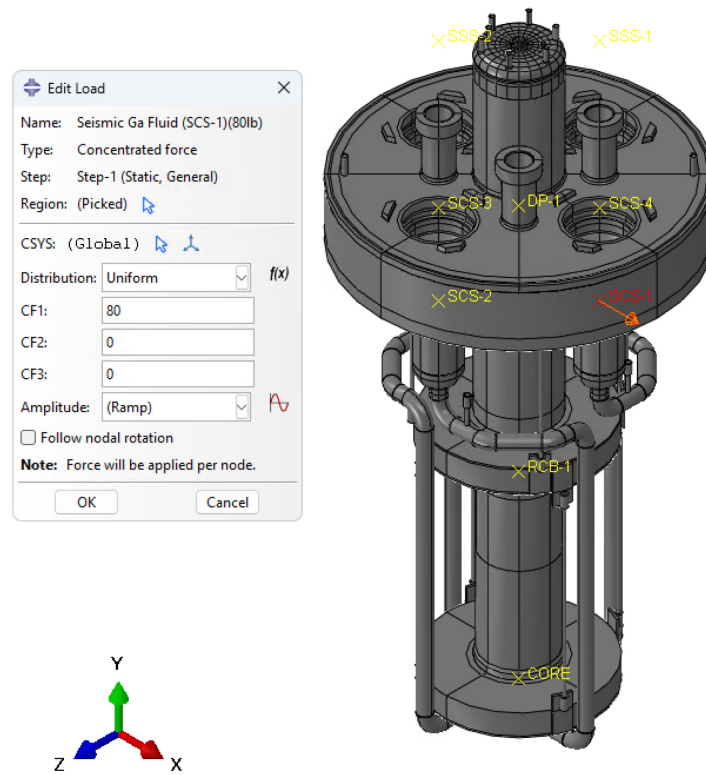
Figure 44. Ga Fluid Overturning Moment Force X Direction Seismic (4x)
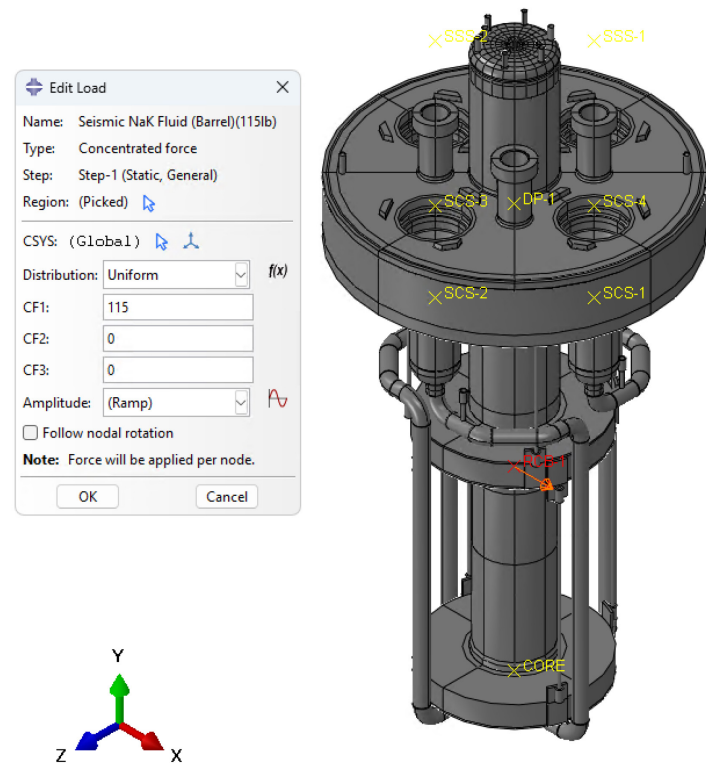
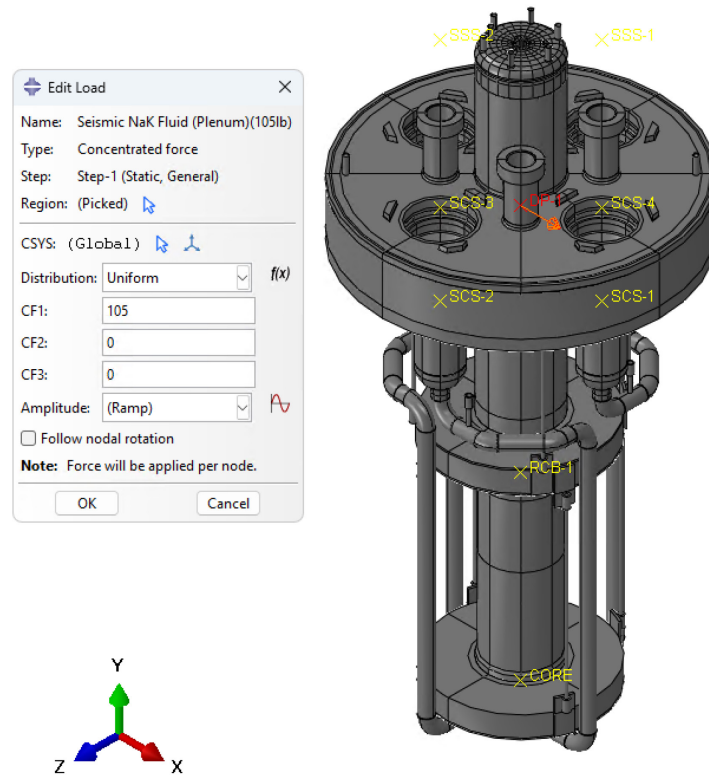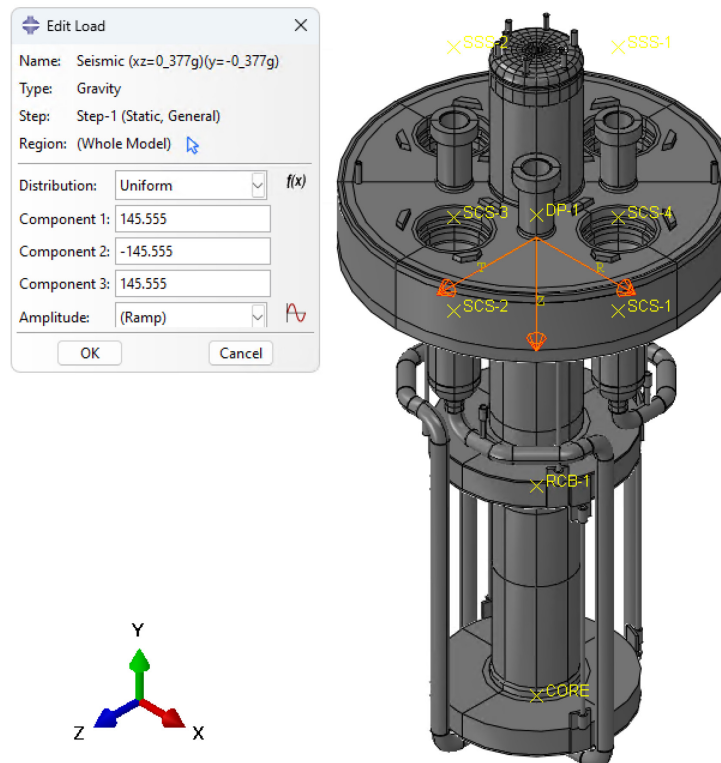Figure 45. NaK Fluid in Core Barrel Overturning Moment X Direction Seismic

TEM-10200-1, Rev. 12 04/12/2021	ENGINEERING CALCULATIONS AND ANALYSIS	ECAR-6564, Rev. 0 Page 83 of 100

MARVEL Project Primary Coolant System ASME BPVC Section III Division 5 Design by Analysis

Figure 46. NaK Fluid in Distribution Plenum Overturning Moment X Direction Seismic
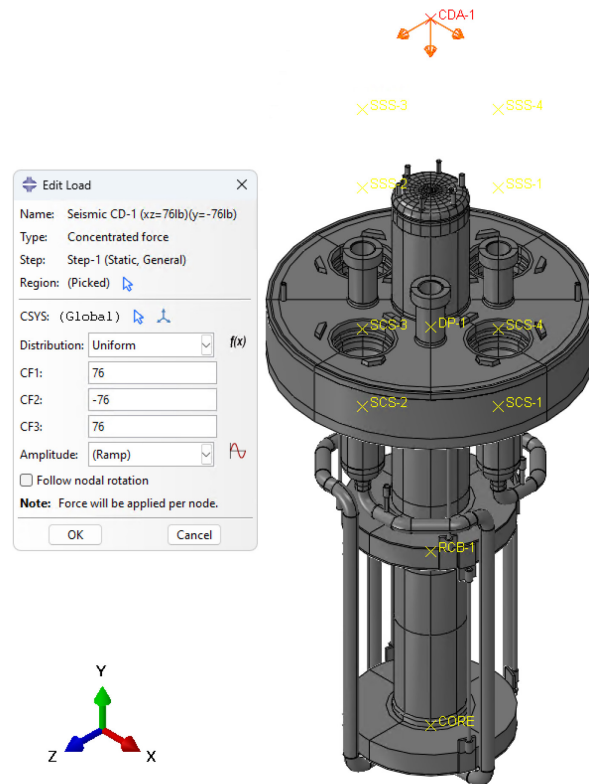

Figure 47. XZ Direction Seismic Gravity

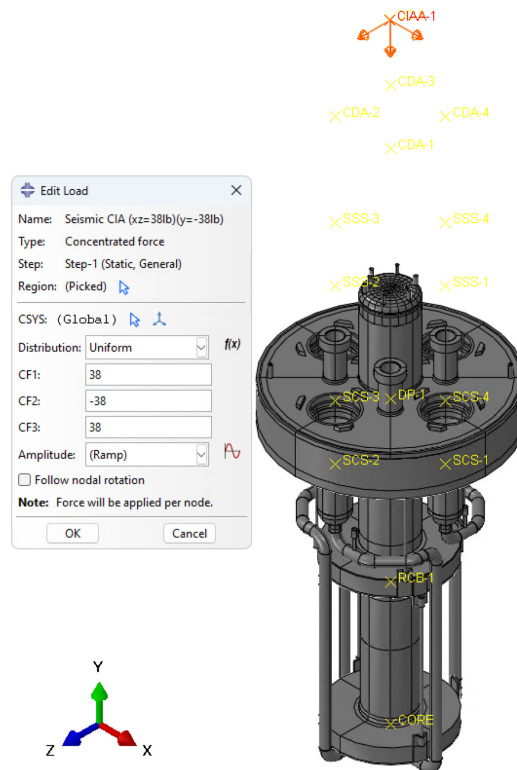Figure 48. CD Actuators XZ Direction Seismic (4x)

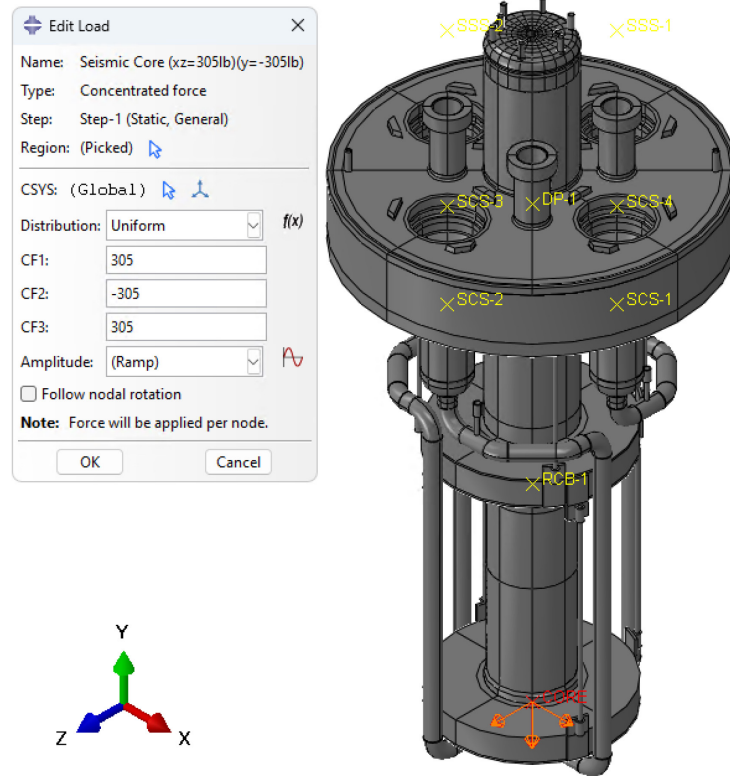

Figure 49. CIA Actuator XZ Direction Seismic

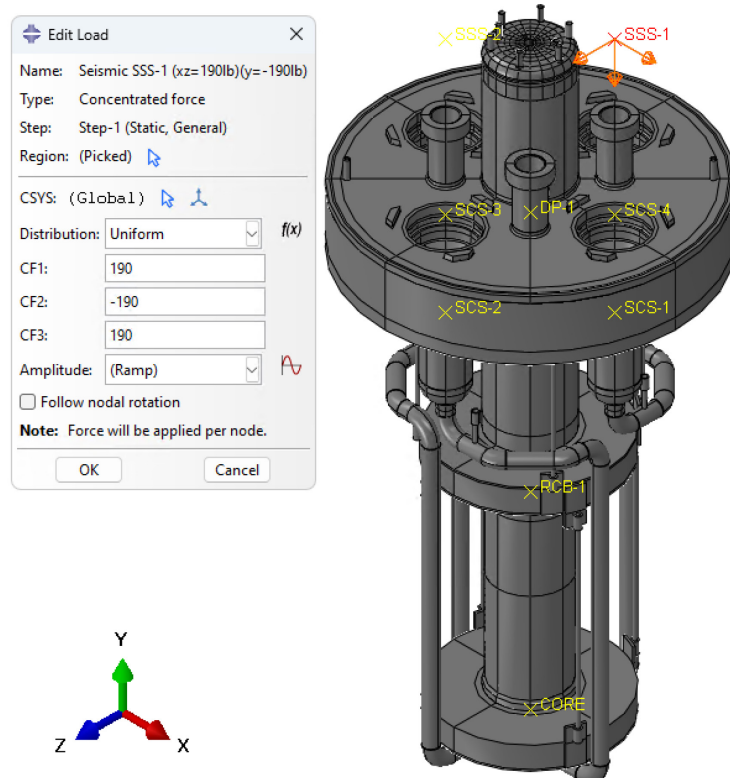Figure 50. Core XZ Direction Seismic

Figure 51. SSS with Stirling Engines XZ Direction Seismic (4x)
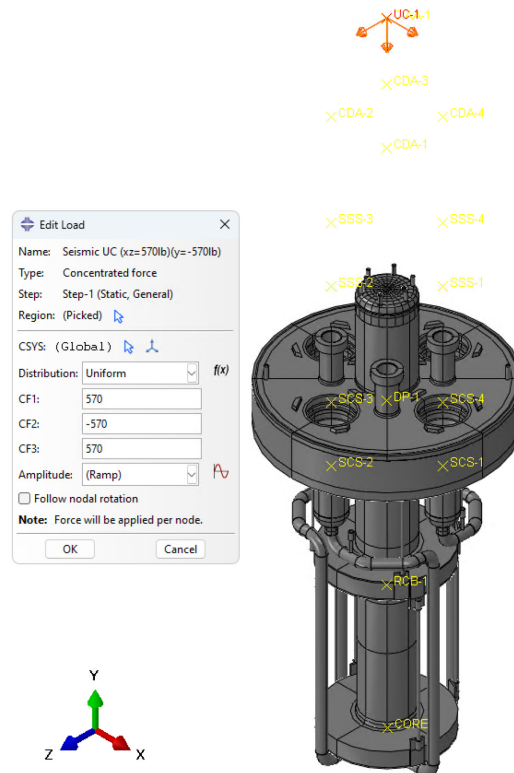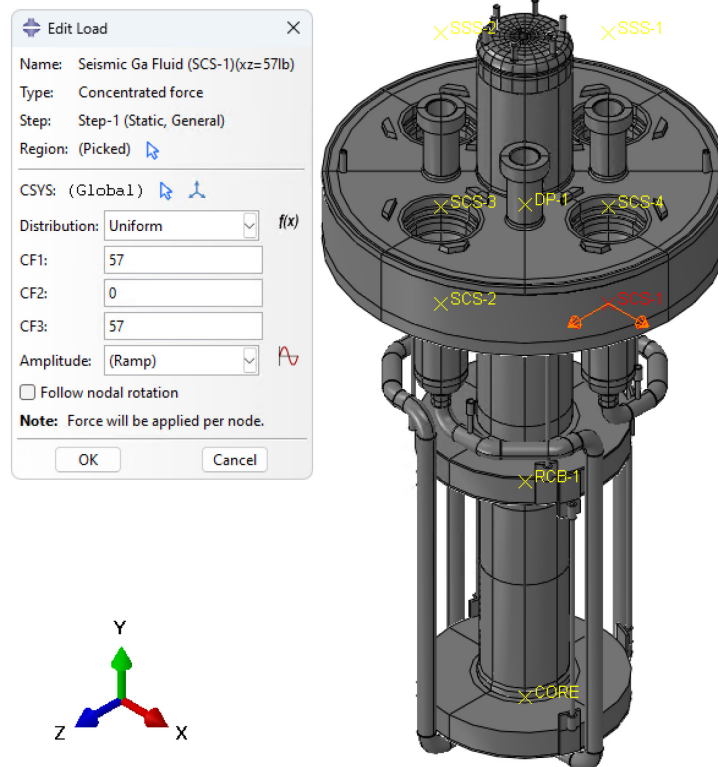
Figure 52. Upper Confinement XZ Direction Seismic

Figure 53. Ga Fluid Overturning Moment Force XZ Direction Seismic (4x)

TEM-10200-1, Rev. 12	**ENGINEERING CALCULATIONS AND ANALYSIS**	ECAR-6564, Rev. 0
04/12/2021		Page 87 of 100

MARVEL Project Primary Coolant System ASME BPVC Section III Division 5 Design by Analysis
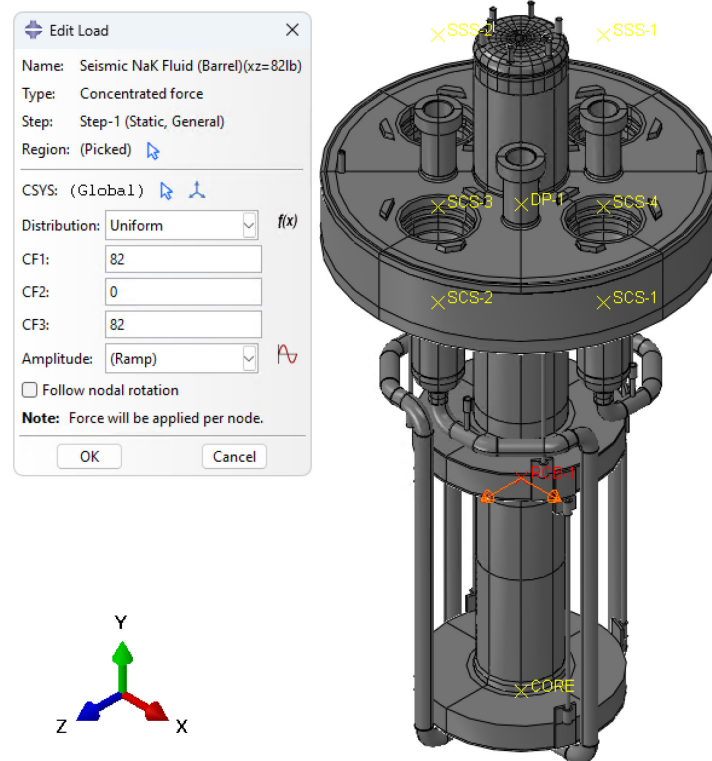
Figure 54. NaK Fluid in Core Barrel Overturning Moment XZ Direction Seismic
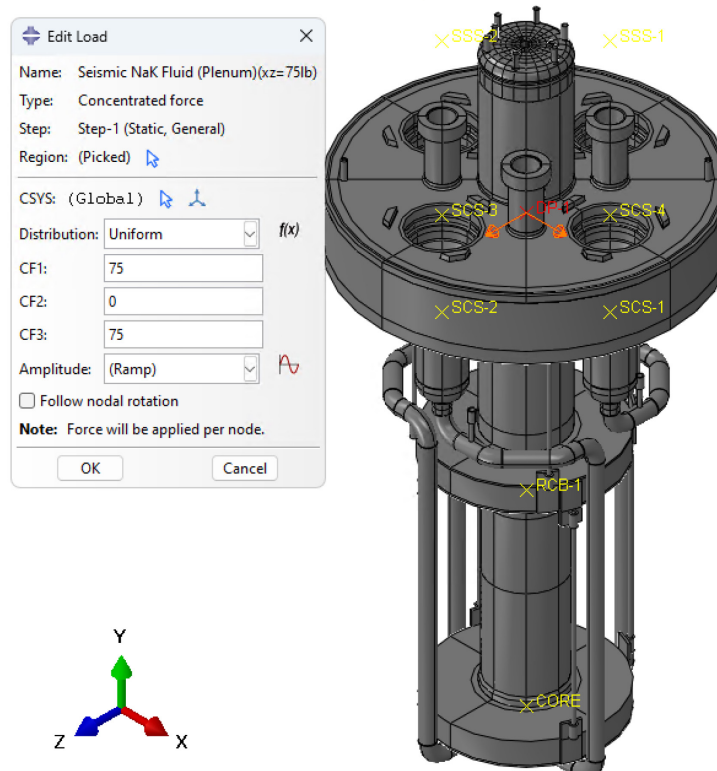

Figure 55. NaK Fluid in Distribution Plenum Overturning Moment XZ Direction Seismic
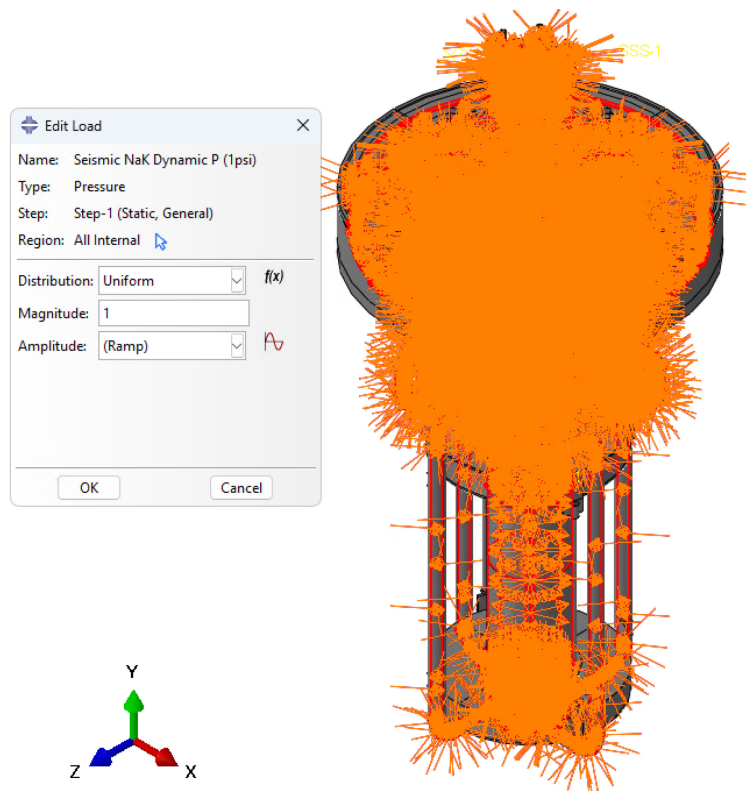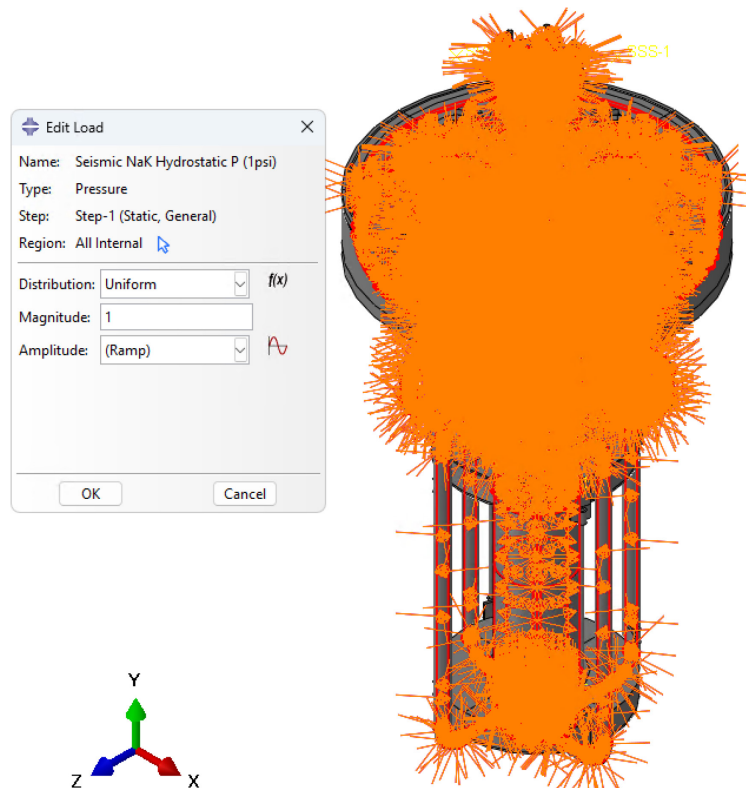
Figure 56. X and XZ Seismic NaK Dynamic Pressure

Figure 57. X and XZ Seismic NaK Hydrostatic Pressure

Appendix F

Boundary Conditions between Divided PCS Model for Service Level A, B, and C

Code Calculations

MARVEL

BOUNDARY CONDITIONS FOR DOWNCOMER CUTS
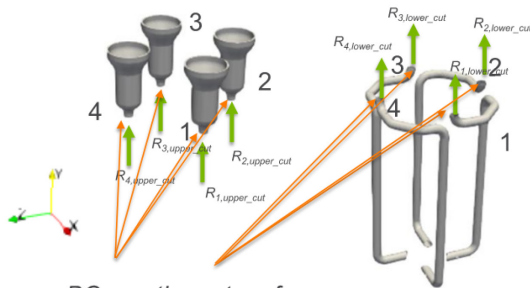
	Design (primary)	SL-A (primary + secondary)	SL-B (primary + secondary)	
$R_{1,upper\_cut}$	-265	-475	-512	DC-1 (upper part along +x axis)
$R_{2,upper\_cut}$	-265	-475	-505	DC-2 (upper part along -z axis)
$R_{3,upper\_cut}$	-265	-475	-491	DC-3 (upper part along -x axis)
$R_{4,upper\_cut}$	-265	-475	-394	DC-4 (upper part along +z axis)

BCs on the cut surface.
1. No out of plane displacement (i.e. equal value y_disp)
2. Apply force (=R)

Unit: lbf

$R_{lower\_cut} = -R_{upper\_cut}$

BOUNDARY CONDITIONS FOR CORE-BARREL CUTS
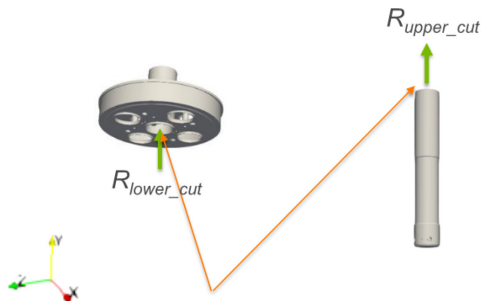
	Design (primary)	SL-A (primary + secondary)	SL-B (primary + secondary)
$R_{1,upper\_cut}$	-7815	-7000	-7025

Unit: lbf
$R_{lower\_cut} = -R_{upper\_cut}$

BCs on the cut surface:
1. No out of plane displacement (i.e. equal value y_disp)
2. Apply force (=R)

3

Argonne
NATIONAL LABORATORY

| TEM-10200-1, Rev. 12 | **ENGINEERING CALCULATIONS AND ANALYSIS** | ECAR-6564, Rev. 0 |
| 04/12/2021 | | Page 92 of 100 |

MARVEL Project Primary Coolant System ASME BPVC Section III Division 5 Design by Analysis

Appendix G

Stirling Engine Tube Helium Rupture in Secondary Coolant System Calculation

| TEM-10200-1, Rev. 12 | **ENGINEERING CALCULATIONS AND ANALYSIS** | ECAR-6564, Rev. 0 |
| 04/12/2021 | | Page 93 of 100 |

MARVEL Project Primary Coolant System ASME BPVC Section III Division 5 Design by Analysis

This appendix documents the impact of a stirling engine tube helium rupture while installed on the PCS. A stirling tube may rupture due to the high corrosion rate of the eGalinstan secondary coolant. The project strategy is to determine a stirling engine replacement cycle that precludes this from happening. All four stirling engines will be replaced at the same interval.

In the unlikely event a stirling engine tube ruptures prior to replacement, this appendix demonstrates that the pressure build-up in the IHX is about 8 psig before the SCGS bellows relieves the pressure in under a second. Since the leak pressure internally to the IHX is less than the PCS pressure externally applied to the IHX, the tube rupture is omitted from the PCS evaluation. Note that the surface stress of less than 3 ksi will be experienced on the IHX liner, which is not part of the primary pressure boundary.

TEM-10200-1, Rev. 12
04/12/2021

ENGINEERING CALCULATIONS AND ANALYSIS

ECAR-6564, Rev. 0
Page 94 of 100

MARVEL Project Primary Coolant System ASME BPVC Section III Division 5 Design by Analysis

Bellows Leak/Rupture
John Stevenson

$P_{He} := 52 \ bar = 754.196 \ psi$ Helium pressure

$T := 350 \ °C$ Operating temperature

$R_{IG} := 8.314 \cdot \dfrac{J}{mol \cdot K}$ Universal gas constant

$M := 4.002602 \ \dfrac{gm}{mol}$ Helium molar mass

$k_{He} := 1.667$ Ratio of specific heats - Helium

$P_w := \dfrac{P_{He} \cdot T}{20 \ °C} = 1603.198 \ psi$ Helium working pressure

$\rho := \dfrac{P_w \cdot M}{R_{IG} \cdot T} = 8.54 \ \dfrac{kg}{m^3}$ Density of helium

$He_v := 12.6 \ L$ Helium volume in Stirling

$D := 9.75 \ in$ Bellows inside diameter - Oakridge Bellows 111522-9

$t := 0.036 \ in$ Bellows thickness - Oakridge Bellows 111522-9

$k := 622.4 \ \dfrac{lbf}{in}$ Spring constant

$n_s := 3$ Number of springs

$k_t := k \cdot n_s = 1867.2 \ \dfrac{lbf}{in}$ Total spring constant

$w := 278 \ lbf$ Stirling engine & SOS weight - 1014740

$n := 1$ Number of tubes ruptured

$ID_{tube} := 0.11 \ in$ Inside diameter of tube

TEM-10200-1, Rev. 12
04/12/2021

ENGINEERING CALCULATIONS AND ANALYSIS

ECAR-6564, Rev. 0
Page 95 of 100

MARVEL Project Primary Coolant System ASME BPVC Section III Division 5 Design by Analysis

$A_{t1} := \pi \cdot \dfrac{ID_{tube}^2}{4} = 0.01 \; in^2$ | Cross sectional flow area of single tube

$A_t := 2 \cdot n \cdot A_{t1} = 0.019 \; in^2$ | Cross sectional flow area comprised of both ends of n ruptured tubes

$R := \dfrac{D}{2} = 4.875 \; in$ | Bellows radius

$C := \pi \cdot D = 30.631 \; in$ | Bellows circumference

$r := 3.86 \; in$ | Stirling Base radius - Stirling model

$v_s := \sqrt{k_{He} \cdot \dfrac{P_w}{\rho}} = 4819.289 \; \dfrac{ft}{s}$ | Sonic velocity in helium

$A_a := \pi \cdot (R^2 - r^2) = 27.853 \; in^2$ | Annulus area

$V := 117.32 \; in^3 = 1.923 \; L$ | Volume in bellows - SCCGS Gas Space Model

$\delta_s := \dfrac{w}{k_t} = 0.149 \; in$ | Spring deflection

$P_a := \dfrac{P_w \cdot He_v}{He_v + V} = 1390.962 \; psi$ | Pressure after tube rupture

$f_v := v_s \cdot A_t = 18.012 \; \dfrac{L}{s}$ | Volumetric flow rate (discharge rate from Stirling limited by sonic velocity)

$W_i := P_w \cdot He_v = (1.393 \cdot 10^5) \; J$ | Initial He work

$W_r := P_a \cdot (He_v + V) = (1.393 \cdot 10^5) \; J$ | He work after tube rupture

$gap := \dfrac{W_i}{v_s \cdot C} \cdot \dfrac{f_v}{W_r} = 0.0006205 \; in$ | Gap required to match discharge from Stirling

$t_b := 3 \; mm$ | Stirling travel allowance

$w_{eff} := w - ((\delta_s - gap - t_b) \cdot k_t) = 221.694 \; lbf$ | Effective weight | Neglects upward force due to coolant displacement

TEM-10200-1, Rev. 12
04/12/2021

ENGINEERING CALCULATIONS AND ANALYSIS

ECAR-6564, Rev. 0
Page 96 of 100

MARVEL Project Primary Coolant System ASME BPVC Section III Division 5 Design by Analysis

$$P_l := \frac{w_{eff}}{A_a} = 7.959 \ psi$$ Leak pressure

$$a := \frac{P_a \cdot A_a}{w} \cdot g = \left(1.367 \cdot 10^3\right) \frac{m}{s^2}$$ Acceleration of Stirling due to pressure

$$t_{gap} := \sqrt{\frac{\frac{P_a \cdot A_a}{g}}{k} \cdot \frac{\pi}{2} \cdot \frac{gap}{\frac{P_a \cdot A_a}{k}}} + \sqrt{\frac{gap}{\frac{1}{2} \cdot a}} = 0.158 \ ms$$ Time to achieve gap

$$V_f := \frac{P_w \cdot He_v}{P_a} = 14.523 \ L$$ Final volume of helium

$$t_r := \frac{V_f}{f_v} = 806.254 \ ms$$ Time to completely leak from rupture

$$\sigma_{hoop} := \frac{P_l \cdot R}{0.036 \ in} = 1.078 \ ksi$$ Hoop stress in bellows

$$F := \rho \cdot A_{t1} \cdot v_s^2 = 25.398 \ lbf$$ Force from impinging jet due to momentum

$$\sigma := \frac{F}{A_{t1}} = 2.673 \ ksi$$ Stress at surface due to impinging jet

Appendix H

PGS Coolant Leak Failure Modes and Effects Analysis

FAILURE MODES AND EFFECTS ANALYSIS

In response to a request to consider a leak of the PGS system onto the top surface of the distribution plate of the PCS, a failure modes and effects analysis was performed. The following three failures were considered and the probability, consequence, and ability to detect the failure were qualitatively assessed to determine the risk to the MARVEL reactor:

- Case 1: A slow leak at the initiation site of a fatigued brazed joint or a fatigued fitting.

- Case 2: A steady leak of water due to continued fatigue or partial failure of the tubing or fittings feeding one of the Stirling engines (spraying of water on the interior of the UCS).

- Case 3: Rapid loss of all water due to complete failure of any fitting, hose, or tubing.

In the first two cases, the resulting risk is considered acceptable to the MARVEL reactor and no additional physical design changes are required. In these cases, there may be additional controls or sequences that should be implemented to minimize any potential impacts. For the last case, the risk is considered high for the MARVEL reactor, but no failures are identified that would create a failure of the primary coolant boundary. It is recommended that further quantitative analysis be performed to better define the risk.

SYSTEM DESCRIPTION AND INTERACTIONS

The PGS system consists of four independent loops with each loop providing the necessary cooling water for a single Stirling engine. The total volume of water in a single PGS loop is approximately 11 gallons which includes the volume in the engine, the tubing, and an expansion tank. The connections to the Stirling engine are made with JIC stainless steel hose. There are a total of four connections, the inlet and outlet, and the two connections between the upper and lower engine chambers. The flow rate of the cooling water is approximately 10-11 gallons per minute. In the final design review meeting, Qnergy (supplier of MARVEL's Stirling engines) reported that approximately 2% of the engines deployed in the field had experienced a fatigue failure of the brazed joints at the exterior of the engine.

The top surface of the PCS distribution plate is covered with fitted pieces of pyrogel insulation (cream material in figure below) to limit heat loss from the PCS into the upper confinement. The insulation is hydrophobic and breathable and is designed to have a snug fit around all components. It's unknown if the hydrophobic agent would breakdown in a radiation environment. However, if that were to occur, water could potentially be absorbed into the insulation which would result in an increase in thermal conductivity.
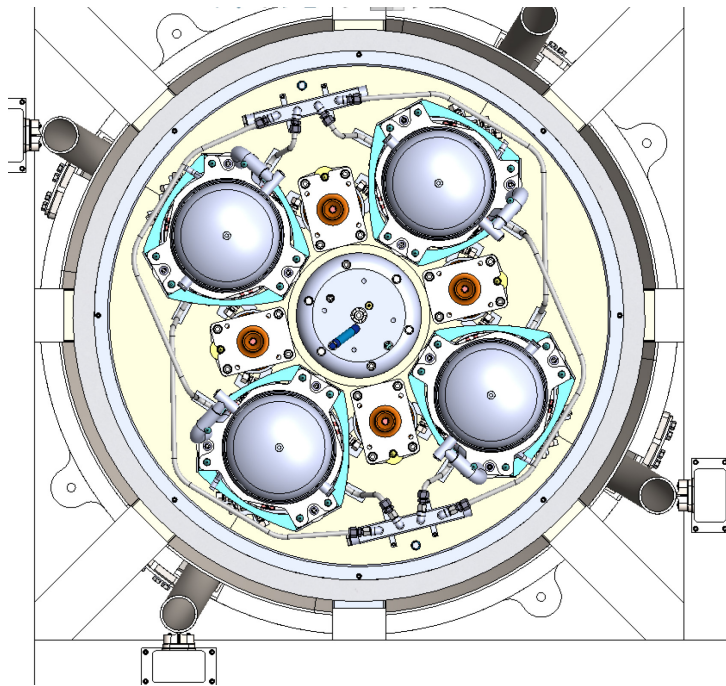
Figure 58. Top View of PCS showing Pyrogel Insulation

CASE 1

It is assumed that any fatigue failure would be initiated with a small fracture in either the brazed joint or with a loss of the compression seal on the JIC fitting. The failure would begin with a slow leak of water directly onto the surface of the PCS or onto the insulation covering the PCS. The thermal mass and temperature of the PCS would vaporize the water as it contacted either bare metal or the insulation. A slow leak could be a detectable failure by a falling volume in the PGS expansion tank. This would alert operations to a problem and the reactor could be safely shut down and the leak investigated and repaired. The resulting risk to the reactor is considered low.

CASE 2

Continued fatigue of a brazed joint or serious failure of a JIC fitting could result in a steady stream of water onto the top of the PCS. This failure is considered less likely than Case 1 as its initiation should be detected prior as a slow leak but is nonetheless anticipated. The fact that coolant water is being pumped limits the rate at which the water would be contacting the surface of the pyrogel insulation. It is assumed that in this case, the level transmitter within the expansion tank would reveal a loss of cooling water and operations could shut down the flow to limit the amount of water in contact with the PCS. The ingress of water to the surface of the PCS would be limited with the presence of the insulation and, like in Case 1, would likely be reduced by vaporization as it moves on top of the insulation towards any gaps in the insulation. The resulting risk to the reactor is considered moderate as there could be some localized straining of the PCS surface with direct contact of the cooling water and the potential binding of one control drum shaft.

CASE 3

In this case, the total volume of water in the PGS loop is rapidly lost to the top of the PCS. This failure is likely only to happen with a complete failure of a fitting or shearing of the stainless-steel braded hose. Because of the severity of the failure, it is considered undetectable and would result in nearly all the 11 gallons of water being deposited onto the top of the PCS. In this case, the fit pattern and hydrophobic nature of insulation would limit water from reaching large areas of the top surface of the PCS but would instead direct the water to the exposed areas near the Stirling engines and control drum pass-throughs. This rapid exposure to the cooling water would in turn quench the exposed surfaces and cause localized strains and thermal stresses. As a best case, the PCS distribution plate would not experience any plastic strains. At worst case the PCS distribution plate is plastically deformed and causes the following potential consequences:

- Misalignment of the Stirling engine stands.

- Binding of the control drum rods, which prevents rotation of the drums.

- Misalignment of the top-hat and CIA rod.

- Fractures or failures of the weld between the PCS distribution plate and guard vessel.

With this case, there are no failures identified that would impact the integrity of the primary coolant boundary. However, with the potential binding of the control drum rods and misalignment of the CIA rod, there is considerable risk in shutting down the reactor.

Although it is highly unlikely that this type of failure would occur, the consequences are high enough that the risk to the MARVEL reactor is also considered to be high. In order to reduce the risk to the MARVEL reactor, it is recommended that further FEA analysis of the PCS distribution plate with the above described transient load being applied to quantify the stress and strain of the distribution plate. Upon completing the FEA analysis, the consequences could be re-evaluated and a more quantitative risk could be determined.